The Cdc48^{Shp1} complex mediates cell cycle progression by positive regulation of Glc7

Dissertation der
Fakultät für Biologie der
Ludwig-Maximilians-Universität
München

vorgelegt von
Diplom-Biochemikerin
Stefanie Böhm

Juni 2011

Ehrenwörtliche Erklärung

Hiermit erkläre ich, dass ich die vorliegende Dissertation selbstständig und ohne unerlaubte Hilfe angefertigt habe. Ich habe weder anderweitig versucht, eine Dissertation einzureichen oder eine Doktorprüfung durchzuführen, noch habe ich diese Dissertation oder Teile derselben einer anderen Prüfungskommission vorgelegt.

Stefanie Böhm
München, den 08. Juni 2011

Promotionsgesuch eingereicht am: 08. Juni 2011
Tag der mündlichen Prüfung: 03. August 2011

Erster Gutachter: Prof. Dr. Stefan Jentsch
Zweite Gutachterin: Prof. Dr. Angelika Böttger

Die vorliegende Arbeit wurde unter der Anleitung von Prof. Dr. Alexander Buchberger zwischen Juli 2006 und März 2009 in der Abteilung von Prof. Dr. Stefan Jentsch am Max-Planck-Institut für Biochemie in Martinsried und von April 2009 bis Juni 2011 am Lehrstuhl für Biochemie der Universität Würzburg durchgeführt.

Table of contents

1. Summary 1

2. Introduction... 5

2.1 The Ubiquitin Proteasome System (UPS) 5

2.1.1 Ubiquitin conjugation 5
2.1.2 The 26S proteasome and degradation 7

2.2 The yeast cell cycle 8

2.2.1 Mitosis 9

2.2.1.1 The spindle assembly checkpoint (SAC)... 10
2.2.1.2 Mitotic exit 13

2.3 The AAA ATPase Cdc48/p97 15

2.3.1 UBX proteins 17
2.3.2 Shp1/p47 19

2.4 Protein phosphatase 1 catalytic subunit- Glc7 21

2.4.1 Targeting subunits mediate Glc7 function 23
2.4.2 Regulation of mitosis by PP1/Glc7 24

2.5 Aim of the work 27

3. Results 29

3.1 Phenotypic characterization of s*hp1* mutants 29

3.1.1 Null mutation of *shp1* causes a general growth defect 29
3.1.2 W303 *Δshp1* is inviable 30
3.1.3 Pleiotropic defects of *shp1* mutants 31

3.2 The Shp1-Cdc48 interaction 32

3.2.1 Cdc48 binding mutants of *shp1* 32
3.2.2 Ubiquitination of Shp1 depends on Cdc48 binding 35

3.3 Shp1 is modified by phosphorylation 36

3.4 Identification of novel Shp1 interactors 37

3.5 Cell cycle defect of *shp1* 40

3.5.1 *shp1* mutants exhibit a cell cycle delay in mitosis 40

3.5.1.1 The cell cycle delay of *shp1* is not due to a defect in mitotic exit 41
3.5.1.2 Null mutants of *shp1* exhibit a metaphase to anaphase delay 43
3.5.1.3 The cell cycle delay of *shp1* is caused by activation of the spindle checkpoint ... 44

3.5.2 The Cdc48^{Shp1} complex is required for the Shp1 cell cycle function 46

3.6 Regulation of Glc7 cell cycle function by Cdc48^{Shp1} 47

3.6.1 Interaction of Shp1 with Glc7 48
3.6.2 Glc7 phosphatase activity is reduced in *shp1* mutants 49

3.6.2.1 Substrates of Glc7 and Ipl1 are hyperphosphorylated in *shp1* 51
3.6.2.2 Overexpression of *GLC7* suppresses the mitotic delay of *shp1* mutants 52

3.6.3 Nuclear localization of Glc7 in wild-type and *shp1* 54
3.6.4 Ubiquitination of Glc7 differs in *shp1* 57

3.7 Shp1 influences the interaction of Glc7 with Glc8 58

3.7.1 Genetic interaction of *shp1* with Glc7 targeting subunits 58
3.7.2 The Glc7-Glc8 interaction is reduced in *shp1* null mutants 60
3.7.3 Overexpression of *GLC8* suppresses *shp1-7* temperature sensitivity 62

4. Discussion 65
4.1 Phenotypic characterization of *shp1* mutants 65
  4.1.1 Null mutants of *shp1* exhibit severe growth defects or lethality 66
  4.1.2 The cell cycle defect of *shp1* 67
  4.1.3 The cell cycle function of Shp1 depends on the Cdc48^{Shp1} complex 69
4.2 Regulation of Glc7 cell cycle function by Cdc48^{Shp1} 70
  4.2.1 Reduction of Glc7 activity in *shp1* mutants 70
    4.2.1.1 Genetic interaction of *shp1* with *glc7* 70
    4.2.1.2 The Ipl1/Glc7 balance at the kinetochore is impaired in *shp1* mutants 70
  4.2.2 Phosphorylation of Shp1 at five major sites is not required for regulation of Glc7 activity .. 73
  4.2.3 Mechanism of Glc7 regulation by Cdc48^{Shp1} 74
    4.2.3.1 Protein levels and localization of Glc7 in *shp1* 74
    4.2.3.2 Glc7 ubiquitination is altered in s*hp1* 75
    4.2.3.3 Interaction of Glc7 with regulatory subunits in *shp1* 76
5. Material and Methods 79
5.1. Material 79
  5.1.1 Chemicals and reagents 79
  5.1.2 Databases 79
  5.1.3 Media and plates 79
    5.1.3.1 *S. cerevisiae* media and plates 79
    5.1.3.2 *E. coli* media and plates 80
  5.1.4 Plasmids 81
  5.1.5 *E. coli* strains 81
  5.1.6 *S. cerevisiae* strains 82
  5.1.7 Antibodies 84
    5.1.7.1 Primary antibodies 84
    5.1.7.2 Secondary antibodies 84
5.2. Methods 84
  5.2.1 Protein biochemical methods 84
    5.2.1.1 SDS-polyacrylamide gel electrophoresis (SDS-PAGE) 84
    5.2.1.2 Western blot 84
    5.2.1.3 Yeast whole cell lysates- TCA precipitation 85
    5.2.1.4 Immunoprecipitation (IP) 85
    5.2.1.5 Denaturing Ni-NTA Pull-down 85
    5.2.1.6 Two step purification of phosphorylated Shp1 for mass-spectrometry 86
  5.2.2 *E. coli* Methods 87
    5.2.2.1 Preparation of competent *E. coli* 87
    5.2.2.2 Transformation of *E. coli* with DNA 87
    5.2.2.3 Plasmid isolation from *E. coli* cultures 87
  5.2.3 Molecular biology methods 87
    5.2.3.1 Polymerase chain reaction (PCR) 87
    5.2.3.2 Site-directed mutagenesis 88
    5.2.3.3 Restriction digest 88
    5.2.3.4 Electrophoresis and DNA extraction from agarose gels 88
    5.2.3.5 Vector dephosphorylation and ligation 88
    5.2.3.6 Sequencing 88
  5.2.4 *S. cerevisiae* methods 89
    5.2.4.1 Preparation of competent yeast cells (Knop et al., 1999) 89
    5.2.4.2 Transformation of competent yeast cells (Knop et al., 1999) 89
    5.2.4.3 Integration of *YIplac* plasmids using homologous recombination 89
    5.2.4.4 Yeast colony-PCR 89
    5.2.4.5 Extraction of genomic DNA (gDNA) 90
    5.2.4.6 Pop-in/ pop-out gene replacement 90
    5.2.4.7 Mating of yeast strains 91
    5.2.4.8 Mating type test 91

5.2.4.9 Sporulation and tetrad dissection 91
5.2.4.10 Spotting of serial dilutions for phenotypic analysis.. 91
5.2.4.11 Interaction studies using directed yeast two hybrid (Y2H) assays 91
5.2.4.12 Robot-based Y2H screen 92
5.2.4.13 Live-cell microscopy (fluorescence and spinning disk confocal)................................. 92
5.2.5 Cell cycle experiments in *S. cerevisiae* 93
5.2.5.1 Analysis of DNA content by flow cytometry (FACS).. 93
5.2.5.2 α-factor arrest/ release 93
5.2.5.3 Nocodazole arrest/ release... 94
6. References 95
7. Abbreviations... 105
Acknowledgements
Curriculum vitae

1. Summary

The conserved, ubiquitin-selective AAA ATPase Cdc48/p97 regulates numerous cellular processes, including protein quality control, membrane fusion, and the cell cycle. Cdc48 specificity is controlled by a large number of different cofactors, regulating substrate binding and processing. The heterodimer Ufd1-Npl4 and the UBX domain protein Shp1/p47 are two mutually exclusive substrate recruiting cofactors of Cdc48, which function in proteolytic and non-proteolytic ubiquitin-mediated pathways, respectively. In contrast to Ufd1-Npl4, cellular functions of Shp1 are still poorly understood. The aim of this work was therefore to further characterize the function of Shp1 in *S. cerevisiae*.

Deletion of the *SHP1* gene resulted in a severe growth defect and hypersensitivity to various drugs. Detailed analysis of *shp1* mutants revealed a cell cycle delay at the metaphase to anaphase transition caused by activation of the spindle assembly checkpoint (SAC).

shp1 alleles were initially identified as suppressors of high-copy protein phosphatase 1. Glc7 is the only protein phosphatase 1 catalytic subunit in *S. cerevisiae* and regulates a large number of diverse cellular pathways. As Glc7 phosphatase activity is reduced in lysates of *shp1* null mutants, Shp1 is believed to be a positive regulator of Glc7. Therefore, the relationship between Shp1 and Glc7 was further investigated. Shp1 was demonstrated to physically interact with Glc7 *in vivo*, and the double mutant of *shp1* and the *glc7-129* allele was found to be inviable. Furthermore, the cell cycle defect of *shp1* could be rescued by *GLC7* overexpression. The balance of Glc7 phosphatase and Ipl1 kinase activity is critical for proper chromosome bi-orientation and cell cycle progression. Consequently, the reduced Glc7 activity in *shp1* null mutants could result in unbalanced Ipl1 activity at the kinetochore. Indeed, a *shp1* null mutation suppressed the temperature sensitivity of *ipl1-321*. Moreover, *shp1* null mutants exhibited hyperphosphorylation of the Ipl1/Glc7 targets Dam1 and histone H3.

An engineered Cdc48 binding-deficient variant of Shp1 enabled the analysis of specific $\text{Cdc48}^{\text{Shp1}}$ complex functions for the first time. Using this *shp1* mutant, it could be demonstrated that the regulation of the metaphase to anaphase transition depends on the $\text{Cdc48}^{\text{Shp1}}$ complex. Similarly to *shp1* null mutants, the binding mutant also suppressed the *ipl1-321* temperature sensitivity and exhibited hyperphosphorylation of histone H3. Taken together, these results establish the $\text{Cdc48}^{\text{Shp1}}$ complex as a critical regulator of Glc7 activity towards Ipl1 substrates.

Finally, potential mechanisms by which $\text{Cdc48}^{\text{Shp1}}$ regulates Glc7 activity were investigated. Glc7 protein levels and sub-cellular localization were found to be unaffected by *shp1* null mutation. Importantly, the interaction between Glc7 and its activator Glc8 was significantly reduced in *shp1*, and overexpression of *GLC8* was able to partially rescue phenotypes of *shp1* mutants. These results suggest that Shp1 controls the binding of Glc8 to Glc7 and thereby enhances Glc7 activation, possibly by facilitating Glc8 nuclear localization.

Zusammenfassung

Die konservierte Ubiquitin-selektive AAA ATPase Cdc48/p97 reguliert eine Vielzahl zellulärer Prozesse, unter anderem Proteinqualtitätskontrolle, Membranfusion und den Zellzyklus. Die Spezifität von Cdc48 wird durch eine große Anzahl Kofaktoren bestimmt, die sowohl Substrat-Bindung als auch -Prozessierung regulieren. Das Heterodimer Ufd1-Npl4 und das UBX- Domänenprotein Shp1/p47 sind zwei sich wechselseitig ausschließende Substrat-rekrutierende Kofatoren von Cdc48, welche in proteolytischen bzw. nicht-proteolytischen Ubiquitin-vermittelten Prozessen wirken. Im Gegensatz zu Ufd1-Npl4 sind die zellulären Funktionen von Shp1 noch weitestgehend unbekannt. Die Zielsetzung dieser Arbeit war daher die Charakterisierung zellulärer Funktionen von Shp1 in *S. cerevisiae*.

Die Deletion des *SHP1* Gens führte zu einem stark ausgeprägten Wachstumsdefekt und zur Hypersensitivität gegenüber zahlreichen Stressbedingungen. Die genauere Analyse von *shp1* Mutanten ergab, dass sie aufgrund der Aktivierung des *spindle assembly checkpoints* (SAC) einen Zellzyklus-Defekt im Übergang von Metaphase zu Anaphase aufweisen.

shp1-Allele wurden ursprünglich als *suppressors of high-copy protein phosphatase 1* identifiziert. Glc7 ist die einzige katalytische Untereinheit von Protein Phosphatase 1 in *S. cerevisiae* und steuert eine große Zahl unterschiedlichster zellulärer Prozesse. Da die Glc7 Phosphatase-Aktivität in *shp1* Lysaten erniedrigt ist, gilt Shp1 als positiver Regulator von Glc7. Deshalb wurde die Beziehung zwischen Glc7 und Shp1 näher untersucht. Es konnte gezeigt werden, dass Shp1 *in vivo* physikalisch mit Glc7 interagiert, und die Doppelmutante aus *shp1* und *glc7-129* erwies sich als letal. Des Weiteren konnte der Zellzyklus-Defekt von *shp1* durch *GLC7* Überexpression gerettet werden Das Gleichgewicht zwischen Glc7 Phosphatase- und Ipl1 Kinase-Aktivität ist für die korrekte Bi-orientierung der Chromosomen während der Mitose und den Zellzyklus-Verlauf kritisch. Daher könnte die verringerte Glc7 Aktivität in *shp1* zu unbalancierter Ipl1 Aktivität am Kinetochor führen. Tatsächlich supprimierte eine Nullmutation von *shp1* die Temperatursensitivität von *ipl1-321*. Außerdem zeigten *shp1* Mutanten eine Hyperphosphorylierung der Ipl1/Glc7 Substrate Dam1 und Histon H3.

Eine Cdc48-Bindemutante von Shp1 ermöglichte erstmals die Analyse spezifischer Cdc48$^{\text{Shp1}}$-vermittelter Funktionen. Mit Hilfe dieser Mutante konnte gezeigt werden, dass die Regulation des Metaphase/ Anaphase-Übergangs von dem Cdc48$^{\text{Shp1}}$-Komplex abhängt. Ähnlich wie *shp1* Mutanten supprimierte auch die Bindemutante die *ipl1-321* Temperatursensitivität und zeigte Hyperphosphorylierung von Histon H3. Diese Ergebnisse etablieren den Cdc48$^{\text{Shp1}}$-Komplex als einen kritischen Regulator der Glc7 Aktivität gegenüber Ipl1 Substraten.

Darüber hinaus wurden mögliche Mechanismen, durch welche Cdc48$^{\text{Shp1}}$ die Glc7 Aktivität reguliert, untersucht. Weder die Proteinmenge noch die Lokalisation von Glc7 waren in *shp1* verändert. Die Interaktion von Glc7 mit dessen Aktivator Glc8 war jedoch in *shp1* deutlich reduziert und die Überexpression von *GLC8* konnte partiell Phänotypen von *shp1* Mutanten retten. Dies legt nahe, dass Shp1 die Bindung von Glc8 an Glc7 kontrolliert und dadurch die Glc7 Aktivierung verstärkt, möglicherweise indem es die nukleäre Lokalisation von Glc8 vermittelt.

2. Introduction

2.1 The Ubiquitin Proteasome System (UPS)

The ubiquitin proteasome system (UPS) is the major system for regulated, selective protein degradation in eukaryotes (Ravid and Hochstrasser, 2008). Short lived proteins, such as cell cycle regulators and misfolded polypeptides, are covalently marked with the small molecule ubiquitin and subsequently degraded by the 26S proteasome (Finley, 2009). However, not every modification with ubiquitin leads to degradation of the target protein. On the contrary, ubiquitin serves as non-proteolytic signal in diverse cellular processes such as endocytosis, intracellular trafficking, DNA repair, histone modification, and regulation of transcription (Pickart and Fushman, 2004; Mukhopadhyay and Riezman, 2007).

2.1.1 Ubiquitin conjugation

Ubiquitin is a small, 76 residue protein, which is highly conserved among all eukaryotes. During a posttranslational process termed ubiquitination or ubiquitinylation the C-terminus of ubiquitin is covalently bound to ε-amino groups of target protein lysine residues via an isopeptide bond, or in case of N-terminal ubiquitination to the α-amino group of the substrate (Ciechanover and Ben-Saadon, 2004; Pickart and Eddins, 2004). The conjugation of ubiquitin to substrates occurs in three sequential steps: ubiquitin activation catalyzed by an E1 enzyme, the transfer of ubiquitin to an E2 conjugating enzyme, and finally conjugation of ubiquitin to the substrate mediated by an E3 ubiquitin ligase (*Fig. 1*).

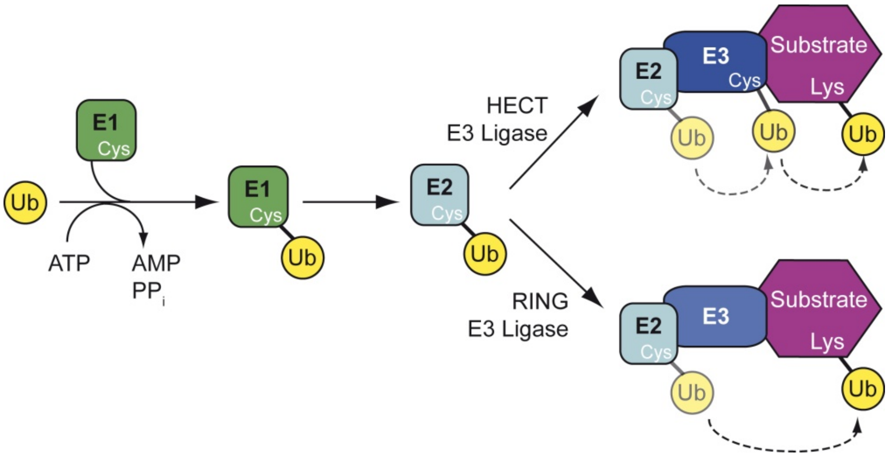

Fig. 1. **The ubiquitin conjugation system.** The catalytic site cysteine of the E1 ubiquitin activating enzyme (green) forms a thioester bond with the C-terminus of ubiquitin in an ATP hydrolyzing reaction. The activated ubiquitin is then transferred to an E2 conjugating enzyme (light blue), where it is again thiol-linked to the catalytic site cysteine. Depending on the type of E3 ligase (blue) present, ubiquitin is either transferred to the E3 catalytic cysteine (HECT ligases) and then to the substrate (purple) lysine residue or, in case of RING E3 ligases, directly transferred from the E2 to the substrate, while the ligase serves as a scaffold. (Adapted from (Ravid and Hochstrasser, 2008))

In most organisms, including yeast and mammals, a single E1 enzyme activates the C-terminus of ubiquitin. During this process of activation, a ubiquitin-AMP intermediate is formed first, and ubiquitin is then transferred to the active site cysteine of the E1 enzyme. Subsequently the thiol-linked ubiquitin is passed to the active site cysteine of an E2 ubiquitin conjugating enzyme. Covalent ligation of ubiquitin to the large number of highly diverse substrates is mediated by numerous E3 ligases, which, in combination with the E2s, control substrate specificity (Pickart, 2001; Pickart and Eddins, 2004).

Three protein families of E3 ubiquitin ligases have been described: HECT (Homologous to E6AP Carboxy Terminus), RING (Really Interesting New Gene), and U-box (UFD2 homology) ligases. RING and U-box E3s mediate ubiquitin ligation by acting as a bridging factor, whereas HECT ubiquitin ligases themselves form a thiol ester intermediate with ubiquitin prior to conjugation to the substrate (*Fig. 1*) (Pickart and Eddins, 2004). In some cases additional U-box containing E4s, such as Ufd2, are required for polyubiquitination of a substrate by extending a pre-existing ubiquitin chain (Koegl et al., 1999).

A target protein can be modified on a single or multiple lysine residues by one or more ubiquitin moieties. The fate of the substrate is determined by ubiquitin chain length and linkage type (Amerik and Hochstrasser, 2004). In *S. cerevisiae* all seven lysines (K6, K11, K27, K29, K33, K48, K63) of ubiquitin allow the formation of different isopeptide linkages (*Fig. 2*), catalyzed by specific E2- E3 combinations that dictate the chain type (Peng et al., 2003).

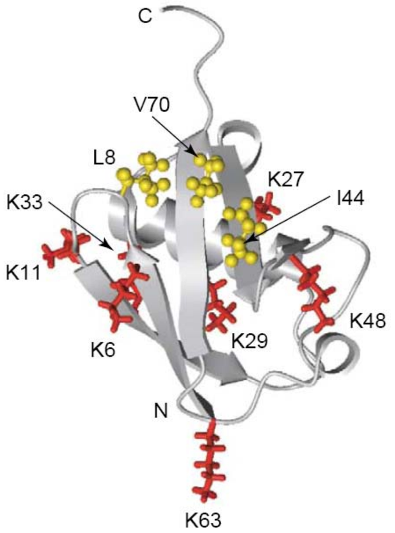

Fig. 2. **Lysine residues of ubiquitin used for conjugation.** Ribbon diagram of ubiquitin and its lysines residues used for chain formation (shown in red). The L8-I44-V70 hydrophobic patch, which mediates interaction of ubiquitin with other factors, is depicted in yellow. (From (Pickart and Fushman, 2004))

Most abundant are K11, K48, and K63 ubiquitin linkages, while K48 has been shown to be essential for viability of yeast (Finley et al., 1994; Peng et al., 2003). Polyubiquitination with more than four K48-linked ubiquitin moieties is thought to mark substrates for degradation by the 26S proteasome, while K63 linkages were shown to act as non-proteolytic signals in several cellular pathways such as DNA repair (Pickart and Fushman, 2004). Recently, it has been demonstrated that all ubiquitin linkages with the exception of K63 are increased upon proteasome inhibition and may therefore target substrates to proteasomal degradation (Xu et al., 2009). Conversely, it has also been found that K48 linkages can serve as non-proteolytic signals, as is the case during repression of the transcription factor Met4 (Flick et al., 2004; Li and Ye, 2008).

Attachment of a single ubiquitin moiety to one or more lysine residues of a target protein, termed monoubiquitination, serves as a non-proteolytic signal in cellular pathways such as endocytosis and regulation of gene expression by histone modification (Hicke, 2001).

Recently, linear polyubiquitin chains have been identified in higher eukaryotes. These chains are formed by conjugation of the C-terminal glycine of one ubiquitin to the α-amino group of the N-terminal methionine of the next ubiquitin. Such linear ubiquitin chains are generated by a ubiquitin ligase complex named LUBAC (linear ubiquitin chain assembly complex) and are involved in canonical NF-κB activation (Iwai and Tokunaga, 2009).

Ubiquitin or ubiquitin chains can be removed by specific deubiquitinating enzymes (DUBs), making ubiquitination a transient and reversible posttranslational modification. In addition to removing conjugated ubiquitin from substrates, DUBs are also necessary to activate ubiquitin, as it is synthesized as an inactive precursor, either as a fusion with certain ribosomal proteins or as head-to-tail fusions of multiple ubiquitins (Amerik and Hochstrasser, 2004).

2.1.2 The 26S proteasome and degradation

The eukaryotic 26S proteasome is a large 2.5 MDa protein complex that sequesters proteolytic sites to the inside of a barrel shaped structure and is therefore also considered to be a chambered protease. Cellular substrates which have been covalently marked with ubiquitin are degraded by the 26S proteasome, which itself consists of the 20S core and two 19S regulatory particles (Pickart and Cohen, 2004; Finley, 2009).

The 20S core particle (CP) is a stack of four heteroheptameric rings $\alpha_7\beta_7\beta'_7\alpha'_7$. Three of the seven β-subunits of each inner ring are catalytically active. A 19S regulatory particle is attached to both ends of the core, itself composed of base and lid. The 19S regulatory particle is responsible for recognizing ubiquitinated substrates, unfolding them, removing the ubiquitin chains, opening the gates of the 20S proteasome, and finally moving the substrates into the proteolytic chamber for degradation (Finley, 2009).

Recognition of the ubiquitinated substrates in yeast is mediated by Rpn10 and Rpn13, two components of the regulatory particle (Wolf and Hilt, 2004; Finley, 2009). Prior to degradation substrates are deubiquitinated and ubiquitin is recycled. Rpn11, a component of the lid, has DUB activity and is critical for proteasome function by coupling deubiquitination to early steps in degradation (Finley, 2009).

Proteasomal degradation of selectively ubiquitinated proteins enables the periodic fluctuation of certain regulators during temporal cellular processes such as cell division. Progression through the eukaryotic cell cycle requires the interdependent regulation of protein phosphorylation, transcription, and ubiquitin-proteasome-mediated degradation of cell cycle regulators, such as cyclins and Cdk1 inhibitors.

2.2 The yeast cell cycle

The eukaryotic cell cycle can be divided into four main phases: G1, S, G2, and mitosis (M), whereas the most prominent events are DNA replication in S-phase and chromosome segregation during mitosis. G1 and G2 are the gap phases needed to prepare these two major events in cell division. During the yeast G1 phase nutrient conditions and cell size are monitored and in late G1 phase START (equivalent to mammalian restriction point) marks the point after which entry into the new cell cycle is irreversible and bud growth begins (*Fig. 3*).

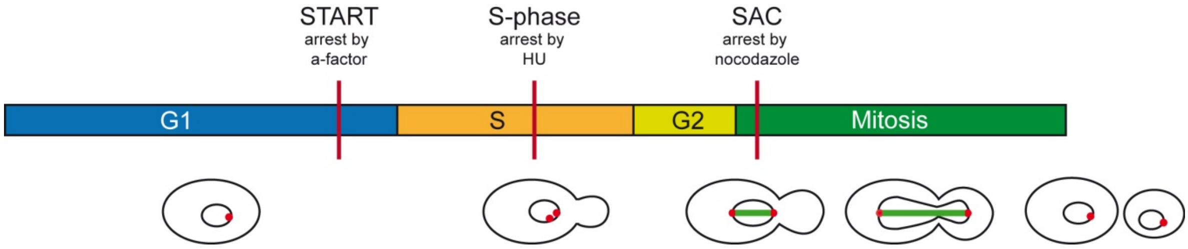

***Fig. 3.* Schematic overview of the yeast cell cycle.** The four cell cycle phases G1 (blue), S (orange), G2 (yellow), and mitosis (green) are depicted according to their approximate duration in an unperturbed WT yeast cell cycle. Three checkpoints that can be targeted are shown. START controls exit from G1 and can be prevented by addition of the mating pheromone α-factor to Mat a yeast cells. The S-phase checkpoint is activated in response to hydroxyurea (HU), while addition of the spindle depolymerizing agent nocodazole leads to activation of the spindle assembly checkpoint (SAC) and cell cycle arrest in mitosis. Schematic drawings of yeast show approximate bud growth, SPB duplication (red) as well as lengths of the mitotic spindle (green) in the corresponding cell cycle stages.

Progression through the cell cycle is controlled by cyclin dependent kinases (Cdks). The activity of these serine/threonine kinases is mainly regulated by the binding of different cyclins (Bloom and Cross, 2007). Cyclin expression and protein levels fluctuate periodically and thereby modulate Cdk activity during cell cycle progression. The best studied Cdk and central regulator of the budding yeast cell cycle is the essential protein Cdc28 (Cdk1) (Hartwell et al., 1974; Mendenhall and Hodge, 1998).
Two groups of cyclins have been classified: the G1 and the B-type cyclins. The G1 cyclins Cln1-Cln3 mainly regulate Cdc28 activity during G1, which involves passage through START, bud emergence, spindle pole body (SPB) duplication, and activation of later cyclins (Bloom and Cross, 2007) (*Fig. 3*). Six B-type cyclins, Clb1-6, are expressed in three waves from START to mitosis (Mendenhall and Hodge, 1998). Clb5 and Clb6 are the earliest and mediate DNA replication and S-phase, whereas Clb1-4 are required for the later mitotic events (Bloom and Cross, 2007).

Protein levels of all cyclins are controlled by ubiquitin-proteasome-dependent degradation. Two multi-subunit RING E3 ligases dominate cell cycle regulation: the SCF (Skp1 Cdc53/ Cullin F-box) and the APC/C (anaphase promoting complex/ cyclosome). Both ligases are modular assemblies consisting of a constitutive core complex and variable substrate binding subunits (Deshaies and Joazeiro, 2009). Different SCF complexes are active throughout the cell cycle and catalyze, mostly phospho-degron dependent, ubiquitination and degradation of a number of substrates, including G1 cyclins and the Cdk1 inhibitor Sic1 (van Leuken et al., 2008). Substrate recruitment of SCF complexes is mediated by different F-box proteins, for example Cdc4 and Grr1 (Deshaies and Joazeiro, 2009). Degradation of the cyclins Cln1 and Cln2 is mediated by SCF^{Grr1}, Clb6 by SCF^{Cdc4} (Bloom and Cross, 2007). The activity of the APC/C on the other hand is restricted to the time between anaphase onset and the end of G1, regulating the degradation of all mitotic cyclins except Clb6, anaphase inhibitors, components of the mitotic spindle, and the APC/C activator Cdc20 (Bloom and Cross, 2007; van Leuken et al., 2008). APC/C activity is in part regulated by binding of either of the two activating subunits Cdc20 and Cdh1, which enhance substrate recognition. APC/C^{Cdc20} controls the metaphase to anaphase transition, while binding of Cdh1 to the APC/C regulates mitotic exit and degradation in G1. Ama1 was described as a third APC/C activator which is only expressed during yeast sporulation (van Leuken et al., 2008).

In addition to cyclin binding, Cdc28 activity is regulated through interaction with inhibitors and by phosphorylation (Mendenhall and Hodge, 1998). Specific Cdk-cyclin complexes are controlled by certain stoichiometric inhibitors, such as Sic1, which blocks activity of Cdc28-Clb, but not Cdc28-Cln complexes (Schwob et al., 1994). Similar to cyclins, Sic1 protein levels are also regulated by ubiquitin-dependent degradation. Cdc28-Cln2 phosphorylates Sic1 in G1, leading to recognition and degradation mediated by SCF^{Cdc4} (Feldman et al., 1997; Skowyra et al., 1997). The Cdc28-Cln inhibitor Far1 mediates a G1 cell cycle arrest in response to the mating pheromone α-factor and is itself also regulated by SCF-dependent degradation (Bloom and Cross, 2007).
Cdc28 is phosphorylated throughout the mitotic cell cycle at residue T169 by Cak1, resulting in its activation (Ross et al., 2000). The morphogenesis checkpoint triggers Swe1 phosphorylation of Cdc28 at residue Y19, which in turn inhibits Cdc28-Clb2 activity during S and G2 and thereby delays entry into mitosis if cells have not formed a bud (Mendenhall and Hodge, 1998; Bloom and Cross, 2007).

2.2.1 Mitosis

Accurate distribution of the replicated genome during cell division is essential for viability and depends on proper chromosome segregation. During mitosis two physically connected sister chromatids must be faithfully segregated to mother and daughter cell, an event controlled by the spindle assembly checkpoint (SAC). After replication of DNA in S-phase, the two sister chromatids are physically connected through cohesin (Scc1). This state is maintained until every chromosome is condensed, aligned, and attached to the mitotic spindle. Attachment to the mitotic spindle occurs by binding of kinetochores to microtubules of the mitotic spindle (*Fig. 4a*). Once all chromosomes are properly attached, the SAC is resolved and chromatid cohesion is removed, enabling chromatid segregation to opposite poles of the mitotic spindle. In late anaphase the nucleus passes the bud neck, and the mitotic exit network (MEN) is activated. This process eventually leads to the release of the phosphatase Cdc14 from the nucleolus, resulting in its activation and dephosphorylation of critical targets needed for the exit from mitosis. Once mitosis is completed the cell undergoes cytokinesis and mother and daughter re-enter G1 (Mendenhall and Hodge, 1998; Lew and Burke, 2003; Bloom and Cross, 2007; Musacchio and Salmon, 2007).

2.2.1.1 The spindle assembly checkpoint (SAC)

In order for the yeast metaphase to anaphase transition to occur each kinetochore is required to attach to a single microtubule of the mitotic spindle (Winey et al., 1995). The attachment branch of the spindle assembly checkpoint is satisfied once both kinetochores of all chromosomes have bound to one microtubule. Additionally, it must be ensured that the two chromatids are pulled to opposite poles of the mitotic spindle. Thus, a second part of the SAC senses tension. Sufficient tension across the two chromatids is only created if the two kinetochores are attached to opposite poles of the mitotic spindle (Musacchio and Salmon, 2007). The SAC prevents anaphase onset until all chromosomes have achieved correct bi-polar attachment (*Fig. 4*).

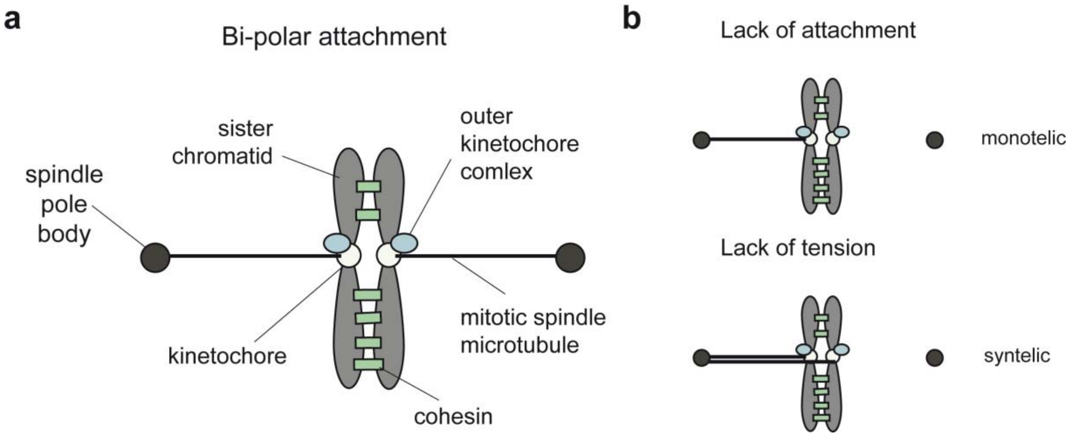

Fig. 4. **Chromosome bi-orientation during metaphase**. a) Proper Chromosome bi-orientation, each kinetochore is attached to one opposite SPB and sister chromatids are tightly linked by cohesin (Scc1). b) The spindle checkpoint can detect monotelic and syntelic attachments. Lack of attachment is sensed if only one kinetochore of either of the two sister chromatids is bound to microtubules. If both kinetochores are attached to the same SPB (syntelic attachment) the SAC senses lack of tension and also triggers a cell cycle arrest. (Adapted from (Musacchio and Salmon, 2007))

If proper bi-polar attachment is not achieved, the SAC is activated and delays or prevents chromosome segregation by keeping the E3 ubiquitin ligase APC/C^{Cdc20} inactive. This prevents APC/C mediated polyubiquitination and subsequent degradation of the two key mitotic substrates Clb2 and Pds1 (Hwang et al., 1998; Kim et al., 1998). Pds1 (securin) is the inhibitor of the cellular protease separase (Esp1), which cleaves the cohesin (Scc1) complex and enables sister chromatid separation (Uhlmann et al., 1999; Nasmyth et al., 2000). By stabilization of the mitotic cyclin Clb2, Cdc28 remains active and mitotic exit is prevented (*Fig. 5*) (Musacchio and Salmon, 2007).

The exact molecular mechanism by which the SAC senses improper chromosome orientation and sends a “wait anaphase” signal that inhibits the APC/C and prevents anaphase onset is still not completely resolved. Genes involved in spindle checkpoint signaling were first identified in yeast screens for mutants unable to arrest mitosis in the presence of the microtubule depolymerizing agents nocodazole and benomyl. The genes *MAD1* (mitotic arrest deficient), *MAD2*, and *MAD3* as well as *BUB1* (budding uninhibited by benomyl), *BUB2*, and *BUB3* were identified in these studies (Hoyt et al., 1991; Li and Murray, 1991). They were then shown to be involved in a pathway preventing premature sister chromatid separation conserved in all eukaryotes (Skibbens and Hieter, 1998).

In addition to the *BUB* and *MAD* genes, the kinase Mps1 was shown to be required for a SAC induced cell cycle arrest (Weiss and Winey, 1996). *MPS1* overexpression causes a constitutive checkpoint arrest dependent on the other SAC components (Hardwick et al., 1996), while *mps1* mutants are checkpoint deficient in response to spindle depolymerization (Weiss and Winey, 1996). One described Mps1 target in spindle checkpoint signaling is Mad1, which is hyperphosphorylated upon checkpoint activation (Hardwick and Murray, 1995).

Mad2 is the central component of the spindle assembly checkpoint and can bind and partially inhibit the APC/C^{Cdc20} until proper chromosome attachment has been achieved. For complete inhibition, however, a complex termed yeast mitotic checkpoint complex (MCC) is required. This complex is composed of the SAC proteins Mad2, Mad3, Bub3, and Cdc20 (Zich and Hardwick, 2010). Additional checkpoint components are Mad1, Bub1 and the kinases Mps1 and Ipl1. Mps1 and Mad1 are required for the interaction of Mad2 with Cdc20 (*Fig. 5a*). The binding of Bub3 and Mad3 to Mad2-Cdc20 completes the MCC, which then fully inhibits the APC/C (*Fig. 5a*). Once the checkpoint is satisfied, the MCC dissociates and Cdc20 activates the APC/C. The active APC/C^{Cdc20} E3 ligase then ubiquitinates Pds1 and Clb2, which results in their degradation by the 26 S proteasome (*Fig. 5b*). This enables sister chromatid segregation and reduces Cdk1 kinase activity (Bloom and Cross, 2007; Musacchio and Salmon, 2007).

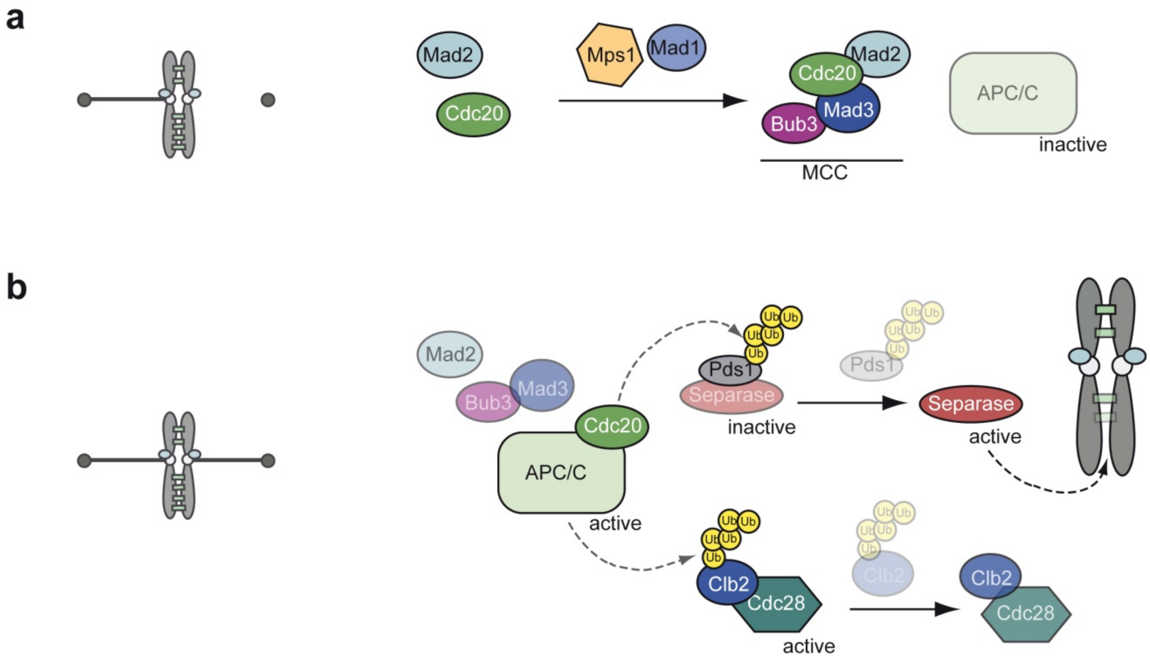

Fig. 5. **Key steps in SAC signaling that lead to APC/C^{Cdc20} activation and anaphase onset.** a) If chromosomes are not properly attached the APC/C is kept inactive by the MCC (mitotic checkpoint complex) containing Mad2, Mad3, Bub3, and Cdc20. Binding of Mad2 to Cdc20 and following formation of the MCC depends on Mps1 and Mad1. b) Once proper bi-orientation is achieved Cdc20 binds and activates the APC/C. Pds1 and Clb2 are ubiquitinated and degraded. Degradation of Pds1 activates the protease separase which cleaves cohesin enabling sister chromatid separation. APC/C^{Cdc20} degrades only part of the mitotic cyclin Clb2, therefore Cdk1 activity is reduced, but not abolished upon metaphase to anaphase transition. (Adapted from (Musacchio and Salmon, 2007))

Most components of the SAC are linked to kinetochores, which are thought to be the source of the majority of checkpoint signals (Bloom and Cross, 2007; Musacchio and Salmon, 2007). If kinetochores lack attachment, binding of the Mad1-Mad2 heterodimer leads to formation of “active” Mad2, which is thought to be a major determinant for MCC assembly. (Musacchio and Salmon, 2007; Zich and Hardwick, 2010). Mad1 and Mad2 are removed directly after attachment has occurred and consequently, the localization of the two proteins can be used as a marker for unattached kinetochores in vertebrates (Skibbens and Hieter, 1998).

In addition to sensing attachment, tension must also be monitored. If both chromatids are connected to the same pole (syntelic attachment, *Fig. 4b*) not enough tension is generated and the checkpoint is activated. This ensures the correct bi-polar attachment of chromosomes and ultimately equal distribution of chromosomes to mother and daughter cell.

The yeast chromosomal passenger complex (CPC), consistent of Ipl1 (the only yeast Aurora kinase), Sli15 (INCENP), Bir1 (survivin), and Nbl1 (borealin), has been shown to promote proper chromosome segregation and, with the exception of Nbl1, to be required for activation of the SAC in response to lack of tension (Biggins and Murray, 2001; Makrantoni and Stark, 2009; Nakajima et al., 2009). Consistent with the inability to activate the SAC in response to lack of tension, both *ipl1* and *sli15* mutants segregate chromosomes unequally due to increased syntelic attachments, while DNA replication, SPB duplication, spindle formation, and cytokinesis are unaffected (Biggins et al., 1999; Kim et al., 1999; Tanaka et al., 2002). *bir1* and *nbl1* mutants also display chromosome missegregation, albeit less severely than *ipl1* or *sli1* (Makrantoni and Stark, 2009; Nakajima et al., 2009).

Ipl1 is required for spindle checkpoint activation in response to lack of tension and has been proposed to activate the SAC by creating unattached kinetochores (Pinsky et al., 2006b). Proper tension occurring from attachment of the two chromatids to opposite poles is presumably sensed by kinetochore proteins. Additionally, kinetochore proteins bind spindle microtubules in a phosphorylation dependent manner (Cheeseman et al., 2002). Consequently, it has been demonstrated that Ipl1 phosphorylates the kinetochore protein Ndc10 *in vitro* (Biggins et al., 1999). In addition to Ndc10, Sli15 and Dam1 have been described as Ipl1 substrates at the kinetochore (Kang et al., 2001). Further mapping of phosphorylation sites within kinetochore proteins revealed additional putative Ipl1 targets, and the outer kinetochore protein Dam1 was identified as a critical downstream target of Ipl1 that regulates kinetochore microtubule attachments (Cheeseman et al., 2002). Phosphorylation of Dam1 by Ipl1 inhibits the kinetochore-microtubule interaction, thereby creating unattached kinetochores (Cheeseman et al., 2002). These unattached kinetochores are thought to result in spindle checkpoint activation (Pinsky et al., 2006b).

Moreover, it has been demonstrated that phosphorylation of the kinetochore component Ndc80 by Mps1 is also required for proper spindle checkpoint signaling. A phospho-mimicking mutant of Ndc80, in which 14 serines have been mutated to aspartate, is inviable dependent on the SAC. The alanine mutant, in turn, is checkpoint deficient and does not arrest after nocodazole treatment (Kemmler et al., 2009). Furthermore, it has been shown that Mps1 phosphorylates Dam1, however, in contrast to the

Ipl1 mediated phosphorylation, modification by Mps1 appears to be required for kinetochore-microtubule attachment (Shimogawa et al., 2006).

These findings demonstrate that the phosphorylation state of kinetochore proteins is critical for SAC signaling. Ipl1 activity is required for checkpoint activation in response to lack of tension (Biggins and Murray, 2001), while Mps1 mediated phosphorylation of Ndc80 is also required for SAC signaling upon spindle depolymerization and therefore lack of attachment (Kemmler et al., 2009). Additionally, Ipl1 phosphorylates Mad3 to further enhance the checkpoint delay (King et al., 2007).

Histone H3 was furthermore demonstrated to be a mitotic substrate of Ipl1 (Hsu et al., 2000). Mitotic phosphorylation of histone H3 at serine ten is conserved among eukaryotes and peaks when chromosomes are most condensed. However, in budding yeast a S10A mutation of histone H3 does not have a significant cell cycle or growth defect, suggesting a more complex regulation of chromosome congression and cell cycle progression (Hsu et al., 2000).

Ipl1 mediated phosphorylation of Ndc10, histone H3, and Dam1 has been proposed to be counteracted by the phosphatase PP1/Glc7 (see 2.4.2) (Sassoon et al., 1999; Hsu et al., 2000; Kang et al., 2001; Cheeseman et al., 2002; Pinsky et al., 2006a).

2.2.1.2 Mitotic exit

Once the spindle checkpoint is satisfied and chromosome separation has occurred, mitotic Cdk1 activity must be inactivated in order for cells to exit mitosis and undergo cytokinesis. In yeast inactivation of this activity is not completed at metaphase to anaphase transition, but is delayed until spindle elongation has occurred (Bardin and Amon, 2001). Degradation of mitotic cyclins as well as stabilization of the inhibitor Sic1 leads to Cdc28-Clb inactivation. The phosphatase Cdc14 is essential for this process and is the effector of a cascade of events called the mitotic exit network (MEN). During most of the cell cycle Cdc14 is bound to Net1 and sequestered in the nucleolus (Bloom and Cross, 2007). In addition to Cdc14, the network comprises the protein kinases Cdc15, Dbf2, Dbf20, the GTP-binding protein Tem1, a putative GEF (guanine nucleotide exchange factor) Lte1, a GTPase activating complex (GAP) consistent of Bfa1 and Bub2, and Mob1, which binds Dbf2/Dbf20 (Dumitrescu and Saunders, 2002).

The mitotic exit network is activated by Tem1-GTP in late anaphase. Active Tem1 triggers a signaling cascade starting with the activation of Cdc15 kinase, which activates Dbf2/Mob1, and in turn leads to activation and release of Cdc14 from the nucleolus (Hoyt, 2000). Cdc14 dephosphorylates and activates the Cdk1 inhibitor Sic1, the *SIC1* transcription factor Swi5, and the APC/C activator Cdh1, all resulting in inhibition of Cdc28-Clb activity (*Fig. 6*) (Sullivan and Morgan, 2007).

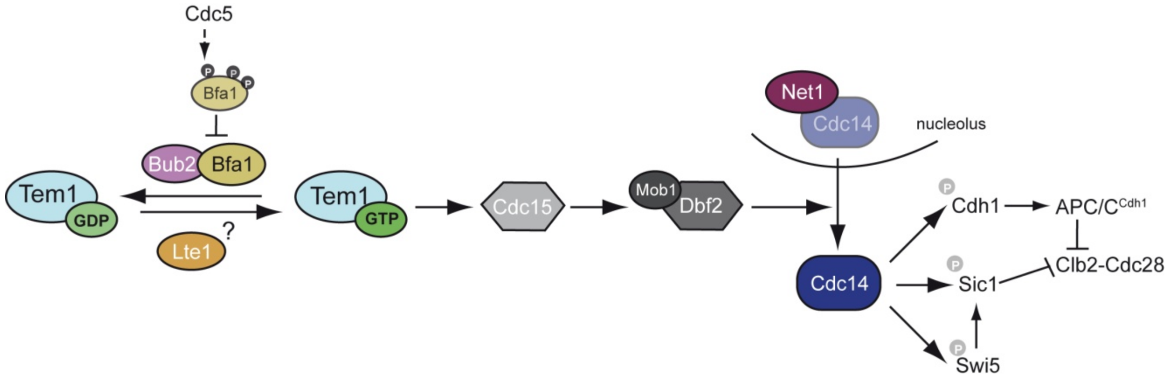

***Fig. 6.* The mitotic exit network (MEN).** Tem1-GDP is kept in this inactive state by the GAP (GTPase activating protein) Bub2-Bfa1. Bub2-Bfa1 can be inhibited by phosphorylation of Bfa1, presumably by Cdc5. Activation of Tem1-GDP to Tem1-GTP may occur through interaction with the GEF (guanine nucleotide exchange factor) Lte1 (see text). Active Tem1-GTP activates the downstream kinases Cdc15 and Dbf2/Mob1 which lead to activation and release of Cdc14. The phosphatase Cdc14 is sequestered in the nucleolus by Net1 during most of the cell cycle. Once it is released it dephosphorylates key targets needed for mitotic exit. By Swi5 dephosphorylation the transcription factor is stabilized and promotes *SIC1* transcription. Additionally, Sic1 is itself stabilized by dephosphorylation and then inhibits Cdc28-Clb2 activity. Cdh1 activates the APC/C and leads to degradation of the remaining mitotic cyclin Clb2, also resulting in inhibition of Cdc28. (Adapted from (Dumitrescu and Saunders, 2002; Lew and Burke, 2003))

Mitotic exit is controlled by the spindle position checkpoint. This branch of the spindle checkpoint ensures that the mitotic spindle is oriented along the mother-bud axis and thereby prevents cytokinesis as long as both sets of chromosomes remain in the mother cell (Lew and Burke, 2003).
During most of the cell cycle Tem1 is kept in its inactive GDP-bound state by the GAP Bub2-Bfa1 (Dumitrescu and Saunders, 2002). Most MEN components display an asymmetric localization that is required for proper mitotic exit to occur. The Bub2-Bfa1 complex localizes only to the daughter-bound SPB during anaphase and recruits Tem1 (Lew and Burke, 2003). How exactly Tem1 is then activated and mitotic exit triggered is considerably unclear. One mechanism proposed is that the position of the nucleus is sensed. The putative GEF Lte1 is localized to the bud cortex and once the nucleus passes the bud neck SPB localized Tem1 could be activated by its GEF. However, Lte1 only becomes essential at cold temperatures and the deletion mutant does not display any significant cell cycle defect at room temperature (Bardin and Amon, 2001). Furthermore, it has been reported that Lte1 does not have GEF activity for Tem1 *in vitro* and thus proposed that Lte1 is rather required for asymmetric localization of Bfa1 to the daughter SPB (Geymonat et al., 2009). Therefore, it is conceivable that Cdc14 release and Tem1 activation are regulated by an additional mechanism (Bardin and Amon, 2001).
Bfa1 and Bub2 are hyperphosphorylated and inactive in late anaphase, which allows activation of the mitotic exit network. Spindle misorientation prevents the phosphorylation of Bfa1 and thereby inhibits mitotic exit, as Tem1 is retained in its inactive GDP-bound state (Lew and Burke, 2003). The yeast Polo-like kinase Cdc5 is thought to be responsible for Bfa1 phosphorylation (Dumitrescu and Saunders, 2002; Lew and Burke, 2003).

In addition to MEN a second network already transiently releases Cdc14 from the nucleolus in early anaphase. The FEAR (Cdc14 fourteen early anaphase release) network allows stabilization of the mitotic spindle, segregation of ribosomal DNA, and activation of MEN (Bloom and Cross, 2007). Cdc14 release caused by the FEAR network is nevertheless not sufficient for cells to exit mitosis (Bloom and Cross, 2007).

2.3 The AAA ATPase Cdc48/p97

Budding yeast *CDC48* (cell division cycle 48) was initially identified in a genetic screen for cold-sensitive (cs) cell cycle alleles. The original cs allele, *cdc48-1*, was found to arrest with large buds, an undivided nucleus, and aberrant microtubules spreading from an unseparated spindle pole body at the non-permissive temperature (Moir et al., 1982; Frohlich et al., 1991). Four additionally identified cs-revertants that exhibit temperature sensitivity, also arrest with large buds at the non-permissive temperature of 37°C (Moir et al., 1982).

In addition to the early mitotic phenotype described in the initial screen, additional functions of Cdc48 during the cell cycle have been reported. The degradation of the G1 SCF substrates Far1 and Cln2 is dependent on Cdc48 (Fu et al., 2003; Archambault et al., 2004). Cao *et. al*. claim that Cdc48$^{\mathrm{Ufd1\text{-}Npl4}}$ is required for spindle disassembly after mitosis, possibly by mediating Cdc5 and Ase1 degradation (Cao et al., 2003). However, these results have been questioned (Heubes and Stemmann, 2007), and no further evidence for a role of Cdc48 in spindle disassembly has been brought forward. Interestingly, in *C. elegans* Cdc48$^{\mathrm{Ufd1\text{-}Npl4}}$ was shown to be required for efficient DNA replication and thereby for cell cycle progression through S-phase (Mouysset et al., 2008). Fission yeast Cdc48, in turn, has been demonstrated to be required for the stability of Cut1 (separase) and therefore necessary for proper sister chromatid separation (Ikai and Yanagida, 2006). Furthermore, p97$^{\mathrm{Ufd1\text{-}Npl4}}$ is essential for nuclear envelope formation after mitosis (Hetzer et al., 2001; Ramadan et al., 2007). Active Aurora B kinase is ubiquitinated, bound by p97$^{\mathrm{Ufd1\text{-}Npl4}}$, and extracted from chromatin allowing chromosome decondensation and nuclear envelope reassembly. Thus, Cdc48 fulfills more than one essential function during the cell cycle, which can either result in G1 or mitotic defects upon depletion or mutation. These diverse functions are possibly regulated by interaction with different sets of cofactors.

The protein Cdc48/p97/VCP (Valosin containing protein) was characterized as an essential, highly conserved AAA ATPase (ATPases associated with various cellular activities), which is involved in a large variety of ubiquitin related cellular processes. Common to all these processes appears to be a “segregase” activity of Cdc48, during which energy derived from ATP hydrolysis is used to extract ubiquitinated proteins from protein complexes or cellular structures (Rape et al., 2001; Braun et al., 2002; Buchberger, 2006; Jentsch and Rumpf, 2007; Buchberger, 2010).

AAA proteins function in a vast number of different cellular processes. Common to all members of this family is the AAA domain, a 200- 250 amino acid ATPase module, which contains Walker-A and –B motifs as well as other conserved elements, most prominent the second region of homology (SRH). Additionally, all AAA proteins assemble into oligomers, often hexamers, and function in structural remodeling, unfolding, and disassembly of macromolecular complexes (Lupas and Martin, 2002; Hanson and Whiteheart, 2005).

Cdc48/p97 is assembled into a homohexameric ring, each monomer composed of an N-terminal domain, followed by two ATPase domains, D1 and D2, and an unstructured C-terminus (*Fig. 7*) (Hanson and Whiteheart, 2005; Buchberger, 2006). Specificity in different processes is conveyed through interaction with numerous cofactors (Buchberger, 2006; Jentsch and Rumpf, 2007; Buchberger, 2010).

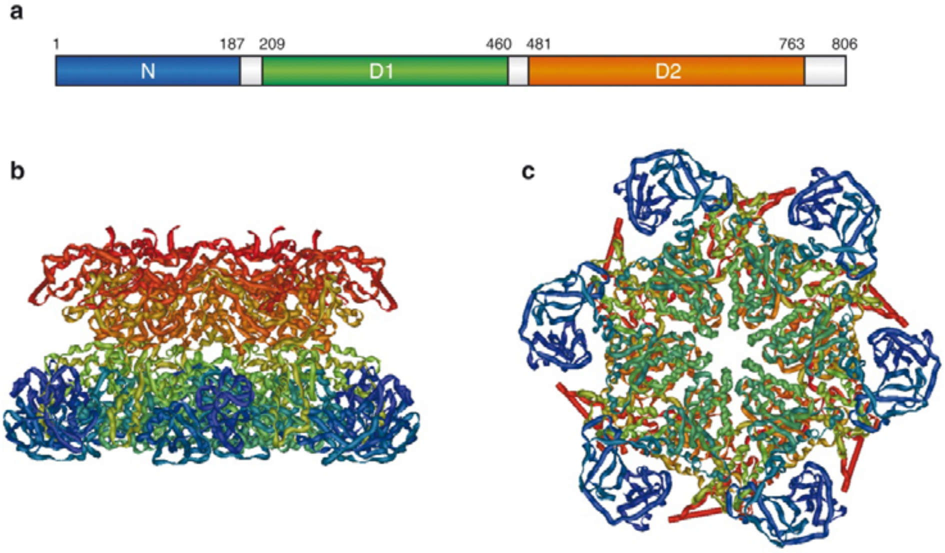

***Fig. 7.* Structure of the AAA ATPase Cdc48.** a) Schematic overview of the domain architecture of Cdc48; the N-domain (blue) is followed by the two ATPase domains D1 (green), and D2 (orange). b) Sideward view of a Cdc48 hexamer (colors as in a) c) View through the central pore (colors as in a). (From (Buchberger, 2006))

Cdc48/p97 cofactors can be divided into two groups: substrate-processing and substrate-recruiting (Jentsch and Rumpf, 2007). Substrate-processing cofactors either directly alter the ubiquitination state of the bound substrate or modify the substrate by other means, such as deglycosylation by peptidyl-N-glycanase (PNGase). The substrate-processing cofactors Ufd2 and Ufd3 bind to the C-terminus of Cdc48 in mutually exclusive manner and antagonistically regulate substrate ubiquitination (Rumpf and Jentsch, 2006; Böhm et al., 2011). The E4 Ufd2 elongates pre-existing ubiquitin chains, whereas Ufd3 cooperates with the DUB Otu1 in antagonizing substrate ubiquitination (Rumpf and Jentsch, 2006).

The two most prominent and mutually exclusive substrate-recruiting cofactors are the heterodimeric Ufd1-Npl4 complex and Shp1/p47. In addition to Cdc48/p97 binding domains, these cofactors possess specific ubiquitin binding modules, such as the UBA domain found in Shp1/p47 (Schuberth and Buchberger, 2008). Substrate-recruiting cofactors mediate the interaction of Cdc48 with substrates and direct Cdc48 to distinct cellular compartments.

The role of Cdc48$^{\text{Ufd1-Npl4}}$ has been clearly demonstrated in ER associated degradation (ERAD) (Ye et al., 2001; Braun et al., 2002; Jarosch et al., 2002; Neuber et al., 2005; Schuberth and Buchberger, 2005), the ubiquitin-fusion degradation (UFD) pathway (Johnson et al., 1995), as well as during mobilization of the membrane anchored transcription factor Spt23 (OLE pathway) (Rape et al., 2001). Additional cellular processes that require Cdc48 function are the mitochondrial stress response (Heo et al., 2010), transcriptional regulation (Wilcox and Laney, 2009), as well as the DNA damage response (Verma et al., 2011).

p97^{p47} has been demonstrated to mediate homotypic membrane fusion (Kondo et al., 1997; Rabouille et al., 1998; Uchiyama et al., 2002), while Cdc48^{Shp1} has been implicated in autophagy (Krick et al., 2010) and chromosome bi-orientation (Cheng and Chen, 2010). p47/Shp1 is a member of a large group of Cdc48 substrate-recruiting cofactors, the so called UBX-proteins.

2.3.1 UBX proteins

The ubiquitin regulatory X (UBX) domain is an 80 amino acid residue module, originally identified in the mammalian protein Y33K (Hofmann and Bucher, 1996). Structural comparison of the UBX domain with ubiquitin itself showed a close structural similarity despite the lack of significant sequence homology (*Fig. 8*) (Buchberger et al., 2001; Yuan et al., 2001). Due to the lack of a di-glycine motif at its C-terminus, the UBX domain is not conjugated like ubiquitin, but has rather proven to be a general Cdc48/p97 binding module (Buchberger et al., 2001; Yuan et al., 2001; Decottignies et al., 2004; Dreveny et al., 2004; Hartmann-Petersen et al., 2004; Schuberth et al., 2004). A conserved surface R…FPR motif, which is absent in ubiquitin and other ubiquitin-like proteins, was shown to mediate the interaction with the N-terminal domain of Cdc48/p97 (Buchberger et al., 2001; Yuan et al., 2001).

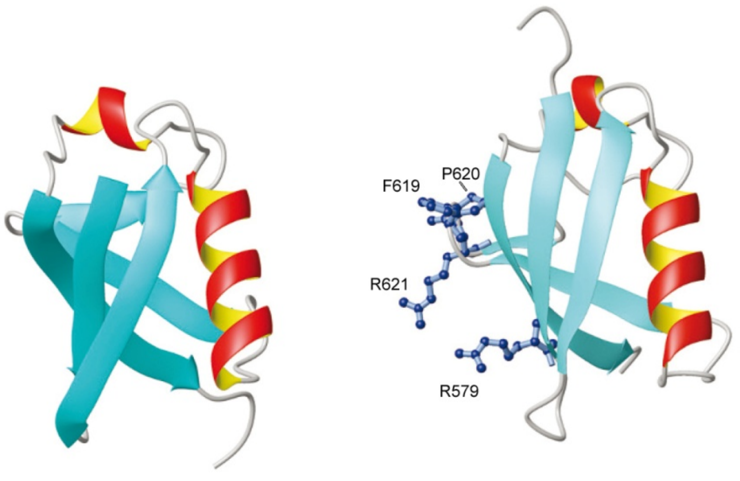

ubiquitin

UBX domain of FAF1

***Fig. 8.* Structural comparison of ubiquitin and the UBX domain.** Ribbon representation of the ubiquitin and tFAF1 UBX domain three-dimensional structure. Residues comprising the conserved p97/Cdc48 interaction motif R…FPR found in UBX domains are depicted in detail. (Modified, from (Schuberth and Buchberger, 2008))

UBX- or UBX-like proteins are the largest family of known Cdc48/p97 cofactors and can be subdivided into five larger groups: p47, FAF1, SAKS1, TUG, and UBXD1, as well as two smaller groups of proteins: Rep-8 and UBXD3 (Schuberth and Buchberger, 2008). In budding yeast seven UBX domain containing proteins have been identified: Shp1 and Ubx2- Ubx7 (*Fig. 9*). All seven proteins have been demonstrated to interact with Cdc48 (Schuberth et al., 2004; Schuberth, 2006). In addition to the Cdc48 binding UBX domain, some members of this group contain additional ubiquitin binding domains or motifs, such as the UBA domain found in Shp1, Ubx2, and Ubx5 (Schuberth and Buchberger, 2008).

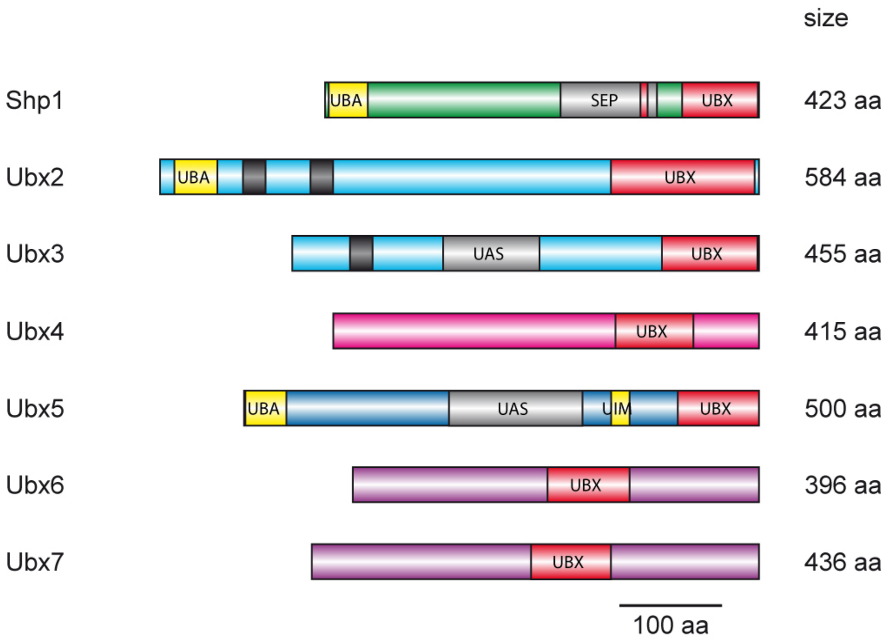

***Fig.9.* Overview of the domain structure of the seven *S. cerevisiae* UBX proteins.** All proteins contain the name-giving UBX-domain, which mediates Cdc48 interaction (shown in red). Ubiquitin binding domains UBA and UIM are depicted in yellow. The SEP domain of Shp1 and the UAS domains of Ubx3 and Ubx5 are shown in gray. (Modified, from (Schuberth and Buchberger, 2008))

It has been demonstrated that most yeast UBX proteins bind to either of the two mutually exclusive complexes of Cdc48, containing Ufd1-Npl4 or Shp1. Ubx6 and Ubx7 can be found in complex with Cdc48$^{\text{Shp1}}$, while Ubx2, Ubx3 and Ubx5 interact with Cdc48$^{\text{Ufd1-Npl4}}$ (Schuberth, 2006). The sub-complexes of Cdc48 are thought to mediate Cdc48 substrate specificity and recruitment to different cellular compartments (Schuberth, 2006; Schuberth and Buchberger, 2008).

The integral membrane protein Ubx2 recruits Cdc48$^{\text{Ufd1-Npl4}}$ to the ER and is required for stable binding of Cdc48$^{\text{Ufd1-Npl4}}$ to ERAD substrates and ligases. Deletion of *UBX2* leads to defects in degradation of all tested ERAD substrates (Neuber et al., 2005; Schuberth and Buchberger, 2005). Ubx4 has also been reported to modulate Cdc48 activity during ERAD (Alberts et al., 2009).

Ubx5, and to some extent Ubx4, in complex with Cdc48$^{\text{Ufd1-Npl4}}$ are involved in the UV-induced turnover of Rpb1, the largest subunit of RNA Pol II (Verma et al., 2011). The authors propose that upon DNA damage Rpb1 is ubiquitinated by Cul3, transferred to Cdc48$^{\text{Ubx5}}$, and then degraded by the proteasome directly on chromatin (Verma et al., 2011).

Although Ubx4 (Cui1), Ubx6 (Cui2), and Ubx7 (Cui3) have been implicated in meiosis (Decottignies et al., 2004), no substrate or interactor required for this process has so far been identified. Ubx3 may be localized to the Golgi and vesicles, therefore it has been speculated that it may play a role in vesicle trafficking (Schuberth, 2006).

2.3.2 Shp1/p47

Mammalian p47 (Shp1 in *S. cerevisiae)* was the first identified p97 interactor and was shown to tightly bind the p97 hexamer in form of a trimer (Kondo et al., 1997; Beuron et al., 2006). This conserved p97/Cdc48 adapter protein contains three domains separated by flexible regions, namely an N-terminal UBA, followed by the SEP (Shp1, eyc, p47), and a C-terminal UBX domain (*Fig. 10*) (Dreveny et al., 2004; Yuan et al., 2004a).

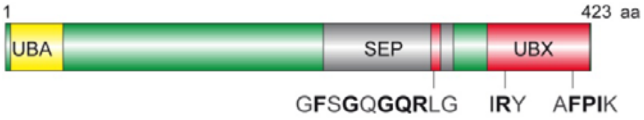

***Fig. 10.* Schematic overview of the Shp1 domain architecture.** The Cdc48 binding modules of Shp1, namely the UBX domain and BS1, are shown in red. Residues within these domains that mediate Cdc48 interaction are depicted in bold letters. The N-terminal UBA (ubiquitin associated domain) is depicted in yellow and the SEP (Shp1, Eyc, p47) domain, which mediates trimerization, in gray. (Modified, from (Schuberth and Buchberger, 2008))

The UBA domain comprises residues 1-45 of p47 and was shown to bind mono-ubiquitin and inhibit polyubiquitination *in vitro* (Meyer et al., 2002). Accordingly, the UBA domain of Shp1 was demonstrated to bind ubiquitin chains *in vitro* and ubiquitinated proteins *in vivo* (Schuberth et al., 2004). Residues 179–246 are spanned by the SEP domain, which is involved in p47 trimerization (Yuan et al., 2004b; Beuron et al., 2006). Both p47 and Shp1 bind to the p97 and Cdc48 N–domain, respectively. This interaction is mediated by (at least) two distinct binding sites in the C-terminus (Uchiyama et al., 2002), the UBX-domain and BS1 at the C-terminal end of the SEP domain (*Fig. 10*) (Bruderer et al., 2004; Dreveny et al., 2004). BS1 (also called SHP box) is a short linear hydrophobic binding motif for p97/Cdc48, which is also found in Ufd1 and other proteins implicated in the UPS (Bruderer et al., 2004; Hitt and Wolf, 2004; Sato and Hampton, 2006).

The $p97^{p47}$ complex is required for homotypic membrane fusion of the Golgi, ER, and nuclear envelope (Latterich et al., 1995; Kondo et al., 1997; Hetzer et al., 2001). It has been proposed that $p97^{p47}$ fulfills a role similar to the AAA ATPase NSF (N-ethylmaleimide-sensitive fusion protein), which disassembles SNARE (soluble NSF attachment protein) complexes formed during membrane fusion. Indeed, p47 binds the SNARE syntaxin 5 *in vitro*, and is required for the efficient interaction of p97 with syntaxin 5. Therefore, p47 is thought to recruit p97 to membrane bound SNARE complexes, leading to their disassembly and thereby priming syntaxin 5 for further membrane fusion events (Rabouille et al., 1998). However, an *in vivo* function of p97 in analogy to SNARE disassembly has also been questioned, as inhibition of p97 ATPase activity *in vivo* did not result in inhibition of Golgi reassembly (Dalal et al., 2004).

Interestingly, the functional UBA domain of p47 is required for $p97^{p47}$ mediated Golgi reassembly *in vitro*, presumably in order to recruit p97 to a ubiquitinated target on the Golgi membrane (Meyer et al., 2002; Meyer, 2005). The deubiquitinating enzyme VCIP135 is also necessary for membrane fusion events of Golgi and ER, and can dissociate the stable complex of $p97^{p47}$ and syntaxin 5 (Uchiyama et al., 2002; Wang et al., 2004; Kano et al., 2005). However, taking into account the requirement for the p47 UBA domain as well as the deubiquitinating activity of VCIP135, it seems improbable that syntaxin 5 is the critical target of p97^{47} during Golgi reassembly, as the interaction with the p97^{p47} complex occurs efficiently *in vitro* without any ubiquitin modification (Rabouille et al., 1998) (discussed in (Buchberger, 2006)). Nevertheless, it is possible that a critical component of the fusion process is ubiquitinated and must be processed, recruited, and/ or extracted by p97^{p47}.

Budding yeast *SHP1* was first identified in a genetic screen for suppressors of the otherwise lethal overexpression of the protein phosphatase 1 catalytic subunit Glc7 (see 2.4). Two *shp1* (suppressor of high-copy PP1) alleles tolerated the overexpression of *GLC7* and, in turn, had phenotypes very similar to those of *glc7* mutants. *shp1-1* and *shp1-2* exhibit a strong growth defect and are deficient in glycogen storage as well as meiosis. Consistent with the model that Shp1 is a positive regulator required for normal Glc7 activity, *shp1* mutants have reduced PP1 activity, determined by the reduced capability of *shp1* cell extracts to dephosphorylate glycogen phosphorylase a (Zhang et al., 1995). Moreover, lysates of cells deleted of *SHP1* were shown to exhibit reduced phosphorylase phosphatase activity, indicative of reduced Glc7 activity (Wilson et al., 2005). The mechanism by which Shp1 influences Glc7 activity is unknown and no direct interaction between Glc7 and Shp1 has been demonstrated.

Employing the yeast knockout libraries available several large-scale screens conducted over the past years have identified a number of phenotypes and sensitivities of *shp1*. Among them was the finding that the deletion of *SHP1* leads to a defect in homotypic membrane fusion, as the knockout was identified in a screen for mutants with defective vacuolar morphology (Seeley et al., 2002). Indeed, Shp1 has been demonstrated to influence vacuolar fusion, possibly by altering localization of certain vacuolar proteins, among them the Glc7 activating subunit Glc8 (Thoms, 2002). However, as the terminal step of vacuolar membrane fusion has been reported to be regulated by Glc7/PP1 (Peters et al., 1999; Bryant and James, 2003), it is difficult to differentiate between secondary effects caused by misregulation of Glc7 in *Δshp1* and phenotypes that are directly related to unique Cdc48^{Shp1} function(s). Accordingly, the *shp1* knockout has been found in several screens investigating chromosome stability and genome maintenance, a phenotype also connected to *glc7* mutants (see 2.4). *shp1* was indentified in three independent screens of a study isolating chromosome instability (CIN) mutants and was shown to have an increased rate in loss of heterozygosity, indicating increased chromosome loss (Yuen et al., 2007; Andersen et al., 2008).

Cdc48^{Shp1} is also involved in protein degradation. Deletion of *SHP1* results in the stabilization and accumulation of the UFD substrate Ub-P-βGal in *S. cerevisiae* (Schuberth et al., 2004), as well as the Cdk inhibitor Rum1 in fission yeast (Hartmann-Petersen et al., 2004).

Very recently, two studies reported novel Cdc48^{Shp1} functions in mitosis and autophagy (Cheng and Chen, 2010; Krick et al., 2010). Cheng and Chen describe a role of Cdc48^{Shp1} in promoting chromosome bi-orientation by regulation of the balance between Ipl1 kinase and Glc7 phosphatase activity at the kinetochore. The authors propose that reduced phosphatase activity at the kinetochore is an effect of abolished nuclear localization of Glc7 in Shp1 depleted cells (Cheng and Chen, 2010) (see following chapters).

Cdc48 and Shp1 were shown to be required for non-selective macroautophagy and for piecemeal microautophagy of the nucleus (PMN), a form of selective autophagy. In analogy to Golgi reassembly the authors speculate on an ubiquitin-proteasome system independent function of $Cdc48^{Shp1}$ in extraction of Atg8 from a complex with the fusion mediator during autophagosome formation (Krick et al., 2010).

2.4 Protein phosphatase 1 catalytic subunit- Glc7

Four families of protein phosphatases have been identified in budding yeast. The PPP family comprises type 1 (PP1), type 2A (PP2A), type 2B (PP2B), and a group of sequence-related Ser/ Thr phosphatases. PP2C family proteins are also Ser/ Thr phosphatases, yet unrelated to PPP phosphatases. Protein tyrosine phosphatases (PTPases) and dual specificity phosphatases form the third group, while low molecular weight PTPases are classified as the fourth family of phosphatases (Stark, 1996).

Glc7 is the only catalytic subunit of protein phosphatase 1 (PP1) found in *S. cerevisiae* and possesses a high degree of sequence homology to mammalian PP1c subunits (*Fig. 11*).

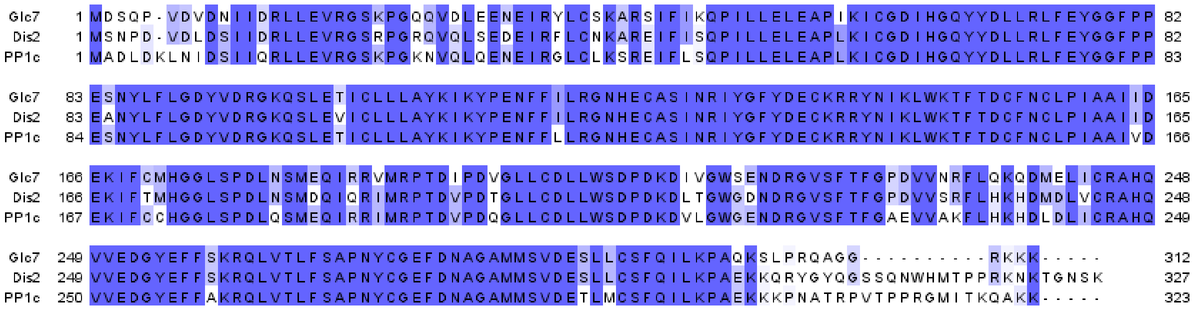

```
Glc7    1 MDSQP-VDVDNIIDRLLEVRGSKPGQQVDLEENEIRYLCSKARSIFIKQPILLELEAPIKICGDIHGQYYDLLRLFEYGGFPP 82
Dis2    1 MSNPD-VDLDSIIDRLLEVRGSRPGRQVQLSEDEIRFLCNKAREIFISQPILLELEAPLKICGDIHGQYYDLLRLFEYGGFPP 82
PP1c    1 MADLDKLNIDSIIQRLLEVRGSKPGKNVQLQENEIRGLCLKSREIFLSQPILLELEAPLKICGDIHGQYYDLLRLFEYGGFPP 83

Glc7   83 ESNYLFLGDYVDRGKQSLETICLLLAYKIKYPENFFILRGNHECASINRIYGFYDECKRRYNIKLWKTFTDCFNCLPIAAIID 165
Dis2   83 EANYLFLGDYVDRGKQSLEVICLLLAYKIKYPENFFILRGNHECASINRIYGFYDECKRRYNIKLWKTFTDCFNCLPIAAIID 165
PP1c   84 ESNYLFLGDYVDRGKQSLETICLLLAYKIKYPENFFLLRGNHECASINRIYGFYDECKRRYNIKLWKTFTDCFNCLPIAAIVD 166

Glc7  166 EKIFCMHGGLSPDLNSMEQIRRVMRPTDIPDVGLLCDLLWSDPDKDIVGWSENDRGVSFTFGPDVVNRFLQKQDMELICRAHQ 248
Dis2  166 EKIFTMHGGLSPDLNSMDQIQRIMRPTDVPDTGLLCDLLWSDPDKDLTGWGDNDRGVSFTFGPDVVSRFLHKHDMDLVCRAHQ 248
PP1c  167 EKIFCCHGGLSPDLQSMEQIRRIMRPTDVPDQGLLCDLLWSDPDKDVLGWGENDRGVSFTFGAEVVAKFLHKHDLDLICRAHQ 249

Glc7  249 VVEDGYEFFSKRQLVTLFSAPNYCGEFDNAGAMMSVDESLLCSFQILKPAQKSLPRQAGG----------RKKK-----   312
Dis2  249 VVEDGYEFFSKRQLVTLFSAPNYCGEFDNAGAMMSVDESLLCSFQILKPAEKKQRYGYQGSSQNWHMTPPRKNKTGNSK   327
PP1c  250 VVEDGYEFFAKRQLVTLFSAPNYCGEFDNAGAMMSVDETLMCSFQILKPAEKKKPNATRPVTPPRGMITKQAKK-----   323
```

***Fig. 11.* Protein sequence alignment of PP1 homologs.** The amino acid sequence of *S. cerevisiae* Glc7, *S. pombe* Dis2, and the γ isoform of human PP1 were aligned and conserved residues depicted in shades of blue. (Jalview (Waterhouse et al., 2009))

The essential gene *GLC7* was first identified in a study that examined a collection of mutants with reduced cellular glycogen levels: *glc1*- *glc8*. *glc7* mutants exhibited strongly decreased amounts of glycogen. Consistently, it was demonstrated that glycogen synthase was hyperphosphorylated and therefore inactive in *glc7* mutants (Peng et al., 1990; Feng et al., 1991; Cannon et al., 1994). Further analysis of Glc7 revealed numerous functions in addition to the regulation of glycogen metabolism (Stark, 1996; Cannon, 2010).

The majority of Glc7 is located in the nucleus, but it is also detectable in the cytosol and at the septum (Bloecher and Tatchell, 2000). Glc7 is stable throughout the cell cycle and enzyme activity does not change substantially, when analyzed by measurement of phosphorylase phosphatase activity. However, it has been reported that Glc7 activity increases as cultures reach stationary phase or glucose becomes limiting, without changes in protein levels, but rather dependent on the subunit Glc8 (Nigavekar et al., 2002).

As *GLC7* is an essential gene in *S. cerevisiae,* many different *glc7* alleles have been used to identify the diverse processes involving Glc7. Most alleles were discovered in screens for one particular Glc7 function, such as glycogen metabolism, and later also utilized to study the other pathways involving PP1 function.

	glc7-1	***glc7-10***	***glc7-12***	***glc7-127***	***glc7-129***	***glc7-T152K***
Mutation	R73C (5, 19)	F135L (2)	N32Y, G227D (3)	K110A, K112A (1)	D137A, E138A (1)	T152K (11)
Altered subunit interaction	defective in Gac1 binding (19)	n.d.	n.d.	n.d.	defective in Bni4 binding (4)	defective in Reg1 binding (18)
Glycogen storage	reduced glycogen (5, 19)	n.d.	n.d.	reduced glycogen (1)	low glycogen (1,6)	normal (11)
Glucose repression	normal (11)	n.d.	n.d.	defective (1)	normal (1)	defective (11)
Sporulation	defect (5)	n.d.	n.d.	reduced (6)	reduced (6)	defect (11)
Mitosis	n.d.	G2/M delay (2,8) dependent on SAC (8)	G2/M delay (3)	no delay (1)	G2/M delay (1,6) dependent on SAC (10)	S-phase delay (7)
Mitotic Glc7 substrates	n.d.	phospho-Ndc10 increased (8) phospho-Dam1 increased (17)	phospho-Dam1 increased (17) phospho-Fin1 increased (16)	phospho H3 enhanced (9)	phospho H3 enhanced (9)	n.d.
Genetic interaction	n.d.	suppresses ts of *ipl1-321* (17)	SL with *cdc48-3* (14)	suppresses ts of *ipl1-2* (9) slow growth with *Δglc8* (6)	suppresses ts of *ipl1-2* (9) SL with *Δglc8* (6)	n.d.
Suppression of pheno-type	n.d.	suppressed by *PKC1*, high osmolarity (1)	mitotic defect suppressed by *SDS22* (3)	n.d.	n.d.	n.d.
Other phenotypes	membrane fusion defect (12,13)	sensitive to high levels of *MPS1* (15)	-	-	sensitive to HU (7)	sensitive to HU (7)

***Table 1*: Commonly used *glc7* alleles and their most prominent phenotypes.** References: 1) (Baker et al., 1997), 2) (Andrews and Stark, 2000), 3) (MacKelvie et al., 1995), 4) (Kozubowski et al., 2003), 5) (Cannon et al., 1994), 6) (Venturi et al., 2000), 7) (Bazzi et al., 2010), 8) (Sassoon et al., 1999), 9) (Hsu et al., 2000), 10) (Bloecher and Tatchell, 1999), 11) (Tu and Carlson, 1994), 12) (Bryant and James, 2003), 13) (Peters et al., 1999), 14) (Cheng and Chen, 2010). 15) (Pinsky et al., 2009), 16) (Akiyoshi et al., 2009b), 17) (Pinsky et al., 2006a), 18) (Tu and Carlson, 1995), 19) (Stuart et al., 1994). SL: synthetically lethal, n.d. not determined, ts: temperature sensitivity, HU: hydroxyurea.

For some identified alleles the molecular basis for the phenotype is evident. The glycogen storage deficiency of *glc7-1* is due to the inability of the mutant Glc7 protein to bind the targeting subunit Gac1, which is mainly responsible for mediating Glc7 function in glycogen synthesis (Baker et al., 1997). In most other cases however, the molecular effects of the point mutations have not been clearly determined. Mutations specific for the different *glc7* conditional alleles could either directly affect activity or stability of Glc7, or alter binding to subunits or substrates.

2.4.1 Targeting subunits mediate Glc7 function

Numerous and highly diverse physiological processes are regulated by Glc7. These cellular pathways include glycogen metabolism, glucose repression, RNA processing, sporulation, DNA damage recovery, actin organization, cell wall morphogenesis, and mitosis (reviewed in (Stark, 1996; Cannon, 2010)). Glc7 itself has little or no substrate specificity, but this is rather mediated through interaction with different regulatory or targeting subunits (*Fig. 12*). These subunits modulate Glc7 phosphatase activity, localization, and substrate binding. At least 28 Glc7 targeting subunits have been demonstrated to regulate Glc7 activity towards certain substrates in *S. cerevisiae* (Cannon, 2010).

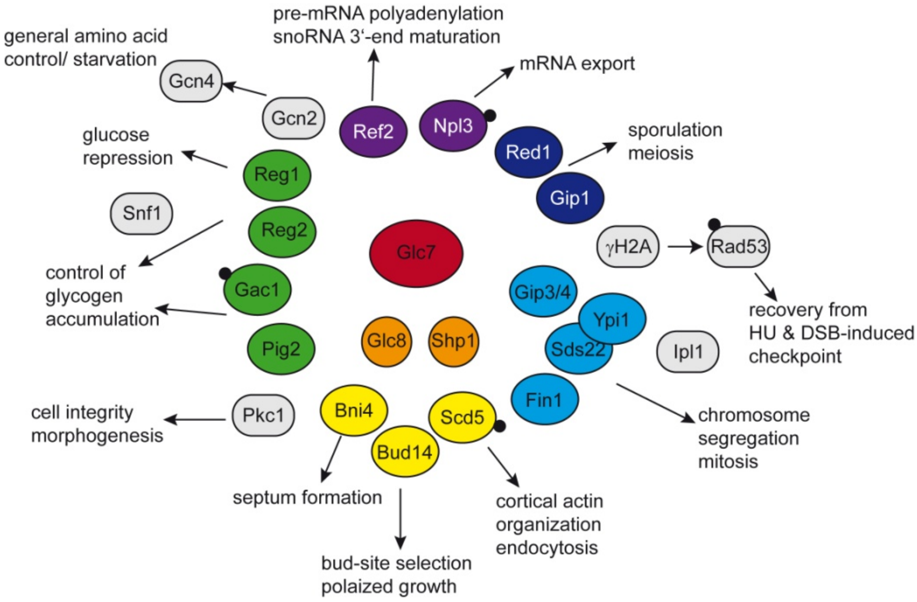
pre-mRNA polyadenylation
snoRNA 3'-end maturation
general amino acid control/ starvation
Gcn4
Gcn2
Ref2
Npl3
mRNA export
glucose repression
Reg1
Red1
sporulation meiosis
Gip1
Snf1
Reg2
Glc7
γH2A
Rad53
control of glycogen accumulation
Gac1
Gip3/4
Ypi1
recovery from HU & DSB-induced checkpoint
Pig2
Glc8
Shp1
Sds22
Ipl1
Fin1
cell integrity morphogenesis
Pkc1
Bni4
Scd5
Bud14
chromosome segregation mitosis
septum formation
cortical actin organization endocytosis
bud-site selection polaized growth

***Fig. 12.* Schematic overview depicting Glc7 regulatory and targeting subunits and their cellular function.** Substrate specificity of Glc7 is achieved by binding of numerous targeting subunits, which regulate Glc7 phosphatase activity towards substrates. Glc7 opposes or regulates the activity of diverse cellular kinases, as well as other factors, such as γH2A (shown in gray). Glc8 and Shp1 are positive regulators of Glc7 (orange), which enhance phosphatase activity by so far mostly unknown mechanisms. Some targeting subunits are themselves substrates of Glc7, indicated by small black dots for phosphorylation.

Binding of many, but not all, Glc7 regulatory subunits is mediated by an (R/K-V/I-X-F) motif (Wu and Tatchell, 2001). This RVxF motif binds to a hydrophobic channel formed by two β-sheets of PP1c, distant from the catalytic core. Mutation of the hydrophobic groove led to reduced affinity of some regulatory subunits towards Glc7 and in severe cases could not fulfill essential functions (Wu and Tatchell, 2001). At least ten regulatory subunits of Glc7 possess this motif, among them Fin1, Scd5, Gac1, and Reg1 (Cannon, 2010). Nevertheless, as about 10% of all mammalian proteins contain this peptide sequence, it is evident that this motif alone is not sufficient to define a PP1 targeting subunit. Additional determinants such as localization, surface exposure of the binding residues as well as changes in tertiary structure depending on the amino acid X play a significant role in defining the capability of PP1 binding (Egloff et al., 1997). In addition, proteins that do not contain an RVxF motif can nevertheless bind PP1. The nuclear protein Sds22 is a major and strong interactor of Glc7, which does not possess an RVxF motif, but rather binds to Glc7 through eleven leucine-rich repeats (Ceulemans and Bollen, 2004; Cannon, 2010).

2.4.2 Regulation of mitosis by PP1/Glc7

Fungal PP1 was first discovered to play a role in mitosis in the fission yeast *S. pombe* (Ohkura et al., 1989; Ishii et al., 1996). *S. cerevisiae* PP1 was also demonstrated to be crucial for chromosome segregation and consequently, several *glc7* mutants arrest at or before anaphase onset (Ohkura et al., 1989; Dombradi et al., 1990; Fernandez et al., 1992; Hisamoto et al., 1994; Black et al., 1995; MacKelvie et al., 1995; Ishii et al., 1996). Furthermore, the conditional alleles *glc7-129* and *glc7-10* exhibit a mitotic delay dependent on the spindle assembly checkpoint (Bloecher and Tatchell, 1999; Sassoon et al., 1999). Protein phosphatase 1 activity is also required for progression through mitosis in different other eukaryotes, such as Drosophila and mammalian cells (Axton et al., 1990; Dombradi et al., 1990).

Glc7 has been demonstrated to oppose Ipl1 kinase activity during chromosome bi-orientation (Biggins et al., 1999; Sassoon et al., 1999; Cheeseman et al., 2002). Additionally, other substrates phosphorylated upon SAC activation must be dephosphorylated for progression through mitosis to commence. This is mediated in part by PP1, as Glc7 is required for spindle checkpoint silencing both in response to lack of attachment and lack of tension (Pinsky et al., 2009).

The finding that overexpression of truncated *glc7* suppressed *ipl1* mutations, whereas overexpression of full length, catalytically active Glc7 was toxic, led to the model that Glc7 and Ipl1 activity need to be balanced in order for proper chromosome segregation to occur (Francisco et al., 1994). Glc7 has been described to oppose Ipl1 kinase activity by dephosphorylating the kinetochore proteins Ndc10 and Dam1, as well as histone H3 (Biggins et al., 1999; Sassoon et al., 1999; Hsu et al., 2000; Kang et al., 2001; Cheeseman et al., 2002). For Ndc10, Dam1, and histone H3 certain *glc7* alleles were used to demonstrate hyperphosphorylation of the substrates at the non-permissive temperature, while they were shown to be hypophosphorylated in *ipl1* mutants. Histone H3 and Dam1 phosphorylation was restored to approximately wild-type levels in *ipl1 glc7* double mutants (Hsu et al., 2000; Pinsky et al., 2006a).

Certain *glc7* alleles suppress the temperature sensitivity of *ipl1* mutants, indicating that kinase and phosphatase activity must be strictly balanced (Francisco et al., 1994; Hsu et al., 2000; Pinsky et al., 2006a). A further indication for the necessity of this kinase to phosphatase balance is the finding that overexpression of Glc7 targeting subunits, which are thought to decrease nuclear Glc7 activity, also partially suppress the *ipl1* ts phenotype. Hence, overexpression of the Glc7 interactors *GLC8*, *SCD5*, *BUD14*, *GIP3*, *GIP4*, and to a lesser extent *SDS22*, *SOL1*, *SOL2*, and *PEX31* suppressed *ipl1* temperature sensitivity (Pinsky et al., 2006a). Furthermore, *ipl1* is suppressed by lack of Shp1 ((Cheng and Chen, 2010) and Results), again arguing in favor of the required balance.

According to the prevalent model, Ipl1 senses incorrect attachments lacking tension during metaphase and phosphorylates a critical kinetochore component, possibly Dam1. Glc7 then reverses this modification and thereby allows microtubule (re-)attachment. This eventually leads to correct bi-polar attachment and cell cycle progression (Pinsky et al., 2006b; Cannon, 2010). Although Dam1 phosphorylation is reduced in response to tension at the kinetochore, the role of Glc7 in (tension-dependent) dephosphorylation of Dam1 has been questioned (Keating et al., 2009). Yet there are other possible targets that may fulfill this function, Ndc10 or Ndc80, the mammalian homolog of which has recently been shown to be a target of PP1 (Deluca et al., 2011).

Furthermore, PP1 reverses phosphorylation events that occur during spindle assembly checkpoint activation (Pinsky et al., 2009; Vanoosthuyse and Hardwick, 2009). *GLC7* overexpression is toxic in wild-type cells (Zhang et al., 1995). Upon release from G1 arrest, overexpression of *GLC7* leads to a Bub2 independent cell cycle arrest before mitotic exit with a high rate of chromosome missegregation. This suggests that *GLC7* overexpression bypasses the spindle checkpoint and causes an additional defect in mitotic exit (Pinsky et al., 2009). Consequently, it could be demonstrated that Glc7 is required for spindle checkpoint silencing, both in response to lack of attachment and lack of tension. Cells overexpressing *GLC7* do not activate the SAC in presence of nocodazole or cohesin defects. *glc7-10* mutants, however, are hypersensitive to constitutive SAC activation by *MPS1* overexpression and are delayed in recovery from transient checkpoint arrest (Pinsky et al., 2009). This was similarly shown in *S. pombe*, where kinetochore localized PP1$^{\mathrm{Dis2}}$ is required for spindle checkpoint silencing (Vanoosthuyse and Hardwick, 2009).

As *ipl1* mutants are checkpoint proficient in response to spindle depolymerization, it is conceivable that Glc7 opposes additional kinases, possibly Mps1, during spindle checkpoint silencing (Pinsky et al., 2009). The mitotic function of Glc7 may therefore not be restricted to opposing Ipl1 kinase activity.

The nuclear targeting subunit(s) required for the mitotic functions of Glc7 has not been identified with certainty. Several targeting subunits localize to the nucleus and could therefore possibly regulate the cell cycle functions of Glc7. Sds22 is an essential nuclear targeting subunit of Glc7, extra copies of which partially suppress the mitotic arrest phenotype of the *glc7-12* allele (Hisamoto et al., 1995; MacKelvie et al., 1995). *sds22* alleles display high rates of chromosome loss, as do *glc7* alleles, but do not have a distinct mitotic arrest phenotype. However, *sds22-6* suppresses the ts phenotype of *ipl1-2*, most likely by reducing nuclear localization of Glc7 (Peggie et al., 2002). Therefore Sds22 was suggested to be the mitotic regulator of Glc7 (Peggie et al., 2002). However, *SDS22* was also isolated as a dosage suppressor of *ipl1-321*, arguing against this model (Pinsky et al., 2006a).

Ypi1 has been shown to form a ternary complex with Sds22 and Glc7 in the nucleus (Pedelini et al., 2007; Bharucha et al., 2008). Depletion of *YPI1* or mutation of its Glc7 binding site leads to a mitotic arrest dependent on the spindle assembly checkpoint, similar to phenotypes of *glc7* alleles. Additionally, the Glc7 binding mutant of Ypi1, and a loss-of function allele, both rescue *ipl1-2* mutants, while being inviable in combination with cell cycle alleles of *glc7* (Bharucha et al., 2008).

Furthermore, the cell cycle regulated protein Fin1 has been demonstrated to be a PP1 targeting subunit that recruits Glc7 to the outer kinetochore. Fin1 was shown to interact with Glc7 and to be required for the majority of the Glc7 interaction with the kinetochore proteins Ndc80 and Dsn1 (Akiyoshi et al., 2009b). A *fin1-5A* phospho-mutant was toxic when overexpressed and led to monopolar spindles without SAC activation (Woodbury and Morgan, 2007). This was caused by misregulation of Glc7 activity at the kinetochore, which resulted in premature SAC silencing (Akiyoshi et al., 2009b). However, *Δfin1* cells do not display a cell cycle or growth defect, are not sensitive to benomyl, and are not defective in SAC silencing, making it very likely that other PP1 targeting subunits that recruit Glc7 to the kinetochore must exist (Akiyoshi et al., 2009b).

The positive regulator of Glc7, Glc8, has also been demonstrated to genetically interact with *ipl1* mutants. *GLC8* was described in the initial genetic screen for mutants with a glycogen storage deficiency (Cannon et al., 1994). *glc8* mutants exhibited the least pronounced reduction of cellular glycogen levels among the indentified mutants. The *GLC8* gene shows sequence homology to the mammalian PP1 inhibitor-2 (I-2) (Cannon et al., 1994), and similar to I-2, Glc8 is a heat-stable protein that inhibits Glc7 and PP1c activity *in vitro*, albeit not as efficiently as I-2 (Tung et al., 1995).

Increased dosage of *GLC8* was found to suppress the temperature sensitivity of *ipl1-1* (Tung et al., 1995). Therefore, as expected, *GLC8* overexpression suppressed the temperature sensitivity of *sli15-3*, a mutant of the Ipl1 activating INCENP homolog Sli15 (see 2.2.1) (Kim et al., 1999). Intriguingly, deletion of *GLC8* also suppressed the ts phenotype of *ipl1-1* and chromosome gain inflicted by *GLC7* overexpression, indicating that Glc8 is required for Glc7 activity (Tung et al., 1995). Consistently, it was demonstrated that lysates of *Δglc8* cells exhibit reduced PP1 activity (Tung et al., 1995; Nigavekar et al., 2002; Wilson et al., 2005). Furthermore, Glc8 has been shown to mediate the increase of Glc7 activity in stationary phase upon glucose reduction (Nigavekar et al., 2002). Glc8 is therefore considered to be a positive regulator of Glc7 activity in *vivo,* becoming inhibitory only when it is overexpressed (Tung et al., 1995).

Mammalian I-2 is phosphorylated at residue T72 (Hemmings et al., 1982; Park et al., 1994). The equivalent residue T118 in Glc8 was shown be phosphorylated and to affect the ability to rescue *ipl1-1*. Mutations of Glc8 T118 to alanine, aspartate, or glutamate enhanced the suppression of the *ipl1* temperature sensitivity (Tung et al., 1995). The cyclin dependent kinase Pho85 in conjunction with the redundant cyclins Pcl6, Pcl7, Pcl8, and Pcl10 was identified to be responsible for the phosphorylation of Glc8 T118 *in vivo* (Tan et al., 2003). Additionally, it was demonstrated that the phosphorylation of T118 is necessary for Glc8 function, as a $glc8^{T118A}$ mutant was defective in glycogen accumulation and not able to rescue the lethality of the *Δglc8 glc7R121K* double mutant. Consistently, a negative genetic interaction between the *glc7R121K* allele and *pho85* or *pcl* mutations has been observed (Tan et al., 2003). The Pho85 cyclins Pcl6 and Pcl7 mainly regulate glycogen metabolism and growth on alternate carbon sources, Pcl8 and Pcl10 regulate glycogen synthase. Interestingly, $\text{Pho85}^{\text{Pcl7}}$ activity is highest in S-phase and it was thus speculated that Glc8 may also regulate cell cycle functions of Glc7 (Tan et al., 2003).

2.5 Aim of the work

In contrast to p97^{p47} in higher eukaryotes, no function or critical substrate of the Cdc48^{Shp1} complex in *S. cerevisiae* had been identified at the beginning of this work. Therefore, this study was initially thought to identify Cdc48^{Shp1} substrates and eventually to determine cellular Cdc48^{Shp1} function(s). To address this, Y2H screens with mutant baits were to be performed and interactors published in large-scale approaches to be verified.

Additionally, the binding of Shp1 to Cdc48 and possible posttranslational modification of Shp1 were to be analyzed in further detail. This should then enable the construction of *shp1* mutants with defined defects in either Cdc48-binding or modification.

Null alleles of *shp1* exhibit reduced Glc7 phosphatase activity, and Shp1 is therefore thought to be a positive regulator of PP1 function *in vivo* (Zhang et al., 1995). However, the mechanism of this regulation is unknown. Therefore, the main focus of the following work was to address the relationship of Shp1 and Glc7. To this end, *shp1* cell cycle phenotypes were to be analyzed in the context of Glc7 deregulation. Furthermore, the involvement of the Cdc48^{Shp1} complex in this process was to be investigated using the engineered *shp1* mutants. Finally, possible mechanisms of Glc7 regulation by Shp1 should be analyzed.

3. Results

3.1 Phenotypic characterization of s*hp1* mutants

The budding yeast gene *SHP1* was first described during a genetic screen for suppressors of high-copy protein phosphatase 1 (Glc7). The two identified *shp1* alleles displayed phenotypes similar to *glc7* alleles (Zhang et al., 1995). Furthermore, it has also been demonstrated that deletion of *SHP1* affects protein degradation (Schuberth et al., 2004; Schuberth, 2006), and numerous large-scale screens have identified drug sensitivities of *shp1* (SGD, www.yeastgenome.org/). In order to gain more insight into the cellular function of Shp1, the phenotypes of *shp1* null alleles in different strain backgrounds were analyzed in further detail.

3.1.1 Null mutation of *shp1* causes a general growth defect

shp1 spores exhibited very strong growth defects directly after tetrad dissection. Deletion of *SHP1* in the DF5 strain background led to impaired growth at all temperatures analyzed and lethality at 37°C or below 16°C (*Fig. 13* and *data not shown*).

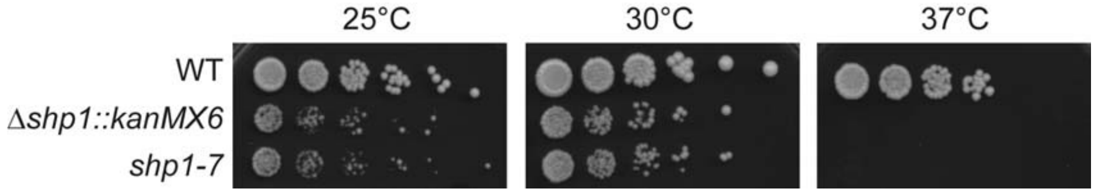

Fig. 13. **shp1 null mutants exhibit a severe growth defect and temperature sensitivity**. Fivefold serial dilutions of cultures of wild-type (WT) and *shp1* null mutant strains were spotted onto YPD plates and incubated at the indicated temperatures.

The *Δshp1*::*kanMX6* strain was constructed by replacing the *SHP1* ORF with a cassette carrying the G418 resistance (Braun et al., 2002; Schuberth, 2006). In some cases this method of gene deletion may lead to unwanted secondary effects caused by partial truncation of promoter or terminator sequences of adjacent genes. *PTH2* is located 100 bp downstream of the *SHP1* locus, making it possible that deletion of *SHP1* interferes with the terminator of *PTH2*. Since Pth2 has been described to negatively regulate the ubiquitin proteasome system (Ishii et al., 2006) this was of concern. To exclude the possibility that some of the phenotypes of *Δshp1* were caused by partial inactivation of *PTH2* further experiments were conducted. First, a new *shp1* deletion strain (*shp1-400*) was constructed, in which the cassette replacing the *SHP1* ORF was truncated at the C-terminus, leaving the last 400 bp of the *SHP1* gene intact and therefore most likely ensuring the integrity of the *PTH2* terminator. Secondly, *Δshp1*::*kanMX6* was transformed with a centromeric plasmid encoding *PTH2.* Both approaches could not suppress or rescue any tested *Δshp1* phenotype, including general growth and temperature sensitivity. To additionally rule out the possibility that the *kanMX6* cassette itself had an unanticipated negative effect on growth, a third step was taken and a null allele of *shp1* was constructed by a pop-in/ pop-out strategy. This method of strain construction enables replacement or mutation of parts of the endogenous ORF without constitutive integration of marker cassettes. In the *shp1-7* allele the *SHP1* start codon was replaced by ACC, leading to a null allele of *shp1* (*Fig. 13*).

This strain is very similar to *shp1-2,* one of the two *shp1* alleles identified in the initial PP1 suppressor screen, which is also a *shp1* null allele in result of a mutated start codon (Zhang et al., 1995). The phenotypes of *Δshp1* and *shp1-7* were compared and no striking differences in growth (*Fig. 13*), sensitivity to drugs, or cell cycle phenotypes (see below) found. One difference, however, was the fact that homologous recombination in *Δshp1* seemed to be partially defective, often yielding unexpected results, such as ORF duplication upon C-terminal epitope tagging or multiple integration events when using integrative plasmids. For all tested strain constructions in *shp1-7,* these aberrant recombination events were not observed. Other recombination defects can, however, formally not be ruled out, as no assays directly addressing homologous recombination activity were performed in either strain. Nonetheless, *Δshp1* and *shp1-7* strains were used in parallel, favoring the *shp1-7* strain when possible.

3.1.2 W303 *Δshp1* is inviable

Surprisingly, it was not possible to delete *SHP1* in certain yeast strain backgrounds and further analysis revealed that *shp1* was lethal in most strain backgrounds derived from W303, but not those directly descending from S288C, like DF5. Heterozygous deletion of *SHP1* in W303 zygotes and subsequent sporulation yielded only wild-type spores, *Δshp1* spores were not viable (*Fig. 14*). The specificity of this lethality was confirmed by rescuing W303 *Δshp1* by plasmid borne *SHP1* (*Fig. 14a*).

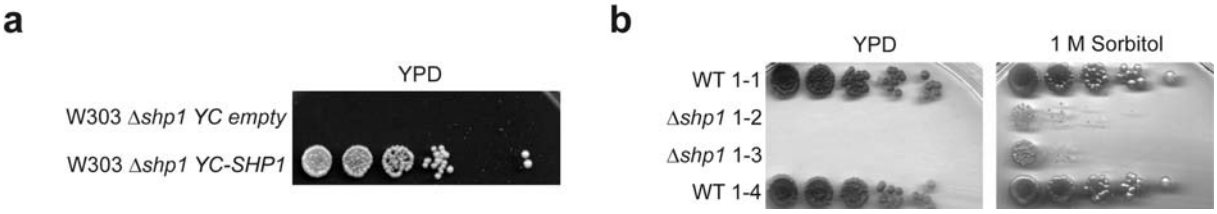

***Fig. 14. SHP1 is* essential in the W303 strain background.** a) Rescue of *Δshp1* lethality in W303 by a plasmid encoding wild-type *SHP1*. Indicated strains were first streaked on 5'FOA to counter-select against the rescuing *YC33-SHP1* plasmid used for sporulation. Cultures of W303 *Δshp1* carrying an empty *YC* plasmid or *YC-SHP1* were then spotted in fivefold dilutions onto YPD plates and incubated at RT. b) Lethality of W303 *Δshp1* is suppressed by 1M Sorbitol. Fivefold serial dilutions of cultures of haploid spores derived from one tetrad of sporulated W303 *Δshp1/SHP1* were spotted on YPD or YPD/1 M Sorbitol. Plates were incubated at RT.

The finding that *shp1* deletion mutants are viable in one yeast strain background, but not the other, prompted the question what the major difference between these two backgrounds is. The *rad5-535* mutation present in the original W303 strain was one obvious possibility (Fan et al., 1996). However, deletion of *SHP1* in W303 *RAD5*+ also did not result in any viable *Δshp1* spores (*data not shown*).

Another described difference between S288C and W303 is the polymorphic gene *SSD1*. Different alleles of *SSD1* have been identified and named according to their ability to suppress the lethality of a *SIT4* deletion. The strain backgrounds W303 and YP6D, in which deletion of *SIT4* is lethal, contain *ssd1-d2* and *ssd1-d1* (d̲ead), respectively. S288C harbors the *SSD1-v1* (v̲iable) allele, which suppresses *Δsit4* lethality (Sutton et al., 1991). Interestingly, *SSD1* was one of two potential suppressors isolated from a high-copy suppressor screen for a *shp1* mutant in W303 (*data not shown*).

Ssd1 has been described to promote cell wall integrity, and *SSD1-v1* can suppress the temperature sensitivity of mutations of the Pkc1 downstream kinase Bck1 (Costigan et al., 1992; Kaeberlein and Guarente, 2002). Pkc1 (protein kinase C) is a central regulator of cell wall integrity and promotes transcription of cell wall biosynthetic genes. Mutants in the Pkc1 kinase pathway undergo cell lysis at high temperatures due to a deficiency in cell wall construction. This cell lysis phenotype can be rescued by high extracellular osmolarity or *PKC1* overexpression (Kamada et al., 1995; Kaeberlein and Guarente, 2002).

Interestingly, both the lethality of W303 *Δshp1* and the temperature sensitivity (ts) phenotype of DF5 *Δshp1* could be suppressed by 1 M Sorbitol (*Fig. 14b* and *data not shown*). This indicates that these phenotypes may be due to cell wall defects resulting in cell lysis. A defect in cell wall morphogenesis could in turn be sensitive to different *SSD1* alleles and thereby cause lethality of W303 *Δshp1.* This assumption is supported by the finding that *shp1* null mutants are sensitive to the fluorescent dye calcofluor white, indicative of a cell wall defect ((Ando et al., 2007) and *data not shown*).

If the mutant allele s*sd1-d2,* which is considered a null allele of *ssd1* in regard to its function in cell wall maintenance (Kaeberlein and Guarente, 2002), were responsible for the lethality of W303 *Δshp1,* then *Δssd1 Δshp1* should be lethal in any strain background. Moreover, expression of *SSD1-v1* in W303 *Δshp1* should rescue the lethality. Indeed, a strong negative genetic interaction between *Δssd1* and *Δshp1* has been reported in a large-scale genetic screen (Collins et al., 2007), performed in the S288C derived background BY4743 (Brachmann et al., 1998). However, expression of DF5 derived *SSD1* did not clearly rescue W303 *Δshp1* when expressed from its endogenous promoter on a low copy plasmid (*data not shown*). Since *Δshp1* in DF5 exhibits a strong growth defect, a low copy number of *SSD1* may not be sufficient to rescue growth. Thus, *SSD1* still is a potential candidate for the difference in *Δshp1* viability between strain backgrounds.

3.1.3 Pleiotropic defects of *shp1* mutants

In addition to temperature sensitivity null mutation of *shp1* led to pleiotropic defects on most stress plates tested. Among others, *Δshp1* was sensitive to the heavy metal Cadmium, the double-strand break inducing drug zeocin, and the translation inhibitor cycloheximide (CHX) (*Fig. 15*). Additionally, *Δshp1* was sensitive to the spindle depolymerizing agent benomyl (*Fig. 25a*) and calcofluor white (CFW) ((Ando et al., 2007) and *data not shown*).

Due to the variability of *Δshp1* phenotypes between individual strain backgrounds, as discussed above for DF5 and W303, drug sensitivities were analyzed not only using DF5 *Δshp1,* but also using the two *shp1* alleles in the RCY background identified in the initial *GLC7* suppressor screen (Zhang et al., 1995) (*Fig. 15*).

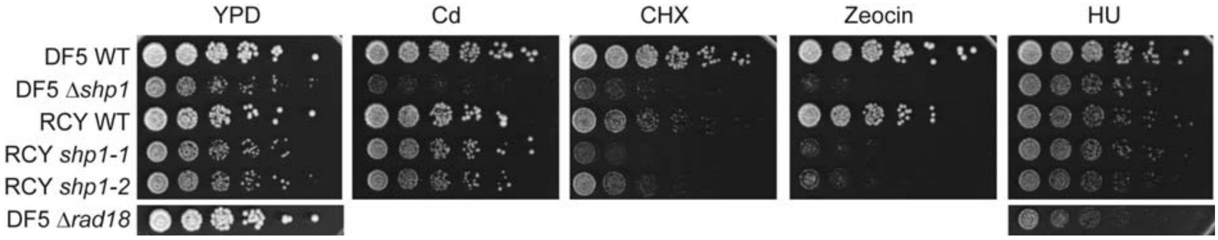

***Fig. 15. shp1* null mutants are hypersensitive to various drugs.** Fivefold serial dilutions of cultures of the indicated strains were spotted on control YPD and plates containing 15μM $CdCl_2$, 0.3 μg/ml cycloheximide (CHX), 1 μg/ml zeocin, or 100 mM hydroxyurea (HU).

Comparing *shp1* null mutations in the DF5 and the RCY strain backgrounds on YPD again demonstrated that lack of Shp1 causes a significant growth defect. This is important to stress, as it further confirms that introduction of the *kanMX6* cassette into the *SHP1* locus did not result in a completely *SHP1*-unspecific impairment of growth. DF5 *Δshp1* and the *shp1* alleles from the original *GLC7* suppressor screen are zeocin and cycloheximide sensitive, whereas the cadmium sensitivity is only pronounced in the DF5 background (*Fig. 15*). Hypersensitivity towards the dNTP depleting agent hydroxyurea (HU) was neither detectable for DF5 *Δshp1,* nor for the *shp1-1* or *shp1-2* allele (*Fig. 15*). This may suggest that *shp1* mutants are more sensitive towards specific forms of DNA damage, such as double strand breaks induced by zeocin.

In summary, null mutation of *shp1* in any strain background resulted in a severe growth defect or even lethality. Furthermore, *shp1* mutants were sensitive to numerous drugs and stress conditions. Shp1 therefore fulfills important functions that are required for normal cell growth and viability. As Shp1 has been described as a cofactor of Cdc48 (Braun et al., 2002; Schuberth et al., 2004; Rumpf and Jentsch, 2006), it is likely to regulate critical cellular pathways as part of the $Cdc48^{Shp1}$ complex.

3.2 The Shp1-Cdc48 interaction

3.2.1 Cdc48 binding mutants of *shp1*

Shp1 has been demonstrated to strongly interact with the N-domain of Cdc48. This interaction is mediated by the UBX domain and a second binding site (BS1) of Shp1 (Bruderer et al., 2004; Hitt and Wolf, 2004; Schuberth et al., 2004; Neves, 2005; Sato and Hampton, 2006). Point-mutations of conserved residues within BS1 and the UBX domain were shown to abolish binding of Shp1 to Cdc48 in yeast two hybrid (Y2H) and *in vitro* GST-pulldown experiments (Neves, 2005). Additionally, further detailed bioinformatic analysis of the Shp1 protein sequence identified a third potential Cdc48 binding site within the unstructured region between the UBA and SEP domains (Kay Hofmann and Alexander Buchberger, *unpublished results*). To further characterize Shp1 binding to Cdc48 *in vivo*, yeast strains only expressing mutant variants of Shp1 were analyzed in co-immunoprecipitation experiments (*Fig. 16*).

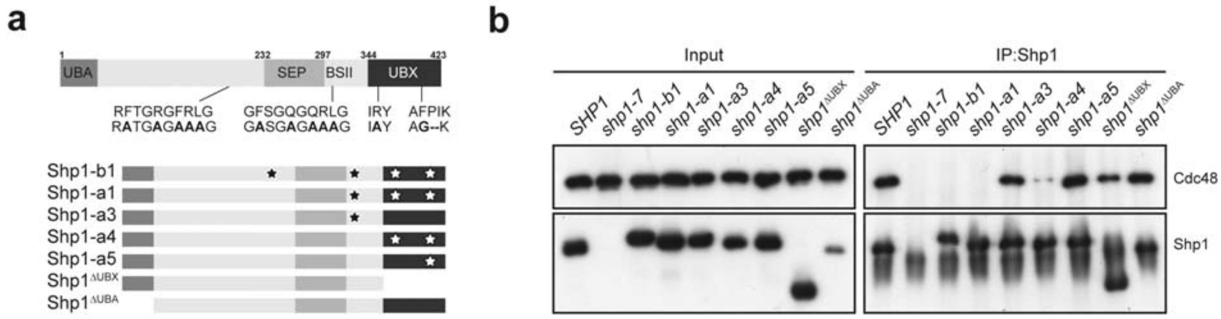

***Fig. 16.* Construction of *shp1* mutants defective in Cdc48 binding.** a) Schematic overview of the different engineered Cdc48 binding mutants of Shp1. Mutated residues are depicted in bold letters or as stars in the schematic overview. b) Co-immunoprecipitation of Cdc48 with the Shp1 mutants. Lysates of the indicated *shp1* mutant strains were subjected to immunoprecipitation with Shp1 antibodies. Co-immunoprecipitation of Cdc48 was detected by Western blot against Cdc48. *SHP1* and *shp1-7* serve as controls.

Different combinations of point-mutations in BS1 and the R…FPR (FPI) motif, as well as deletion mutants of the UBA and UBX domains, were tested for their ability to interact with Cdc48 (*Fig. 16*).

Deletion of the UBX domain noticeably reduced the interaction of Shp1$^{\Delta UBX}$ with Cdc48, but did not abolish binding completely (*Fig. 16b*). Mutation of the FPR motif to G—or deletion of the UBA domain (Shp1-a5 and Shp1$^{\Delta UBA}$, respectively) did not influence the interaction with Cdc48 (*Fig. 16b*). This was expected for the deletion of the UBA domain, but somewhat surprising for Shp1-a5, as additional mutation of the arginine of the R…FPI motif strongly reduced Cdc48 binding (Shp1-a4). Thus, these results suggest that the arginine in strand 1 of the UBX domain is the major determinant in mediating the interaction of the Shp1 UBX domain with Cdc48. This is in some contrast to what has been reported for p47, as the FPR motif was demonstrated to mediate the interaction of p47 with p97. However, mutation of the preceding arginine in p47 also significantly reduced binding of p97 (Dreveny et al., 2004). This discrepancy may reflect a difference between p47 and Shp1 or could be an effect of the different introduced amino acid substitutions.

As expected from previous results of Y2H and *in vitro* studies (Neves, 2005), the Shp1-a1 mutant was unable to co-immunoprecipitate detectable amounts of Cdc48 (*Fig. 16b*). This Shp1 variant contains mutations in BS1 and the R…FPR motif of the UBX domain (*Fig. 16a*).

Even though no interaction of Shp1-a1 with Cdc48 was detectable in Y2H, GST pull-down (Neves, 2005), or co-immunoprecipitation, the possibility of a residual transient interaction remained. Considering the identification of a third putative Cdc48 binding motif within Shp1 (Kay Hofmann and Alexander Buchberger, *unpublished results*), a further binding mutant of Shp1 was constructed. Mutation of the UBX domain, BS1 and the newly identified third putative binding motif resulted in the triple binding mutant Shp1-b1 (*Fig. 16a*). As expected, Shp1-b1 did not bind any detectable amounts of Cdc48 (*Fig. 16b*). However, the mutated Shp1 protein migrated more slowly than all other full length Shp1 variants in SDS-PAGE, possibly indicating an altered posttranslational modification. Mutating this third binding site alone was sufficient to induce the altered migration pattern (*data not shown*), indicating that this was a direct effect of the introduced point-mutations and not an additive effect of mutating all Cdc48 interacting motifs.

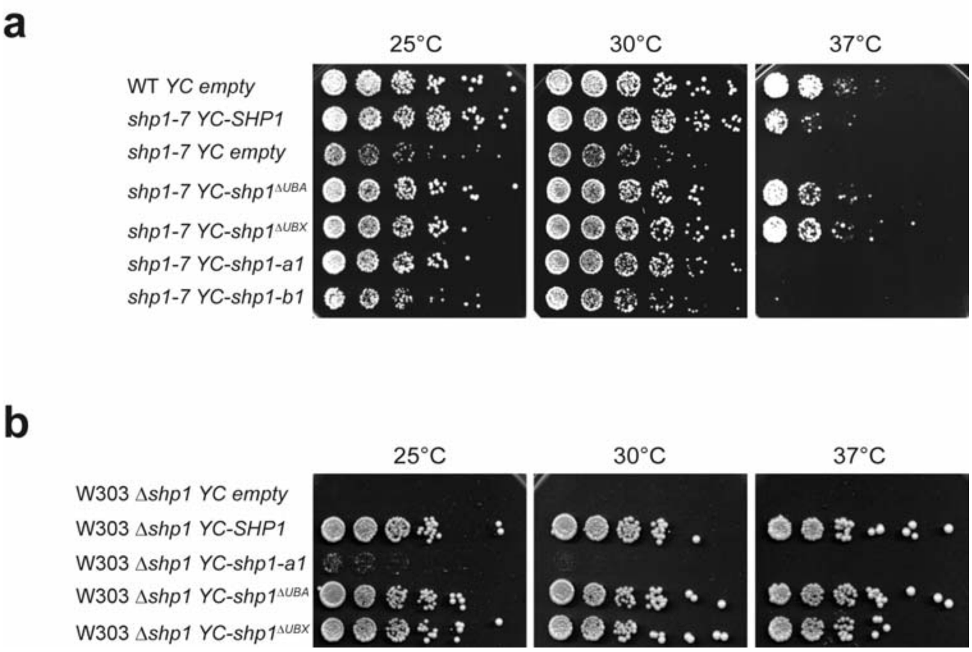

***Fig. 17.* Binding of Shp1 to Cdc48 is required for normal growth.** a) Loss of Cdc48 binding leads to temperature sensitivity in DF5. Fivefold serial dilutions of DF5 wild-type (WT) or *shp1-7* cultures carrying the indicated *shp1* binding mutants on *YCplac111* plasmids were spotted on SC-Leu plates. Plates were incubated at the indicated temperatures. b) The binding mutant *shp1-a1* causes a severe growth defect in W303. W303 *Δshp1::kanMX6 YC33-SHP1* additionally transformed with the indicated plasmids was first streaked on 5'FOA to counter-select against the wild-type *SHP1* plasmid. Cultures were then spotted in fivefold serial dilutions on SC-Leu plates and incubated at the respective temperatures.

To address the cellular importance of the Cdc48-Shp1 interaction, different *shp1* mutants were analyzed for possible growth defects (*Fig. 17*). Deletion of the UBX or UBA domains of Shp1 alone did not result in any general growth defect or temperature sensitivity, neither in the DF5 nor in the W303 strain background (*Fig. 17a,b*). This is consistent with previous reports that deletion of the UBA domain of Shp1 does not affect Cdc48 binding of Shp1 or general growth (Schuberth, 2006).

shp1-7 transformed with a plasmid encoding the Cdc48 binding mutant *shp1-a1* was temperature sensitive at 37°C, but did not have a strong general growth defect resembling a *shp1* null mutation (*Fig. 17a*). This was surprising, as it is expected that Shp1 fulfills most, if not all, of its cellular functions in complex with Cdc48. Therefore, abolishing the Shp1-Cdc48 interaction should result in a phenotype similar to the *shp1* null allele. This could indicate that Shp1 either fulfills critical cellular functions independently of Cdc48, or that transient interaction with Cdc48 remains possible. Further strain construction and phenotypic analysis of a *shp1-a1* mutant constructed by a pop-in/ pop-out strategy (*shp1-a1* in *Fig. 27,32,33*) revealed that this strain did have growth defects similar to *shp1* null mutants, albeit less severe. Therefore, the growth defect of *shp1-a1* at normal temperatures appears to be less pronounced when analyzing *shp1-7* transformed with *YC-shp1-a1*. This could be due to sporadic accumulation of suppressors, or reflect growth with or without additional plasmids.

In contrast, the triple binding mutant, *shp1-b1*, exhibited phenotypes nearly identical to the *shp1* null mutant (*Fig. 17a*). This was not due to the altered modification state of Shp1-b1, as the *shp1* variant containing only mutations within the third binding site exhibited wild-type growth (*data not shown*).

That abolishing Shp1 binding to Cdc48, however, results in a relevant growth defect is supported by the finding that *YC-shp1-a1* suppresses the lethality of W303 *Δshp1,* but exhibits severely impaired growth (*Fig. 17b*). Given the difference between W303 and S288C, which makes *SHP1* essential, a full rescue of W303 *Δshp1* by *shp1-a1* would not have been expected. Furthermore, the phenotype observed in W303 would be consistent with the current model that Shp1 fulfills all of its critical cellular functions in complex with Cdc48. If Shp1-a1 indeed transiently interacts with Cdc48, and this is required for viability in W303, then the triple binding mutant *shp1-b1* should be inviable in W303.

3.2.2 Ubiquitination of Shp1 depends on Cdc48 binding

In Western blot analysis of Shp1 several more slowly migrating species could be observed, indicating possible posttranslational modification. Indeed, Shp1 was distinctly ubiquitinated by multiple ubiquitin moieties (*Fig. 18*). Lysates of a strain expressing endogenous Shp1^{7His} and overexpressing ^{myc}ubiquitin were subjected to denaturing Ni-NTA pull-down and subsequent stringent myc-immunoprecipitation (*Fig. 18a*). This two step purification that first enriches Shp1 and then ubiquitinated proteins, clearly demonstrated that Shp1 is covalently modified by ubiquitin *in vivo*.

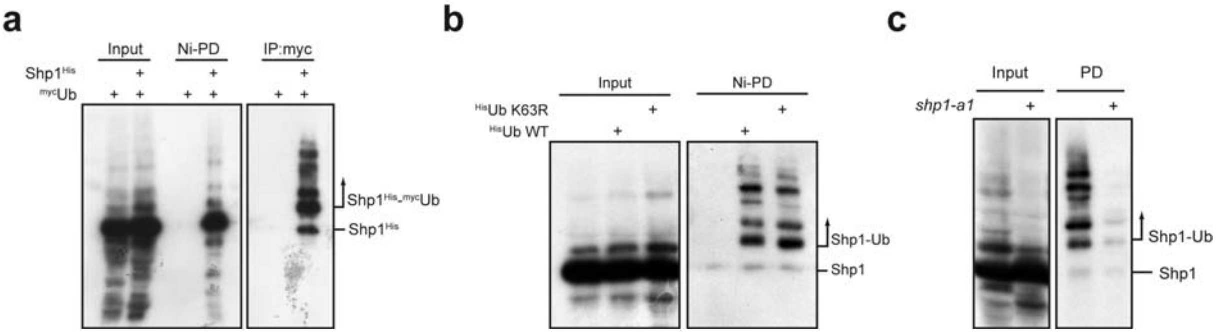

***Fig. 18.* Shp1 is ubiquitinated *in vivo*.** a) Two-step purification of ubiquitinated Shp1. Yeast strains expressing Shp1^{7His} and strains additionally overexpressing ^{myc}ubiquitin were first subjected to a denaturing Ni-NTA pull-down (PD) and subsequently to myc immunoprecipitation. Ubiquitinated Shp1 was detected by Western blot using Shp1 antibodies. b) Shp1 is not modified by K63-linked ubiquitin chains. Denaturing Ni-NTA pull-down from lysates of wild-type (WT) and WT overexpressing either ^{His}ubiquitin or ^{His}ubiquitin K63R. Western blot against Shp1. c) Shp1 ubiquitination depends on Cdc48 binding. Denaturing Ni-NTA pull-down of ^{His}ubiquitin from lysates of WT or *shp1-a1* cells overexpressing ^{His}ubiquitin. Western blot against Shp1.

As five to six distinct bands of modified Shp1 could be detected, it is unlikely that these are K48-linked ubiquitin chains marking the protein for proteasomal degradation. Additionally, Shp1 is very stable over hours and therefore the majority of the protein is presumably not subjected to proteasomal degradation ((Schuberth, 2006) and *data not shown*). Since K63-linked ubiquitin chains do not result in proteasomal degradation of the substrate, it was addressed if Shp1 is modified by a ubiquitin chain of this linkage type. Overexpression of wild-type and mutant K63R ^{His}ubiquitin in the DF5 background did not result in significantly different ubiquitination patterns of Shp1 (*Fig. 18b*). Since the effect of K63R ubiquitin may have been masked by endogenous wild-type ubiquitin, this experiment was repeated in a strain background in which K63R ubiquitin is the only source of ubiquitin (Spence et al., 1995). However, pull-downs of K63R ^{His}ubiquitin in this strain led to the same result, K63R had no effect on the pattern of Shp1 modification (*data not shown*).

As the modified bands of Shp1 are very distinct and highly reproducible, multiple mono-ubiquitination is conceivable. A further possibility could be mixed chains of Smt3 (SUMO) and ubiquitin assembled on Shp1. ^{His}Smt3 pull-downs, however, did not contain any detectable Shp1 species, while the low abundant Smt3-modified Cdc48 was detectable (*data not shown*).

Interestingly, the Cdc48 binding mutant of Shp1 (Shp1-a1) was not ubiquitinated (*Fig. 18c*). Mutation of the Cdc48 binding sites, BS1 and the R…FPR motif, did not affect any lysine residues. It is therefore unlikely that the loss of ubiquitination is a direct consequence of the introduced point mutations in Shp1-a1. Furthermore, ubiquitination of Shp1$^{\Delta UBX}$ was also reduced, but not completely abolished (*data not shown*). Hence, the reduction of Shp1 ubiquitination presumably correlates with the degree of residual Cdc48 binding. Therefore it is plausible that Shp1 is ubiquitinated upon Cdc48 binding. The *in vivo* function of this ubiquitination remains to be identified.

To address the functional aspect of this modification the critical lysine residue was thought to be identified and later specifically mutated for phenotypic analysis. However, mutagenesis of random combinations of all 23 lysines failed to identify a critical target for ubiquitination (*data not shown*). Nonetheless, the fact that one or two forms of Shp1 ubiquitination could be reduced, while others were unaffected, argues against a chain of any linkage type.

As the critical lysine(s) could not be determined, attempts to identify the responsible E2 conjugating enzyme were undertaken. The only reduction of Shp1 ubiquitination was detected in deletion mutants of the redundant "housekeeping" E2s Ubc1, Ubc4, and Ubc5 (*data not shown*). Thus, no relevant information regarding the potential Shp1 function was gained from this approach.

3.3 Shp1 is modified by phosphorylation

In addition to the demonstrated ubiquitination, Shp1 was also reported to be posttranslationally modified by phosphorylation (Ficarro et al., 2002; Gruhler et al., 2005; Li et al., 2007; Smolka et al., 2007; Albuquerque et al., 2008). The mammalian homolog of Shp1, p47, is phosphorylated on residue S140 by Cdc2 (Cdk1). p47 is mainly localized to the nucleus in interphase cells. During mitosis, as p47 enters the cytoplasm due to nuclear envelope breakdown, phosphorylation by Cdk1 inhibits binding of p47 to Golgi membranes. In late mitosis p47 is dephosphorylated by an unknown phosphatase, enabling binding of p47 to Golgi membranes and Golgi reassembly (Uchiyama et al., 2003).

However, yeast undergoes a closed mitosis, and phosphorylation would not be necessary to inhibit premature binding to cytosolic targets. Furthermore, this specific Cdk1 target site is not conserved in Shp1. Nevertheless, phosphorylation could regulate Shp1 function or localization. Five major phosphorylation sites within Shp1 have been identified in several large-scale mass-spectrometric analyses: S106 (Ficarro et al., 2002; Albuquerque et al., 2008), S108 (Ficarro et al., 2002; Smolka et al., 2007; Albuquerque et al., 2008), S315 (Gruhler et al., 2005; Li et al., 2007; Smolka et al., 2007; Albuquerque et al., 2008), S321 (Smolka et al., 2007; Albuquerque et al., 2008), S322 (Li et al., 2007; Albuquerque et al., 2008). Additionally, six further putative phosphorylation sites within Shp1 have been identified (S93, S94, S97, S155, S210, S226) (Albuquerque et al., 2008).

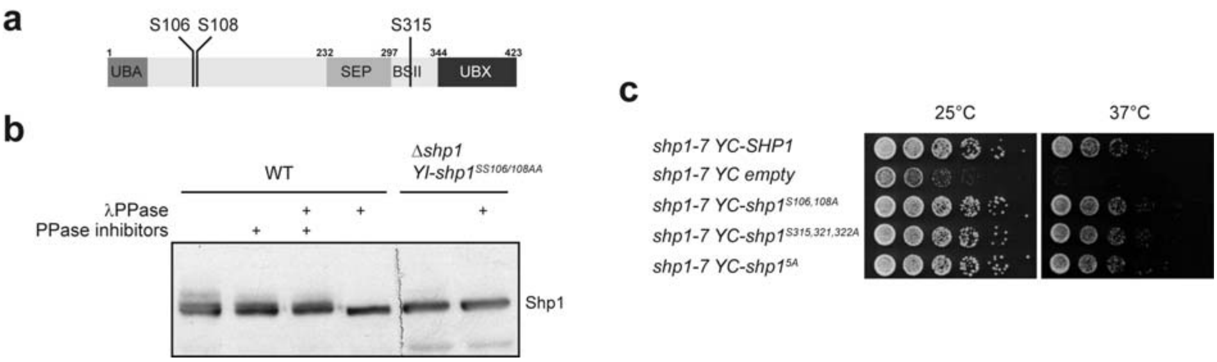

Fig. 19. **Phosphorylation of Shp1 at residues S106, S108, S315, S321, and S322 is not required for normal growth.** a) Schematic overview of phosphorylated residues identified by mass-spectrometry of affinity purified Shp1^{myc7His}. b) λ-phosphatase assay of yeast whole cell lysates. Lysates of stationary WT or *Δshp1 YI-shp1*$^{SS106/108AA}$ strains were incubated with phosphatase inhibitors and, or λ-phosphatase. Multiple phosphorylated forms of Shp1 could be detected by Western blot against Shp1. c) Temperature sensitivity of *shp1-7* is rescued by all tested combinations of serine to alanine mutants of Shp1. *shp1-7* was transformed with plasmids encoding the indicated serine to alanine mutants of Shp1. Fivefold serial dilutions were spotted on SC-Leu plates and incubated at 25°C and 37°C. *shp1*^{5A} is a mutant containing all five serine to alanine mutations.

To address potential phosphorylation, modification of Shp1 in asynchronously growing cells under non-stressed conditions was analyzed. In order to increase sensitivity and to reduce unspecific background, Shp1^{myc7His} was purified using denaturing Ni-NTA pull-downs and subsequent stringent myc-immunoprecipitation. Mass-spectrometric analysis without prior enrichment of phosphorylated peptides (Frank Siedler; MPI of Biochemistry, Martinsried) identified the known phosphorylation sites S106, S108, and S315 (*Fig. 19a*). Treatment of yeast lysates with λ-phosphatase further demonstrated that Shp1 was indeed phosphorylated *in vivo*. Stationary yeast cultures were lysed and treated with λ-phosphatase, phosphatase inhibitors, or both (*Fig. 19b*). Several more slowly migrating forms of Shp1 were noticeably reduced in samples treated with λ-phosphatase, but still detectable in samples to which phosphatase inhibitors had been added. This indicates that Shp1 is phosphorylated *in vivo*. Furthermore, a variant of Shp1, in which the two phosphorylation sites S106 and S108 had been mutated to alanine, migrated similarly to the dephosphorylated form of Shp1 in SDS-PAGE independently of phosphatase treatment. This indicates that S106/108 is a major phosphorylation site in Shp1 during stationary phase (*Fig. 19b*). However, the Shp1 serine to alanine mutants of residues 106, 108, 315, 321, and 322 were able to suppress the growth defect as well as the temperature sensitivity of *shp1-7* (*Fig. 19c*), demonstrating that phosphorylation at these sites is not required for normal growth.

3.4 Identification of novel Shp1 interactors

To identify Shp1 interactors and possibly substrates of the Cdc48^{Shp1} complex, robot-based yeast two hybrid (Y2H) screens and co-immunoprecipitation experiments were conducted.

First two individual Y2H screens were performed, one using full-length wild-type Shp1 and the other using a mixture of two Cdc48 binding mutants as baits (Shp1$^{\Delta UBX}$ with a mutated BS1 and Shp1-a1). It was reasoned that potential substrates of Cdc48^{Shp1} may be processed very quickly, making an interaction undetectable using the Y2H system. Therefore the Cdc48 binding mutants were used, as

potential substrates could interact with Shp1 but not subsequently be turned over by Cdc48. Over all, the screen using the mixture of two binding mutants as baits resulted in a much higher number of false positive interactors. The ten most strongly interacting candidates were cloned, but could not be verified in directed Y2H experiments (*data not shown*). However, Ndc80 (Tid3) was identified as a potential interactor on the less stringent plates during this screen. Interestingly, this candidate had previously also been found in a conventional Y2H screen using the same Shp1 mutants as baits (Neves, 2005).
The robot-based screen using full-length Shp1 as the bait identified Cue3, Ygl108c, and Ynl155w as potential Shp1 interactors. The latter two candidates as well as Hda2, Tem1, and Nut2 had been identified as Cdc48 and Shp1 interactors in a large-scale TAP-approach (Krogan et al., 2006).

YGL108c and *YNL55w* are two non-essential uncharacterized yeast ORFs that have no described function or reported sensitivities of the corresponding deletion mutants. Ynl155w contains a predicted N-terminal AN1-type zinc finger domain and localizes to the cytoplasm and the nucleus (SGD, www.yeastgenome.org/). Ygl108c is predicted to be palmitoylated and distinctly localizes to the cell periphery ((Ren et al., 2008) and *data not shown*). Additionally, it has been demonstrated that Ygl108c binds to Cdc48 via a distinct linear binding motif within its C-terminus (Christopher Stapf et al., *manuscript in preparation*). Hda2 is a subunit of the Hda1 histone deacetylase complex required for function (Wu et al., 2001). The essential protein Nut2 is a component of the mediator complex, which is a co-activator of RNA Polymerase II dependent transcription (Gustafsson et al., 1998). The GTP binding protein Tem1 controls mitotic exit and Ndc80 is a central component of the outer kinetochore (see Introduction).

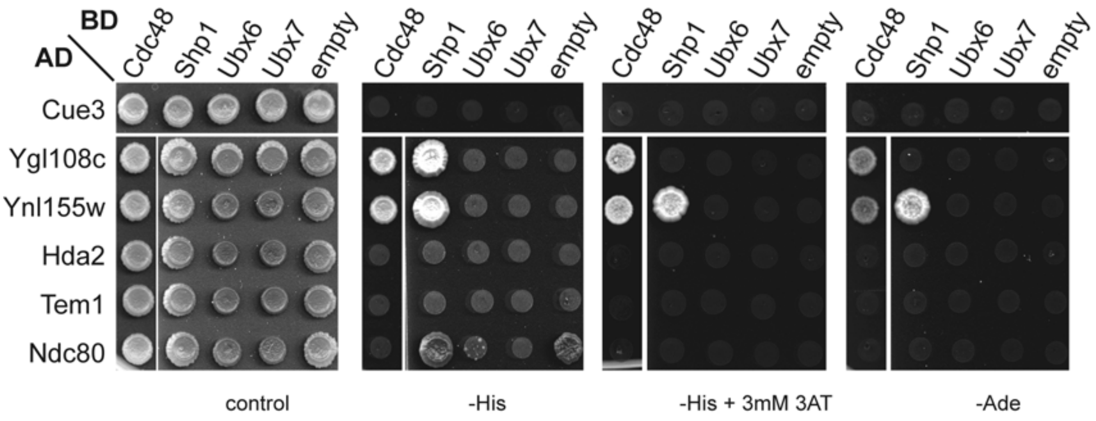

Fig. 20. **Yeast two hybrid interaction analysis of Cdc48, Shp1, Ubx6, and Ubx7 with Cue3, Ygl108c, Ynl155w, Hda2, Tem1, and Ndc80.** PJ69-4A cells were transformed with the indicated combinations of bait (BD) and prey (AD) plasmids and were spotted on SC plates lacking tryptophan and leucine (control) or additionally lacking histidine (-His), lacking histidine and supplemented with 3 mM 3AT (-His + 3AT), or lacking adenine (-Ade).

To confirm that the identified candidates indeed interact with Shp1, they were analyzed in directed Y2H assays. In addition, candidates were also tested for their interaction with Cdc48, Ubx6 and Ubx7 (*Fig. 20*). Yet none of the tested candidates interacted with Ubx6 or Ubx7. Among the putative interactors Ynl155w interacted most strongly with Shp1 and Cdc48 and allowed growth on all plates, including the stringent SC–Ade plate. The interaction of Ynl155w with Shp1 was dependent on Cdc48 binding of Shp1, as it was completely abolished when the binding mutant Shp1-a1 was used as the bait (*data not shown*). Ygl108c showed interaction with Shp1 and Cdc48 on the least stringent SC-His plate, but grew only in combination with Cdc48 on the more selective SC-His+3 AT and SC-Ade plates. Interaction of Cue3, Hda2, Tem1, and Nut2 with Shp1 or Cdc48 could not be confirmed using the Y2H system (*Fig. 20* and *data not shown*). Ndc80 and Shp1 interact, as growth on the SC-His plate indicates. This interaction was not abolished when the binding mutants of Shp1 were used as baits (*data not shown*). However, the Ndc80 construct was also partially auto-activating, allowing some growth on SC–His when only the empty vector was co-transformed. Nonetheless, no growth was observed in combination with Cdc48, Ubx6, and Ubx7, making Ndc80 a possible direct interactor of Shp1.

To further verify the Y2H results and to address interaction *in vivo*, co-immunoprecipitation experiments were performed. All candidate interactors were C-terminally tagged with either 9myc or 3HA epitopes and immunoprecipitated from yeast lysates. Co-immunoprecipitation of Shp1 or Shp1^{9myc}, as well as Cdc48 was analyzed by Western blot (*Fig. 21a,b*).

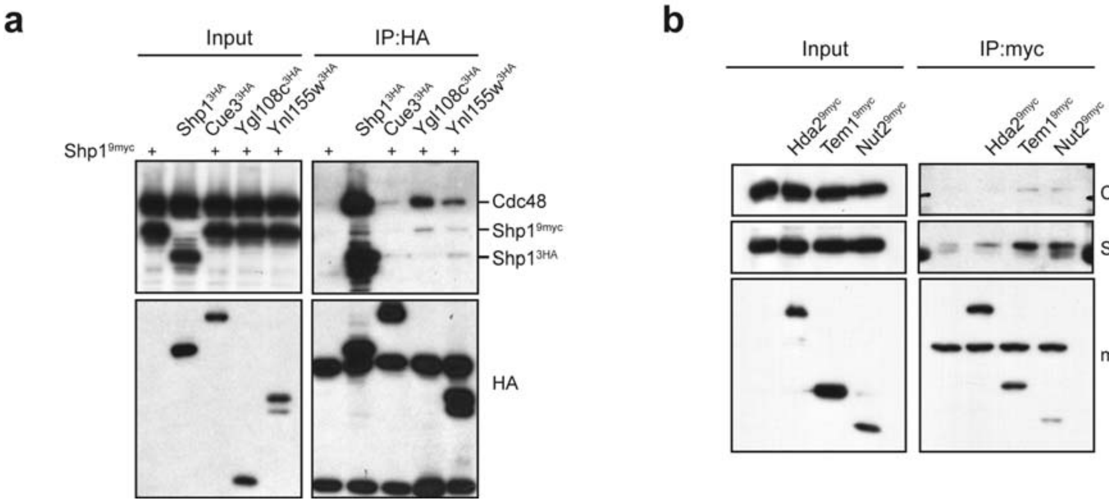

Fig. 21. **Verification of putative Shp1 interactors by co-immunoprecipitation.** a) Co-immunoprecipitation (IP) of Shp1^{9myc} and Cdc48 with C-terminally 3HA epitope tagged potential interactors Cue3, Ygl108c, and Ynl155w. Western blot against Cdc48, Shp1 and HA. Immunoprecipitation of Shp1^{3HA} and co-IP of Cdc48 serves as a control. b) Co-IP of Shp1 and Cdc48 with C-terminally 9myc tagged potential interactors Hda2, Tem1, and Nut2. Western blot against Cdc48, Shp1 and myc.

With the exception of Cue3 all tested candidates could be verified as *in vivo* interactors of Shp1, and in most cases interactors of Cdc48. However, analysis of co-immunoprecipitation of Shp1 with Ndc80 from asynchronous cultures was not conclusive, as the immunoprecipitation of kinetochore structures resulted in a high degree of unspecific background binding (*data not shown*).

Taken together, the strongest candidates as Cdc48^{Shp1} interactors are the uncharacterized proteins Ygl108c and Ynl155w. However, these candidates do not bind Shp1 directly, but rather bind to Cdc48. Nonetheless, these interactors could be substrates of a Cdc48 sub-complex and were therefore further analyzed.

All potential interactors were stable in a cycloheximide shut-off experiment, independent of proteasomal inhibition by MG132 (*data not shown*). Ynl155w expression was induced by MG132 addition, which may not be unexpected, as an Rpn4 binding site has been predicted in its promoter. Therefore, there is no indication that these proteins are substrates of Cdc48 that are processed and subsequently degraded.

Nevertheless, ubiquitination *in vivo* was detected for all epitope tagged interactors with the exception of Cue3 (*data not shown*). Most strikingly ubiquitinated was the essential MEN activator Tem1, although this did not noticeably depend on Shp1 (*data not shown*). However, as Tem1 levels have been reported to fluctuate during the cell cycle (Bardin et al., 2000) and Tem1 was confirmed as a Shp1 interactor (*Fig. 21b*), a potential role of Shp1 in cell cycle regulation was addressed in the following experiments.

3.5 Cell cycle defect of *shp1*

3.5.1 *shp1* mutants exhibit a cell cycle delay in mitosis

Further analysis of *shp1* phenotypes revealed that asynchronous *shp1* cells accumulate with replicated DNA, indicating a cell cycle delay after S-phase. Analysis of the DNA content by flow cytometry (FACS analysis) showed a significant accumulation of cells with 2 n DNA content in *Δshp1* compared to wild-type (*Fig. 22a*). In asynchronous wild-type cultures the ratio of cells in G1/S to G2/M is nearly equal with 43 ± 3% in G1/S and 56 ± 3% in G2/M (*Fig. 22b*). Asynchronous *Δshp1* cultures, however, contain only 27 ± 6% cells in G1/S and 73 ± 6% in G2/M (*Fig. 22b*). The accumulation of *Δshp1* cells in G2/M was further confirmed by releasing wild-type and *Δshp1* cultures from a G1 arrest induced by addition of α-factor (*Fig. 22c*). Wild-type and *Δshp1* strains both entered G2/M approximately 60 min after release. While wild-type cells initiated G1 of the following cell cycle after about 120 min, the majority of *Δshp1* cells remained in G2/M throughout the entire time course of the experiment.

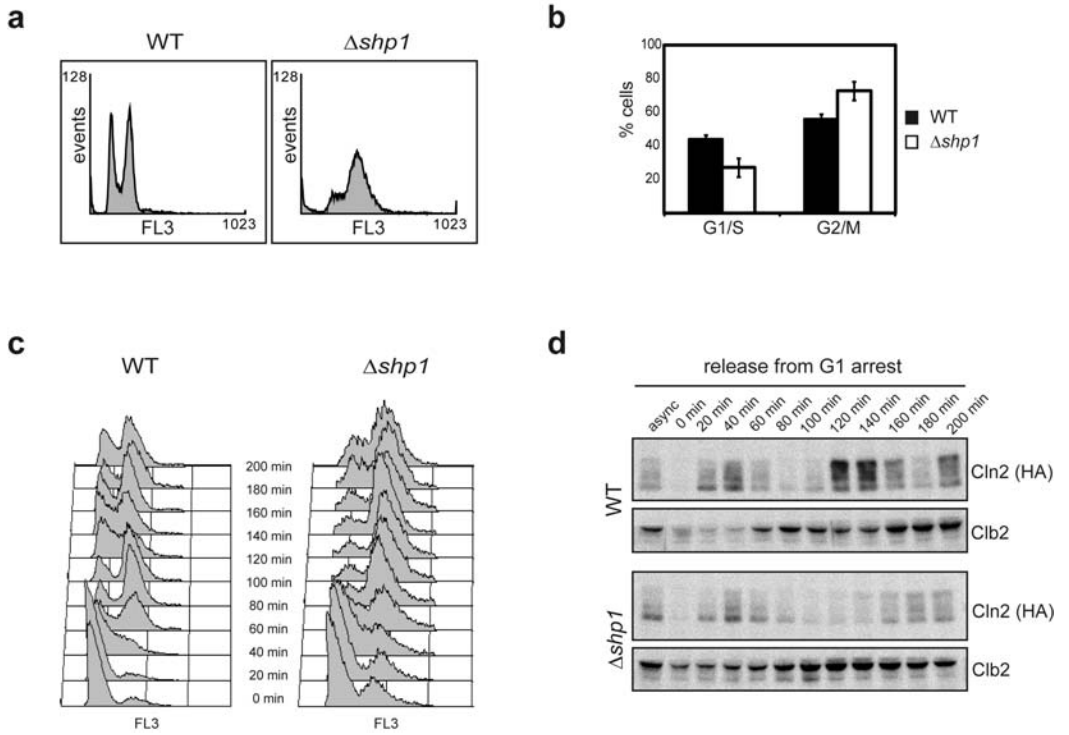

***Fig. 22. Δshp1* cells exhibit a cell cycle delay in mitosis**. a) FACS analysis of DNA content. Cultures of asynchronously growing wild-type (WT) and *Δshp1* strains were fixed and the DNA was stained with propidium iodide. DNA content was measured by flow cytometry. b) Quantification of the percentage of cells in G1/S and G2/M. DNA content of cells during 14 (WT) or 18 (*Δshp1*) independent FACS experiments, using asynchronous logarithmic cultures, was quantified. c) FACS analysis of a release from a G1 arrest. Cultures of WT and *Δshp1* strains were arrested in G1 with α-factor, released, and DNA content was monitored by flow cytometry. FACS samples were collected every 20 min and DNA was stained with propidium iodide. d) α-factor arrest/ release. Exponentially growing WT and *Δshp1 CLN2*^{3HA} strains were arrested in G1 with α-factor and released. Samples were taken every 20 min and Clb2 and Cln2 (HA) levels analyzed by Western blot.

In order to obtain direct evidence for a mitotic delay, the protein levels of the G1 cyclin Cln2 and the mitotic cyclin Clb2 were analyzed. Cln2 is required for progression through START and is rapidly degraded after S-phase entry dependent on SCF^{Grr1} (Bloom and Cross, 2007). The mitotic cyclin Clb2 is expressed during mitosis, ubiquitinated by APC/C^{Cdc20} in early anaphase and by APC/C^{Cdh1} upon mitotic exit, and completely degraded prior to the following G1 phase (Bloom and Cross, 2007). Wild-type and *Δshp1* strains expressing Cln2^{3HA} were arrested in G1 by α-factor, released, and cell cycle progression was monitored by Western blot against Cln2 and Clb2 (*Fig. 22d*). Consistent with the FACS data, the fluctuation of Cln2 protein levels in wild-type and *Δshp1* also indicated that *Δshp1* cells are delayed after the G1/S transition. Clb2 levels persisted significantly longer in *Δshp1* upon release from G1 arrest, again indicating a mitotic delay of *Δshp1* cells.

3.5.1.1 The cell cycle delay of shp1 is not due to a defect in mitotic exit

The activator of the mitotic exit network (MEN), Tem1, was confirmed as a Shp1 interactor (*Fig. 21b*) and *shp1* cells were demonstrated to exhibit a mitotic defect (*Fig. 22*). Therefore, one possibility was that Shp1 directly regulates or influences Tem1 and thereby mitotic exit. Deletion of *SHP1* could cause deregulation of Tem1 activity and subsequently lead to defects in mitotic exit. This would in turn increase the G2/M cell population observed in FACS analysis and cause elevated Clb2 levels. To test if Shp1 is involved in regulating mitotic exit several experimental approaches that had been previously used to identify MEN mutants were employed (Dumitrescu and Saunders, 2002).

The main effector of the mitotic exit network is the phosphatase Cdc14, which is released from the nucleolus and activated. This release and activation of Cdc14 is essential for cells to exit mitosis (Dumitrescu and Saunders, 2002; Bloom and Cross, 2007). Consequently, mutants of the mitotic exit pathway can be rescued by *CDC14* overexpression (Dumitrescu and Saunders, 2002).

CDC14 overexpression was induced in *Δshp1* and the MEN mutant *cdc15-2*. While overexpression of *CDC14* clearly rescued *cdc15-2* at the non-permissive temperature, it had no effect on *Δshp1* growth at 37°C (*Fig. 23a*) or other temperatures, nor did it suppress the G2/M accumulation observed in FACS analysis (*data not shown*).

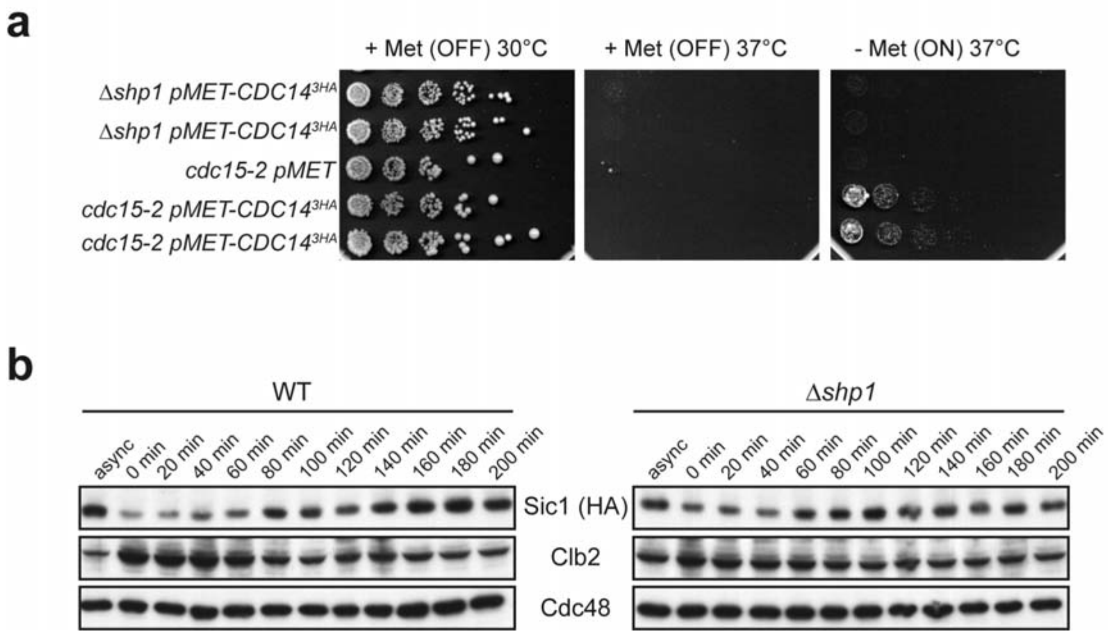

Fig. 23. **Shp1 is not an essential component of the mitotic exit network (MEN)**. a) Overexpression of $CDC14^{3HA}$ to test for mitotic exit network (MEN) involvement. Cultures of the indicated strains were serially diluted and spotted on plates with (promoter off) or without methionine (promoter on). *Δshp1* temperature sensitivity is not rescued by $CDC14^{3HA}$ overexpression, in contrast to the positive control *cdc15-2.* b) Mitotic exit is not delayed in *Δshp1*. Cultures of exponentially growing wild-type (WT) and *Δshp1* $SIC1^{3HA}$ strains were arrested in metaphase with nocodazole and then released. Samples were taken every 20 min and Clb2, HA (Sic1), and Cdc48 (loading control) levels analyzed by Western blot.

Upon release from the nucleolus, Cdc14 dephosphorylates and stabilizes the APC/C activator Cdh1, the Cdc28-Clb inhibitor Sic1 and the transcriptional activator of *SIC1* expression, Swi5 (Dumitrescu and Saunders, 2002; Lew and Burke, 2003). Hence, Sic1 levels rise as mitotic exit is executed and drop again in late G1, when Sic1 is degraded in an SCF^{Cdc4} dependent manner (Feldman et al., 1997; Skowyra et al., 1997).

Wild-type and *Δshp1* $SIC1^{3HA}$ cultures were released from a mitotic arrest induced by nocodazole treatment and Sic1 protein levels were analyzed (*Fig. 23b*). Both strains displayed a stabilization of Sic1 approximately 60- 80 min after the release, coinciding with a strong decrease in Clb2 levels in wild-type and to a lesser extent in *Δshp1* cells. The less pronounced decrease of Clb2 levels in *Δshp1* indicates that the release from the nocodazole arrest did not occur as efficiently as in wild-type.

However, Sic1 levels in *Δshp1* fluctuated similarly to wild-type, indicating that mitotic exit, i.e. Cdc14 release, was not delayed or defective.

Furthermore, some mitotic exit mutants can also be rescued by overexpression of the Cdk1 inhibitor *SIC1* (Dumitrescu and Saunders, 2002). Overexpression of *SIC1* also did not affect growth of *Δshp1* (*data not shown*), again indicating that the cell cycle delay observed is not due to insufficient Clb-Cdc28 kinase inactivation.

Taken together, these experiments demonstrate that Shp1 is not required for mitotic exit and that the cell cycle delay observed in *shp1* mutants is not due to a defect in mitotic exit, despite the observed interaction between Tem1 and Shp1.

3.5.1.2 Null mutants of shp1 exhibit a metaphase to anaphase delay

Δshp1 cells delay cell cycle progression after the G1/S transition but before mitotic exit. To identify the time-point of the delay more precisely, the spindle morphology was analyzed in live-cell fluorescence microscopy. Spindle pole body (SPB) duplication starts in G1, whereas separation of the two SPBs requires the early mitotic cyclins. Only after separation has occurred, two SPBs can be observed *in vivo* (Jaspersen and Winey, 2004). Once the SPBs have separated the mitotic spindle starts to form and reaches about 1.5- 2 µm in length before anaphase onset (Yeh et al., 1995).

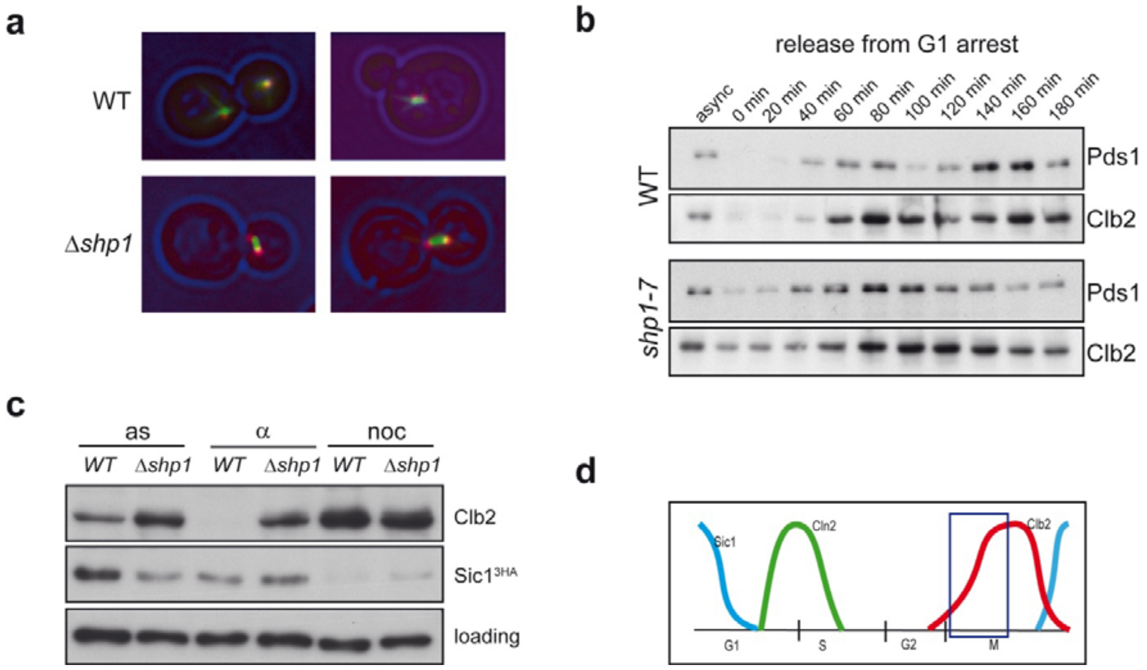

Fig. 24. **Loss of Shp1 results in a delay of cell cycle progression at the metaphase to anaphase transition**. a) *Δshp1* cells arrest with separated spindle pole bodies and short spindles after shift to 14°C. Live-cell fluorescence microscopy of cultures of cells wild-type (WT) or *Δshp1* strains expressing ^{GFP}tubulin1 and SPC42^{Mars}, incubated at 14°C for 7,5h prior to microscopic analysis. b) α-factor arrest/release of WT and *shp1-7 PDS1*^{18myc} strains. Cultures of the indicated strains were arrested in G1 by α-factor, released, and samples were taken every 20 min. Cell cycle progression was monitored by Western blots against Clb2 and Pds1 (myc). c) Steady-state protein levels of Sic1^{3HA} and Clb2. Yeast whole cell lysates of WT and *Δshp1* cultures during logarithmic growth (as, asynchronous), G1 arrest (α, α-factor), and mitotic arrest (noc, nocodazole). Western blot against Clb2 and Sic1 (HA), as well as Cdc48 (loading). d) Schematic overview of cell cycle proteins used as markers for distinct cell cycle stages in c). The blue box indicates the assumed delay time-point of *Δshp1* cells.

Δshp1 and wild-type cells expressing a C-terminal Mars fusion of the spindle pole body protein Spc42 and ^{GFP}tubulin were first grown at the permissive temperature and then shifted to 14°C (*Fig. 24a*). Wild-type cells continued cycling normally (*data not shown*), and as expected cells with one or two separated SPBs and mitotic spindles of different lengths were observed (*Fig. 24a*). *Δshp1* cells, however, arrested in G2/M (*data not shown*), and the majority of cells had two separated SPBs and a short mitotic spindle that divided the nucleus (*Fig. 24a*), indicating a delay in metaphase or early anaphase. In some cases the short mitotic spindle did not align perpendicular to the bud neck, but was rather found in the bud or at the opposite end of the mother cell (*Fig. 24a* and *data not shown*). This could be due to stochastic movements of the nucleus and the spindle along astral microtubules during the duration of the arrest, or alternatively reflect a defect in spindle positioning.

Pds1 (securin) is degraded dependent on the APC/C^{Cdc20} upon metaphase to anaphase transition (Musacchio and Salmon, 2007). Wild-type and *shp1-7 PDS1*^{18myc} strains were arrested in G1, released, and Pds1 levels were analyzed. Consistent with a metaphase to anaphase delay, Pds1 degradation was impaired in *shp1-7* cells (*Fig. 24b*). When released from the G1 arrest, Pds1 was expressed and degraded approximately 40- 80 min after release in wild-type. However, Pds1 was stabilized and detectable until the end of the time course in *shp1-7*, demonstrating that the metaphase to anaphase transition is impaired. The fact that Pds1 and Clb2 levels still decreased in *shp1-7*, albeit with much slower kinetics than in wild-type, reflects the fact that *shp1-7* cells do not arrest but only delay the cell cycle at 25°C. Some cells appear to be able to overcome the mitotic defects and continue to progress through the cell cycle.

A delay at the metaphase to anaphase transition was again confirmed by analysis of the steady-state protein levels of Clb2 and Sic1 in asynchronous wild-type and *Δshp1* cultures. Clb2 levels were high and yet Sic1 levels still low in *Δshp1* cultures (*Fig. 24c,d*), as would have been expected for cells that accumulate in metaphase.

3.5.1.3 The cell cycle delay of shp1 is caused by activation of the spindle checkpoint

The metaphase to anaphase transition is controlled by the spindle assembly checkpoint (SAC) through inhibition of the APC/C^{Cdc20} ubiquitin ligase complex until chromosome bi-orientation is achieved. The delayed metaphase to anaphase transition of *shp1* mutants could therefore be the result of a constitutively active or malfunctioning checkpoint.

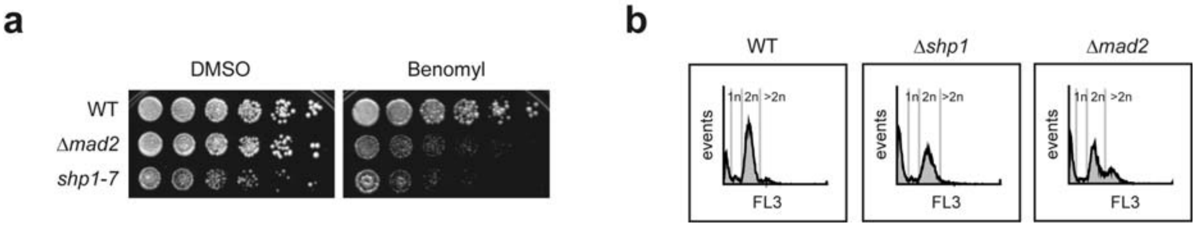

Fig. 25. **Shp1 is not essential for the spindle assembly checkpoint**. a) Benomyl sensitivity of *shp1-7*. Cultures of the indicated strains were spotted in serial dilutions on YPD/DMSO or YPD/10 μg/ml benomyl plates and incubated at 25°C. b) Nocodazole arrest of wild-type (WT), *Δmad2*, and *Δshp1*. FACS analysis of nocodazole arrested cultures of WT, *Δshp1* and *Δmad2*. 1n, 2n and >2n DNA content is indicated in the histograms by vertical gray lines. *Δmad2* shows the expected checkpoint override leading to higher DNA content.

SAC mutants and strains with spindle or kinetochore defects are sensitive to spindle depolymerizing agents, such as benomyl or nocodazole (Hoyt et al., 1991; Li and Murray, 1991; Wang and Burke, 1995). To test for such defects, wild-type, *shp1-7,* and the SAC mutant *Δmad2* were spotted on plates containing benomyl (*Fig. 25a*) and indeed, *shp1-7* and the control strain *Δmad2* both were sensitive to benomyl. This could either indicate that Shp1 is required for SAC activity or that *shp1-7* mutants possess other defects that result in benomyl sensitivity. Hence, the ability of *shp1-7* cells to activate the SAC was analyzed. *Δshp1* cells were clearly proficient in SAC activation in response to lack of attachment, as they arrested in G2/M upon nocodazole treatment and did not accumulate a DNA content larger than 2n, as observed for the *Δmad2* control strain (*Fig. 25b*). Therefore, the sensitivity towards benomyl indicates that *shp1* cells have certain spindle or kinetochore defects that are exacerbated and result in decreased viability upon spindle depolymerization. Consistently, *shp1* null alleles exhibited a strong negative genetic interaction with *Δmad2,* indicating that an intact SAC is critical in these cells (*Fig. 26a*). The very slow growing double mutant *shp1-7 Δmad2* displayed a more equal G1/S versus G2/M distribution of cells in FACS analysis compared to the *shp1-7* null mutant (*Fig. 26b*). This implies that *shp1* cells possess a delayed cell cycle due to activation of the spindle checkpoint, and that deletion of the essential SAC component *MAD2* leads to a “rescue” of this delay. However, as the cause of the checkpoint activation is not resolved, abrogation of the SAC results in more severe defects, possibly missegregation of chromosomes, and in turn in an even stronger growth defect.

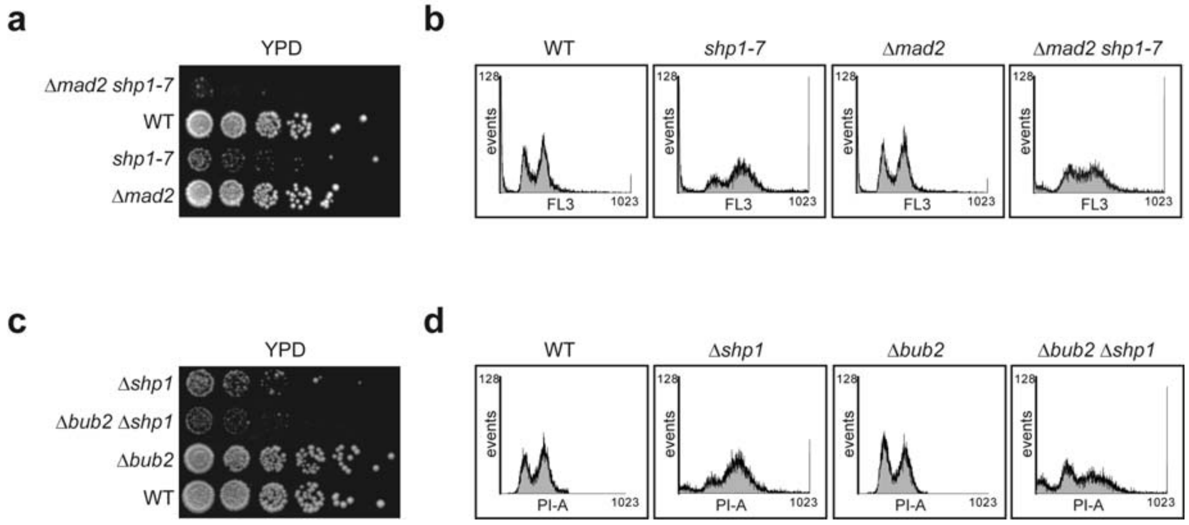

***Fig. 26.* The cell cycle delay of *shp1* mutants is dependent on the spindle checkpoint.** a) The double mutant *Δmad2 shp1-7* displays a strong synthetic growth defect. Fivefold serial dilutions of the haploid spores of one *Δmad2 x shp1-7* tetrad were spotted on YPD plates and incubated at 25°C. b) FACS analysis of *Δmad2 shp1-7* shows more cells in G1 than in *shp1-7*. Cultures of strains as in a) were asynchronously grown and the propidium iodide stained DNA content was measured by flow cytometry. c) *Δbub2 Δshp1* exhibits a synthetic growth defect. Cultures of the haploid spores of one *Δbub2 x Δshp1* tetrad were spotted in serial dilutions on YPD plates and incubated at 25°C. d) FACS analysis of indicated strains as in b).

A similar effect could be demonstrated for the double mutant of *Δshp1* and *Δbub2* (*Fig. 26c,d*). Bub2 is a component of the spindle positioning branch of the spindle checkpoint (Dumitrescu and Saunders, 2002; Lew and Burke, 2003), and is required to prevent mitotic exit upon spindle damage, spindle misorientation, and DNA damage (Wang et al., 2000). The double mutant *Δshp1 Δbub2* exhibits a synthetic growth defect, while the FACS profile is more equally distributed (*Fig. 26c,d*), suggesting that the spindle checkpoint is activated and crucial in *shp1* cells.

3.5.2 The Cdc48^{Shp1} complex is required for the Shp1 cell cycle function

Shp1 is thought to mainly, if not exclusively, function as a Cdc48 cofactor. If Shp1 is required to recruit Cdc48 to certain substrates or cellular compartments during the cell cycle, it would be expected that the observed cell cycle defects should depend on its ability to bind Cdc48. Therefore the Cdc48 binding mutants of *shp1* were analyzed for cell cycle defects and their ability to rescue *shp1* phenotypes.

Even though the two engineered Cdc48 binding mutants *shp1-a1* and *shp1-b1* exhibited growth defects to a slightly different degree (*Fig. 17a*), they both displayed a cell cycle defect very similar to that of *shp1* null mutants (*Fig. 27*).

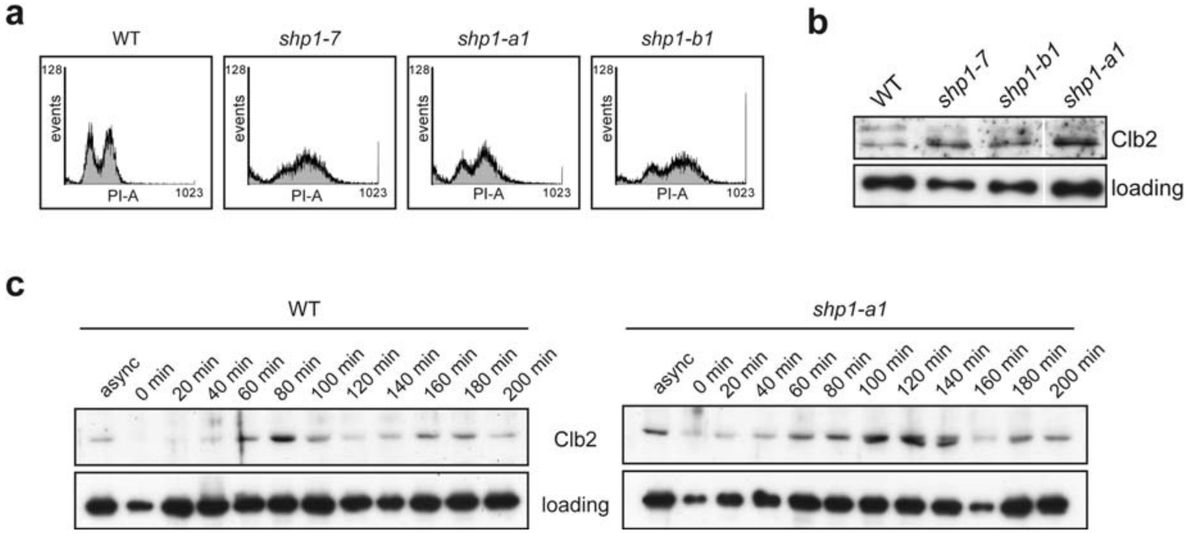

Fig. 27. **The cell cycle function of Shp1 depends on Cdc48 binding.** a) FACS analysis of the DNA content of wild-type (WT), *shp1-7,* and the binding mutants *shp1-a1* and *shp1-b1*. Cultures of the indicated strains were grown asynchronously, DNA was stained with propidium iodide, and the DNA content was measured by flow cytometry. b) Clb2 levels are elevated in *shp1* mutants. Cell lysates from logarithmic, asynchronous cultures of WT and respective *shp1* strains were probed for the mitotic cyclin Clb2. Western blot against Cdc48 serves as a loading control. Note that an irrelevant lane between *shp1-b1* and *shp1-a1* was removed from the figure. All samples depicted were on the Western blot membrane and film, and therefore exposed identically. c) α-factor arrest/release of WT and the binding mutant *shp1-a1*. Cultures of WT and *shp1-a1* were arrested in G1, released, and samples taken every 20 min. Western blot against Clb2 and Cdc48 (loading control). Note that time-points 0 min in both strains and 160 min in *shp1-a1* are of lower total protein concentration, as evident by comparison of the loading control Cdc48.

FACS analysis of asynchronous cultures of the Cdc48 binding mutants *shp1-a1* and *shp1-b1* showed a significant G2/M delay (*Fig. 27a*). All *shp1* mutants consistently exhibited increased levels of the mitotic cyclin Clb2 in asynchronous cultures at room temperature, indicating that the increased G2/M population was indeed due to an increase in mitotic cells (*Fig. 27b*). Finally, release of wild-type and the *shp1-a1* binding mutant from a G1 arrest confirmed a mitotic delay of this mutant (*Fig. 27c*). As observed for the *shp1* null mutation, sustained Clb2 protein levels indicate prolonged mitosis also in *shp1-a1*.

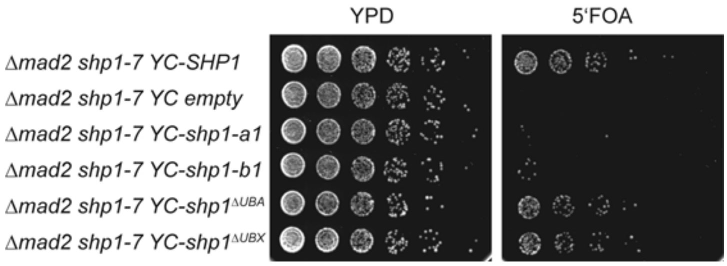

Fig. 28. **Cdc48 binding mutants of *shp1* are synthetically lethal with *Δmad2*.** *shp1-7 Δmad2* cells carrying a *YC33-SHP1* (URA) plasmid were additionally transformed with *YC111* plasmids encoding the indicated *shp1* mutants. Cultures of these strains were spotted in fivefold serial dilutions onto YPD control plates or 5'FOA plates to counter-select against *YC33-SHP1*. Plates were incubated at 25°C.

The double mutant *shp1-7 Δmad2* has a strong growth defect, indicating that a functional spindle assembly checkpoint is required in *shp1-7* cells (*Fig. 26a*). To address if this phenotype results from the lack of a Cdc48$^{\text{Shp1}}$ mediated function, different Shp1 mutants were assayed for their ability to rescue *shp1-7 Δmad2* growth at 25°C (*Fig. 28*). Plasmids encoding *SHP1* or *shp1*$^{\Delta UBA}$ fully rescued growth after counter-selection against the additional wild-type *YC33-SHP1* plasmid on 5'FOA plates. This was expected, as deletion of the UBA domain does not affect Cdc48 binding (*Fig. 16b*). Deletion of the UBX domain reduces binding of Shp1 to Cdc48 and consistently this mutant suppressed the growth defect of *shp1-7 Δmad2* at 25°C (*Fig. 28*), and slightly less well at higher temperatures (*data not shown*). The two Cdc48 binding mutants *shp1-a1* and *shp1-b1* both failed to rescue *shp1-7 Δmad2*, indicating that the negative genetic interaction between *shp1* and *mad2* is linked to the Cdc48$^{\text{Shp1}}$ complex.

Together, these results demonstrate that mutations in Shp1 which abolish Cdc48 binding result in cell cycle phenotypes nearly indistinguishable from those of the *shp1* null mutant. The Cdc48 binding mutants of *shp1* exhibit a cell cycle delay in mitosis and negatively interact with *Δmad2.* This indicates that the Cdc48$^{\text{Shp1}}$ complex is required for proper cell cycle progression at the metaphase to anaphase transition. As Shp1 has been reported to positively regulate Glc7 activity, the role of Cdc48$^{\text{Shp1}}$ in Glc7 mediated cell cycle regulation was analyzed in more detail.

3.6 Regulation of Glc7 cell cycle function by Cdc48$^{\text{Shp1}}$

shp1 mutants were first identified as suppressors of high-copy protein phosphatase 1 (Glc7) (Zhang et al., 1995). These *shp1* alleles displayed phenotypes very similar to those of certain *glc7* alleles (Zhang et al., 1995). Some *glc7* alleles result in a G2/M accumulation dependent on the SAC at the non-permissive temperature (Bloecher and Tatchell, 1999; Sassoon et al., 1999). Shp1 has been proposed to be a positive regulator of Glc7, as deletion of *SHP1* results in reduced phosphatase activity (Zhang et al., 1995; Stark, 1996; Wilson et al., 2005; Cannon, 2010). Since the phenotypes identified for *shp1* widely overlap with those described for *glc7* alleles, they may in part be caused by reduced phosphatase activity and not reflect a direct role of Cdc48^{Shp1} in a certain cellular pathway. In order to be able to differentiate between Cdc48^{Shp1} functions and secondary effects caused by reduced phosphatase activity, experiments addressing the relationship of Shp1 and Glc7 were conducted.

3.6.1 Interaction of Shp1 with Glc7

Even though Shp1 has been described as a positive regulator of Glc7, no physical interaction has been reported so far (Cannon, 2010). The RVxF motif that mediates binding of some targeting subunits to Glc7 could also not be identified within the Shp1 sequence. As most Glc7 targeting subunits have been shown to interact with Glc7 using the Y2H system, these experiments were also conducted with Glc7, Shp1, and Cdc48.

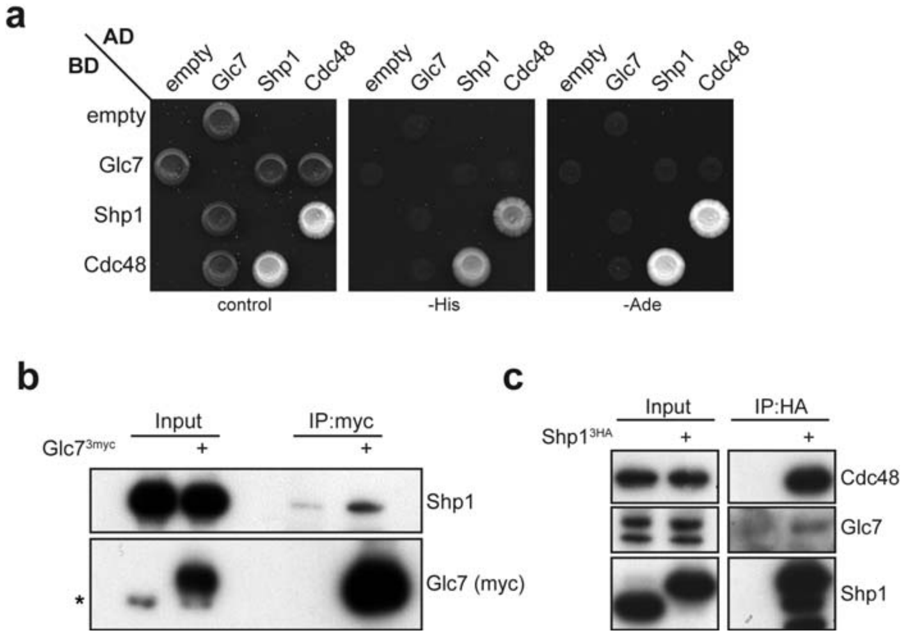

Fig. 29. **Shp1 interacts with Glc7**. a) The directed Y2H assay indicates no interaction of Glc7 and Shp1. PJ69-4A cells were transformed with the indicated combinations of bait (BD) and prey (AD) plasmids and spotted on SC plates lacking tryptophan and leucine (control) or additionally lacking histidine (-His) or lacking adenine (-Ade). The strong Cdc48-Shp1 interaction serves as a positive control. b) Co-immunoprecipitation of Shp1 with Glc7. Glc7^{3myc} was immunoprecipitated from lysates of asynchronous, logarithmic cultures of *SHP1*^{3HA} and *SHP1*^{3HA} *GLC7*^{3myc} strains. Co-immunoprecipitation of Shp1^{3HA} with Glc7^{3myc} was detected by Western blot using Shp1 antibodies. * denotes an unspecific cross-reactive band in the myc-blot. c) Co-immunoprecipitation of Glc7 with Shp1^{3HA}. Shp1^{3HA} was immunoprecipitated from lysates and co-immunoprecipitation of endogenous untagged Glc7 and Cdc48 analyzed by Western blot against Glc7 and Cdc48, as well as Shp1.

No interaction between Glc7 and Shp1, nor Glc7 and Cdc48 could be detected in directed Y2H assays (*Fig. 29a*). However, a weak but reproducible interaction of Shp1 with Glc7^{3myc} could be demonstrated in co-immunoprecipitation experiments (*Fig. 29b*). This interaction was further confirmed by immunoprecipitating Shp1^{3HA} and weak co-immunoprecipitation of untagged endogenous Glc7 (*Fig. 29c).* Interaction between Glc7 and its targeting subunits seems to be somewhat difficult to detect in co-immunoprecipitation experiments with endogenous proteins. Sds22 apparently forms the most stable and abundant complex with Glc7, while other subunits are hardly detectable (Walsh et al., 2002). Therefore the weak but reproducible, and previously undetected, co-immunoprecipitation of Shp1 and Glc7 is presumably significant.

To test for a potential genetic interaction of *shp1* and *glc7,* the *glc7-129* allele was chosen. The phenotype of this cell cycle allele of Glc7 at the non-permissive temperature is a cell cycle arrest in G2/M as large budded cells with separated SPBs and a short mitotic spindle (Baker et al., 1997). Furthermore, the mitotic arrest was reported to be dependent on the SAC (Bloecher and Tatchell, 1999). Sporulation and tetrad analysis revealed that *shp1-7 glc7-129* was inviable at all temperatures tested (*Fig. 30a* and *data not shown*).

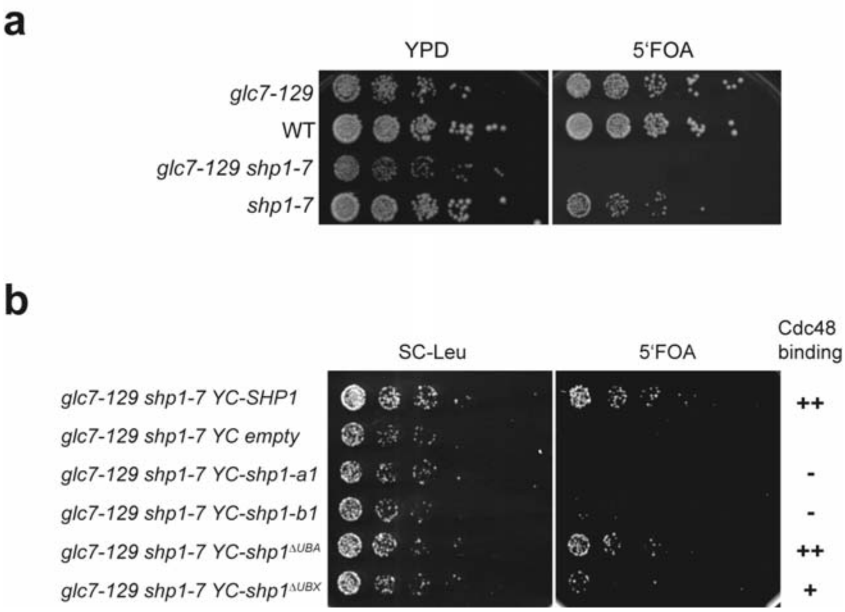

***Fig. 30. shp1-7*-is synthetically lethal with *glc7-129* in a Cdc48 binding dependent manner.** a) The double mutant *shp1-7 glc7-129* is inviable. Cultures of wild-type (WT), single mutants and *shp1-7 glc7-129,* all carrying an additional *YC33-SHP1* plasmid (URA), were spotted in fivefold dilutions either on control (YPD) and 5'FOA plates to counter-select against the wild-type *SHP1* plasmid. The plates were then incubated at 25°C. b) Synthetic lethality of *glc7-129 shp1-7* depends on the Cdc48-binding ability of Shp1. *glc7-129 shp1-7* cells carrying the *YC33-SHP1* plasmid were additionally transformed with plasmids encoding the indicated *shp1* mutants. Cultures of these strains were spotted in fivefold serial dilutions on control SC-Leu plates and 5'FOA plates to counter-select against *YC33-SHP1*. All plates were incubated at 25°C.

As expected, the synthetic lethality of *glc7-129* and *shp1-7* was dependent on the Cdc48-binding ability of Shp1 (Fi*g. 30b*). Viability of *shp1-7 glc7-129* transformed with plasmids encoding mutant forms of *shp1* was analyzed after counter-selection against the wild-type *SHP1* plasmid on 5'FOA. Plasmids encoding *SHP1* or *shp1*$^{\Delta UBA}$ were able to fully rescue growth of the double mutant. *shp1-7 glc7-129* transformed with plasmids encoding either of the two Cdc48 binding mutants of *shp1* or the empty vector was inviable. *shp1*$^{\Delta UBX}$ weakly suppressed the synthetic lethality (*Fig. 30*), most likely reflecting its reduced ability to interact with Cdc48 (*Fig. 16*). These results demonstrate that the Cdc48^{Shp1} complex is required for viability of *glc7-129.*

3.6.2 Glc7 phosphatase activity is reduced in *shp1* mutants

As deletion of *SHP1* reduces Glc7 phosphatase activity (Zhang et al., 1995; Wilson et al., 2005), Glc7 substrates are expected to be hyperphosphorylated in *shp1* null mutants. Glc7 has been described to counteract Ipl1 kinase (the yeast Aurora B homolog) during chromosome bi-orientation (Francisco et al., 1994). A tight balance of kinase and phosphatase activity is required for proper cell cycle progression and growth. Consistently, some mutants of *glc7* suppress the *ipl1* temperature sensitivity (Francisco et al., 1994; Hsu et al., 2000; Pinsky et al., 2006a).

If Glc7 activity is reduced in *shp1*, then a double mutant of *shp1* and *ipl1* should also be able to suppress the temperature sensitivity of *ipl1* mutants. To test this *shp1-7* was crossed with the temperature sensitive allele *ipl1-321,* and viability of the haploid spores was analyzed at different temperatures (*Fig. 31a*). Indeed, the temperature sensitivity of *ipl1-321* at 33°C and partially at 37°C was suppressed by the *shp1* null mutant. Importantly, *shp1-7 ipl1-321* in turn also suppressed the growth defect of *shp1-7* at higher temperatures, indicating that the temperature sensitivity of *shp1-7* may in part be caused by reduced Glc7 activity towards a critical Ipl1 substrate.

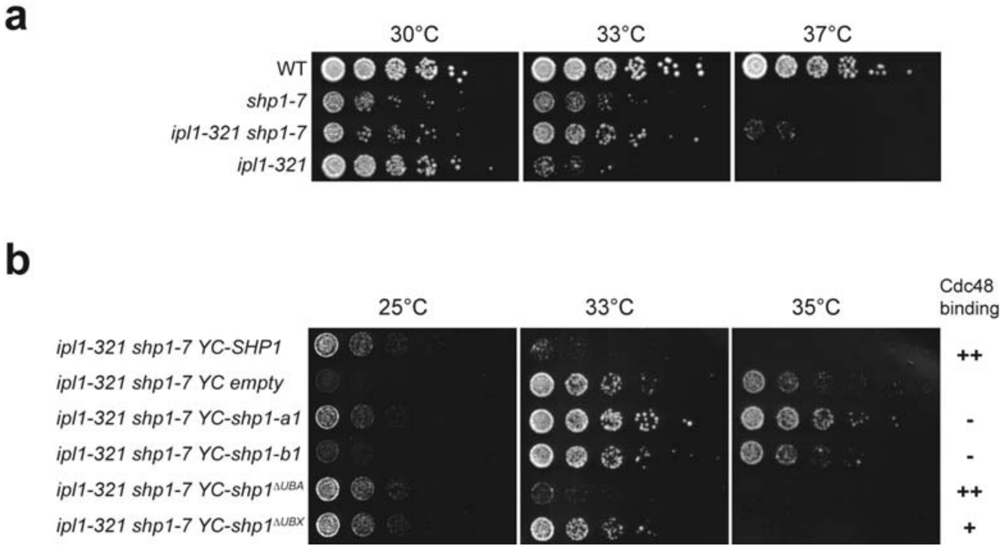

***Fig. 31. shp1* mutants suppress the temperature sensitivity of *ipl1-321* dependent their ability to bind Cdc48.** a) *shp1-7* suppresses the temperature sensitivity of *ipl1-321*. Cultures of the haploid spores of one *shp1-7 x ipl1-321* tetrad were spotted in serial dilutions on YPD plates. The plates were incubated at the indicated temperatures. b) Suppression of temperature sensitivity of *ipl1-321* is dependent on Shp1 binding to Cdc48. *shp1-7 ipl1-321* cells were transformed with the indicated *shp1* mutant plasmids, and serial dilutions of cultures were spotted on SC-Leu plates. The plates were incubated at the denoted temperatures. Note that *shp1-a1* partially rescues the *shp1* growth defect, therefore resulting in improved growth of the double mutant at 35°C.

As for the genetic interaction with *glc7*, the involvement of Cdc48 in the suppression of the *ipl1-321* temperature sensitivity by *shp1* was tested using the *shp1* binding mutants. Indeed, the Cdc48 binding mutants of *shp1* were able to suppress the temperature sensitivity of *ipl1-321* as well as the *shp1* null mutant (*Fig. 31b*). *shp1*$^{\Delta UBX}$, which displays reduced binding to Cdc48 (*Fig. 16*), was able to suppress the temperature sensitivity at 33°C, but not at 37°C. As expected, *shp1*$^{\Delta UBA}$ did not rescue the ts phenotype to any extent, as this mutation does not affect the Shp1- Cdc48 interaction.

These results again indicate that the genetic interaction of *shp1* with *ipl1* and *glc7* is dependent on the Cdc48^{Shp1} complex.

3.6.2.1 Substrates of Glc7 and Ipl1 are hyperphosphorylated in shp1

To directly address if substrates of Glc7 are hyperphosphorylated in *shp1*, modification of the kinetochore protein Dam1 and Histone H3 was analyzed. Both Dam1 and Histone H3 have been described as common substrates of Ipl1 and Glc7 that are regulated by phosphorylation during the cell cycle (Hsu et al., 2000; Kang et al., 2001).

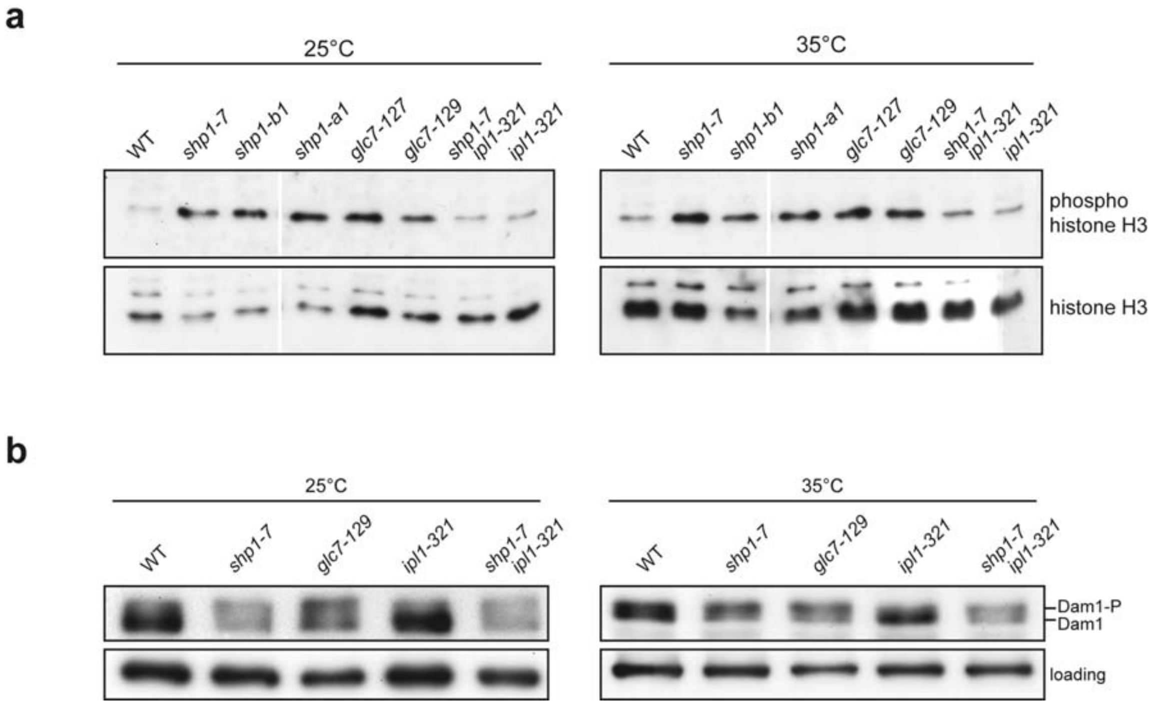

***Fig. 32.* Hyperphosphorylation of Glc7 substrates in *shp1-7*.** a) Histone H3 phosphorylation is increased in *shp1* mutants. Logarithmic cultures were either grown at 25°C or shifted to the non-permissive temperature (35°C) for 3 h. Whole cell lysates were prepared and were analyzed by Western blot against phosphorylated histone H3 S10 and total histone H3. Note that an irrelevant lane between *shp1-b1* and *shp1-a1* was removed from all blots. All samples were exposed identically, since they were on the same Western blot membrane and film. b) The kinetochore protein Dam1 is hyperphosphorylated in *shp1-7*. Asynchronous cultures of wild-type (WT), *shp1-7*, *glc7-129*, *ipl1-321*, and *shp1-7 ipl1-321 DAM1*^{9myc} strains were either grown at 25°C or shifted to the non-permissive temperature for 3 h. Cell lysates were analyzed by Western blot against Dam1 (myc) and Cdc48 (loading control). Dam1-P indicates the more slowly migrating phosphorylated forms of Dam1.

Residue S10 of histone H3 is phosphorylated by Ipl1 during mitosis (Hsu et al., 2000). In addition to being a marker for mitotic cells, H3 S10 phosphorylation has also been shown to depend on the balance of Ipl1 kinase and Glc7 phosphatase activity (Hsu et al., 2000).

Thus, phosphorylation of histone H3 was analyzed by Western blot of cell lysates from asynchronous cultures at the permissive and non-permissive temperature (*Fig. 32a*). For this purpose an antibody specifically detecting histone H3 S10 phosphorylation was used. The phosphorylated form of H3 was strikingly increased in *shp1-7* cells compared to wild-type. This effect was similar to the hyperphosphorylation observed in *glc7-127* and *glc7-129* cells. Interestingly, the increase in phosphorylated histone H3 was also observed for the Cdc48 binding mutants of *shp1* (*shp1-b1* and *shp1-a1*). As expected, the *ipl1-321* mutant exhibited decreased phosphorylation of histone H3 at the non-permissive temperature. However, the double mutant *shp1-7 ipl1 321* restored a wild-type phosphorylation state of histone H3 at both temperatures. This demonstrates that first, Ipl1 kinase activity is already partially reduced at the permissive temperature and secondly, that residual kinase activity is still present at 35°C. Notably, reduction of Glc7 phosphatase activity, by loss of Shp1, restores the kinase to phosphatase balance and results in wild-type phosphorylation of histone H3 in *ipl1-321 shp1-7*. As *shp1* mutation leads to an accumulation of cells in mitosis, an increase in phosphorylated H3 would have been expected regardless of Glc7 activity. Therefore, an additional Ipl1/Glc7 substrate was analyzed.

As the previous results infer that *shp1* null mutants reduce mitotic Glc7 activity, it would be expected that Dam1 is also hyperphosphorylated in *shp1-7*. To assess this, strains expressing $\mathrm{Dam1}^{9myc}$ were shifted to the non-permissive temperature and phosphorylation of Dam1 was analyzed by Western blot (*Fig. 32b*). Dam1 was indeed hyperphosphorylated in *shp1-7* cells, as judged by the altered ratio of upper and lower bands in the Dam1 Western blot. This increase of Dam1 phosphorylation in *shp1* occurred to a similar degree as in the control strain *glc7-129*. It has been demonstrated that the hypophosphorylation of Dam1 in *ipl1* mutants can in part be rescued by reducing Glc7 phosphatase activity (Pinsky et al., 2006a). As expected, *ipl1-321* mutants exhibited a significant reduction of Dam1 phosphorylation at the non-permissive temperature (*Fig. 32b*). Importantly, the phosphorylation state of Dam1 was shifted to a wild-type like situation upon additional null mutation of *shp1*, indicating that the phosphatase to kinase balance was restored (*Fig. 32b*).

Suppression of the *ipl1* temperature sensitivity as well as the hyperphosphorylation of two Glc7/Ipl1 substrates, Dam1 and histone H3, demonstrated that *shp1* mutants exhibit reduced Glc7 activity towards Ipl1 substrates. Furthermore, these results indicate that the $\mathrm{Cdc48}^{Shp1}$ complex is required for the regulation of Glc7 towards these substrates. The reduction of Glc7 activity in *shp1* cells impairs the balance of kinase (Ipl1) and phosphatase (Glc7) required during chromosome bi-orientation and could therefore lead to the observed cell cycle delay in *shp1* mutants.

3.6.2.2 Overexpression of GLC7 suppresses the mitotic delay of shp1 mutants

A general reduction of Glc7 activity in *shp1* is thought to cause the pleiotropic defects observed in this strain (Zhang et al., 1995; Wilson et al., 2005; Cannon, 2010). Consequently, overexpression of functional *GLC7* should, in the most direct possible mechanism of regulation, partially rescue these phenotypes. Overexpression of *GLC7* has been described to be toxic in wild-type cells. *shp1* alleles, however, tolerate *GLC7* overexpression, presumably due to reduced basal Glc7 activity (Zhang et al., 1995).

GLC7 overexpression was induced in wild-type and *shp1-7* strains and growth was analyzed (*Fig. 33a*). Consistent with published results, overexpression of *GLC7* was toxic in wild-type, but tolerated by the *shp1* null mutant. The binding mutants of *shp1*, *shp1-a1* and *shp1-b1,* also tolerated *GLC7* overexpression (*Fig. 33a* and *data not shown*), again indicating that the regulation of Glc7 activity by Shp1 is linked to a $\mathrm{Cdc48}^{Shp1}$ function.

GLC7 is one of less than 5 % of *S. cerevisiae* genes that contain an intron (Spingola et al., 1999). To rule out the possibility that the toxicity of *GLC7* overexpression is caused by overloading the splicing machinery, overexpression of *GLC7* with and without the intron was compared. Both constructs were toxic to wild-type but tolerated by *Δshp1* (*data not shown*). Furthermore, toxicity of *GLC7* overexpression is dependent on a fully functional version of *GLC7*, as indicated by the failure of the partial loss of function variant Glc7^{3HA} to cause toxicity upon overexpression (*data not shown*).

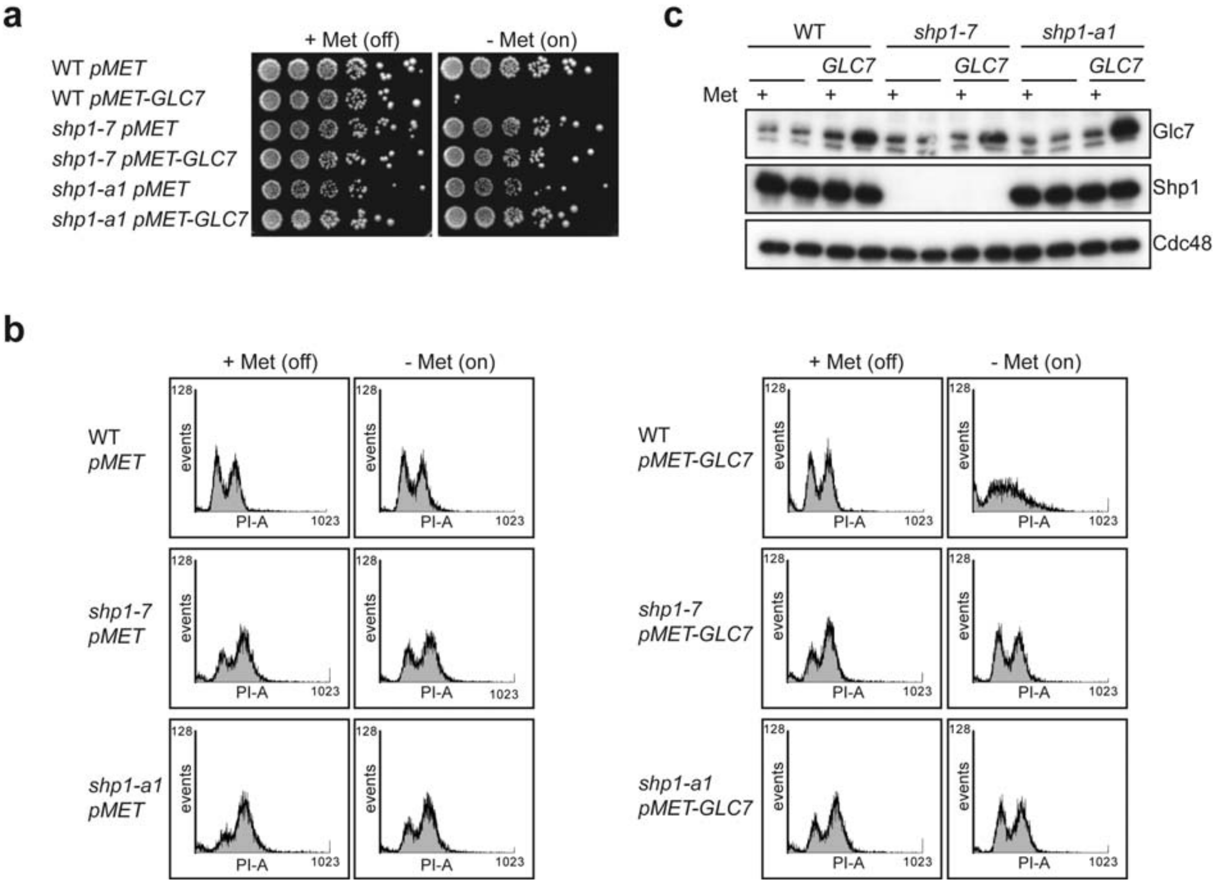

Fig. 33. *GLC7* overexpression suppresses the G2/M delay of *shp1* mutants. a) *shp1-7* and *shp1-a1* tolerate *GLC7* overexpression. *GLC7* was overexpressed by fully inducing the *MET25* promoter. Cultures of the indicated strains were serially diluted and spotted on plates containing (promoter off) or lacking methionine (promoter on). The plates were incubated at 30°C. b) Overexpression of *GLC7* in wild-type (WT), *shp1-7* and *shp1-a1* cells suppresses the G2/M accumulation of *shp1* cells. FACS analysis of logarithmic, asynchronous cultures of WT, *shp1-7* and *shp1-a1 pMET* controls (left) in medium with and without methionine, and of WT, *shp1-7,* and *shp1-a1 pMET-GLC7* (right) with uninduced (+Met) or induced (-Met) *GLC7* overexpression. c) Expression levels of Glc7 during the FACS experiment in b). Whole cell lysates of cultures from b) were analyzed for Glc7 expression by Western blot against Glc7.

FACS analysis of the DNA content of wild-type cells with repressed or induced *GLC7* overexpression confirmed that *GLC7* overexpression was highly toxic (*Fig. 33b, upper right row*). Remarkably, *GLC7* overexpression was not only tolerated by *shp1* mutants, but even suppressed the G2/M accumulation to yield a G1/S to G2/M distribution similar to that of wild-type (*Fig. 33b*). This demonstrates that the cell cycle phenotype of *shp1* presumably results from limiting Glc7 activity. Intriguingly, the rescue observed for cell cycle progression did not lead to a suppression of the growth defect at any temperature (*Fig. 33a* and *data not shown*), indicating that the growth defect, especially the temperature sensitivity, and cell cycle progression are not directly linked.

3.6.3 Nuclear localization of Glc7 in wild-type and *shp1*

All evidence provided so far is consistent with reduced Glc7 activity being the cause of severe phenotypes of *shp1*. However, the mechanism by which the Cdc48$^{\text{Shp1}}$ complex modulates Glc7 phosphatase activity is unknown. One straightforward possibility would be that deletion of *SHP1* reduces Glc7 protein stability. However, the *shp1* alleles identified in the initial *GLC7* overexpression suppressor screen were shown to have reduced PP1 activity, while Glc7 protein levels were not affected (Zhang et al., 1995). Indeed, steady-state protein levels of untagged endogenous Glc7 were not altered in *shp1* mutants (*Fig. 33c, 35b*, *36* and *data not shown*), consistent with the published data (Zhang et al., 1995).

Alternatively, localization of Glc7 could be altered in *shp1* mutants. Glc7 localizes to the nucleus, the cytosol, and the septum (Bloecher and Tatchell, 2000). The Glc7 targeting subunits Ypi1 and Sds22 have been demonstrated to mediate Glc7 nuclear localization (Peggie et al., 2002; Pedelini et al., 2007). Depletion of Ypi1 leads to a cell cycle arrest similar to *glc7* mutants, most likely due to reduced nuclear Glc7 levels (Bharucha et al., 2008).

Therefore, nuclear Glc7 localization was analyzed in wild-type and *shp1* using strains expressing Glc7$^{\text{GFP}}$ as the only source of Glc7. Functionality of the C-terminal GFP-fusion of Glc7 was ensured, as it did not significantly impair growth at any tested temperature (*Fig. 34c)*. Furthermore, FACS analysis of a WT *GLC7*^{GFP} strain demonstrated that this variant of Glc7 did not lead to a cell cycle defect (*Fig. 34d*), suggesting that Glc7$^{\text{GFP}}$ localizes normally to the nucleus and fulfills the critical cell cycle function(s) of Glc7.

As reported (Bloecher and Tatchell, 2000), the majority of Glc7$^{\text{GFP}}$ was detected in the nucleus in wild-type, *shp1-7*, and *shp1-b1* cells (*Fig. 34a*). In all three strains medium and large budded cells also showed distinct localization of Glc7$^{\text{GFP}}$ at the septum. Furthermore, the diffuse cytosolic staining of Glc7$^{\text{GFP}}$ was not altered in either *shp1* mutant, nor could any aberrant localization or aggregation of Glc7$^{\text{GFP}}$ be observed. Quantification of the intensity of the GFP signal in the nucleus compared to the cytosol revealed a slight decrease of nuclear Glc7 to approximately 80% in the *shp1* mutants (*Fig. 34b*).

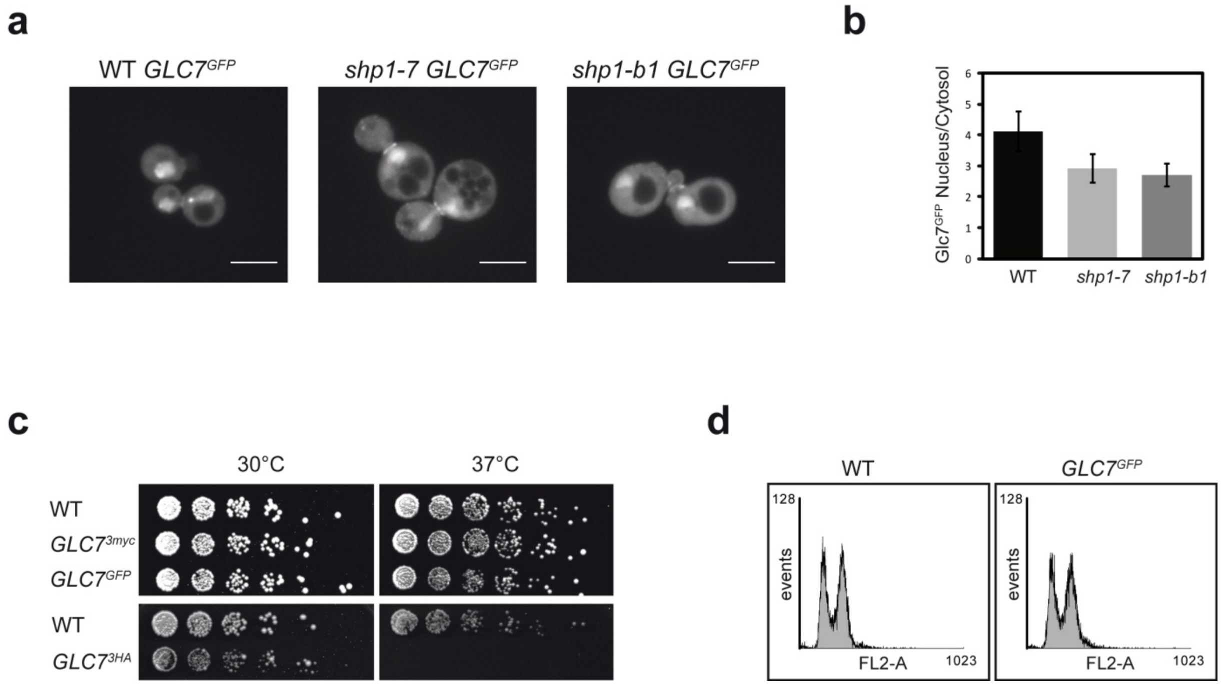

Fig. 34. **Loss of *SHP1* slightly impairs nuclear accumulation of Glc7**. a) Localization of Glc7^{GFP}. Glc7^{GFP} localization in asynchronous logarithmic cultures of indicated yeast strains was analyzed using a confocal spinning disk microscope (scale bar: 5μm). Z-stack projection (sum) performed using ImageJ. b) Quantification of the GFP-signal in nucleus/cytosol in the analyzed strains. Average GFP fluorescence intensity was measured in an area of equal size in the nucleus and cytoplasm and the ratio was calculated. Single z-slices of confocal images were used for the analysis with ImageJ. c) Effect of chromosomal C-terminal epitope tagging of Glc7 on growth. Serial dilutions of cultures of the indicated strains, expressing the respective C-terminally tagged Glc7 variant as the only source of PP1, were spotted on YPD plates. The plates were incubated at 30°C and 37°C. Glc7^{3HA} causes a significant growth defect and temperature sensitivity. d) C-terminal GFP tagging of Glc7 does not cause a cell cycle defect. FACS analysis of asynchronous cultures of wild-type (WT) and *GLC7*^{GFP} strains.

Interestingly, in the course of these experiments, it became evident that the nuclear localization of Glc7^{GFP} is influenced by the presence of untagged Glc7 in *shp1* mutants. The additional expression of Glc*7* in *shp1-7 GLC7*^{GFP} strains resulted in a notable reduction of the nuclear Glc7^{GFP} signal (*Fig. 35a*). This was dependent on the amount of untagged Glc7 additionally expressed, as a high-copy plasmid encoding *GLC7* under control of the constitutively active *ADH* promoter reduced the nuclear Glc7^{GFP} signal even further (*Fig. 35a,b*). This effect was not observed for wild-type strains, indicating that null mutation of *shp1* does affect Glc7^{GFP} localization. However, lack of Shp1 does not abolish nuclear localization of Glc7^{GFP} if this is the only source of Glc7.

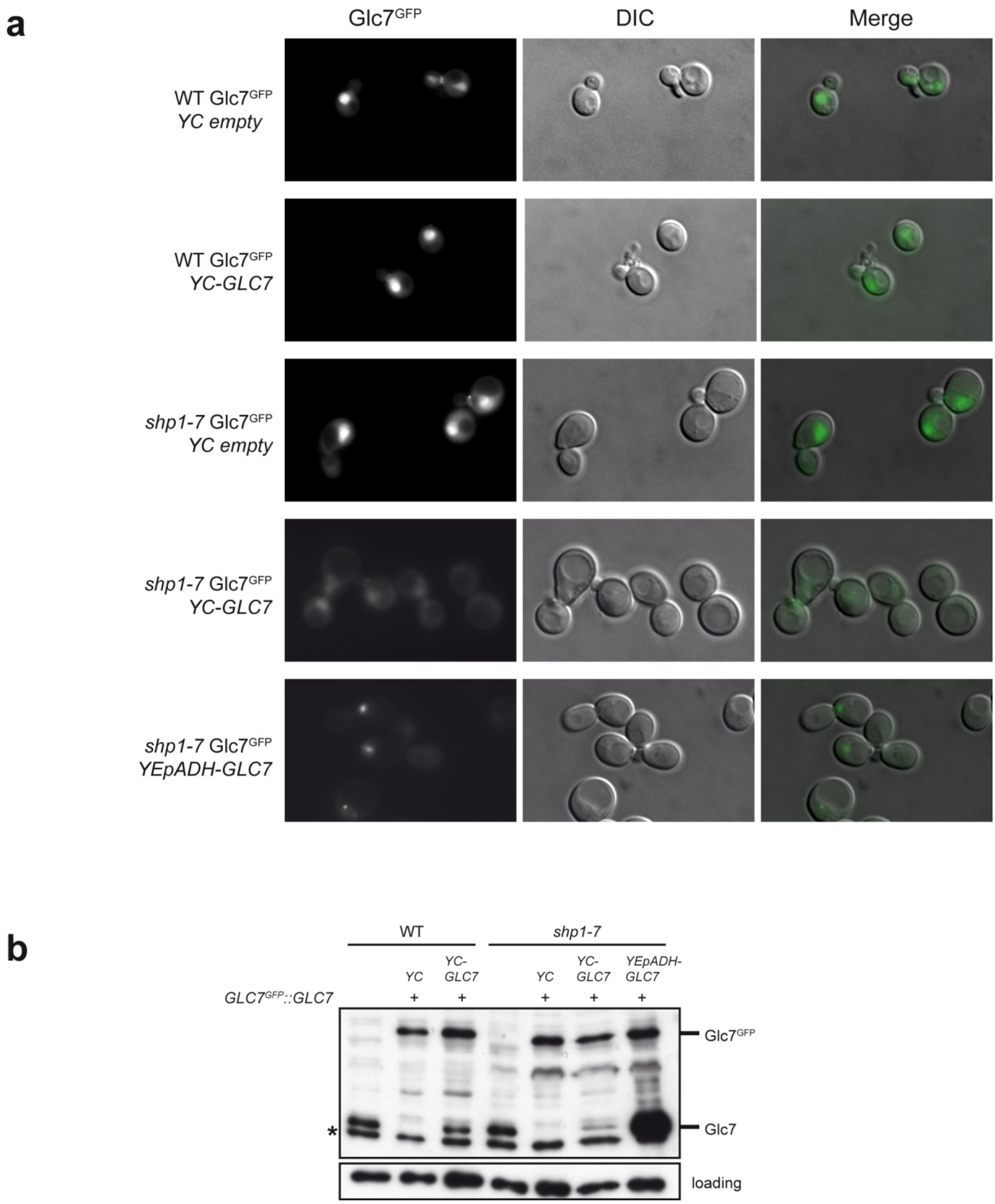
a
Glc7GFP
DIC
Merge
WT Glc7GFP YC empty
WT Glc7GFP YC-GLC7
shp1-7 Glc7GFP YC empty
shp1-7 Glc7GFP YC-GLC7
shp1-7 Glc7GFP YEpADH-GLC7
b
WT
shp1-7
YC
YC-GLC7
YC
YC-GLC7
YEpADH-GLC7
GLC7GFP::GLC7
+
+
+
+
+
Glc7GFP
*
Glc7
loading

Fig. 35. **Additional copies of *GLC7* in *shp1-7* negatively influence the nuclear signal of Glc7$^{\mathrm{GFP}}$.** a) Wild-type (WT) or *shp1-7* strains, expressing Glc7$^{\mathrm{GFP}}$ as the only source of Glc7, were transformed with either empty *YC* plasmids or plasmids encoding the *GLC7* gene under control of the wild-type promoter (*YC-GLC7*) or the ADH promoter (*YEpADH-GLC7*). Asynchronous logarithmic cultures of the indicated strains were used for live-cell fluorescence microscopy. GFP (Glc7) fluorescence, DIC images, and the overlay are depicted. b) Lysates of cultures used for microscopy in a) were analyzed by Western blot against Glc7 and Cdc48 (loading control). Additionally WT and *shp1-7* without endogenously GFP tagged Glc7 are shown. * denotes an unspecific cross-reactive signal in the Glc7 Western blot.

The nuclear localization of Glc7 was further analyzed by testing the interaction of untagged Glc7 with the targeting factor Sds22, which is required for nuclear localization of Glc7 (Peggie et al., 2002; Pedelini et al., 2007; Bharucha et al., 2008).

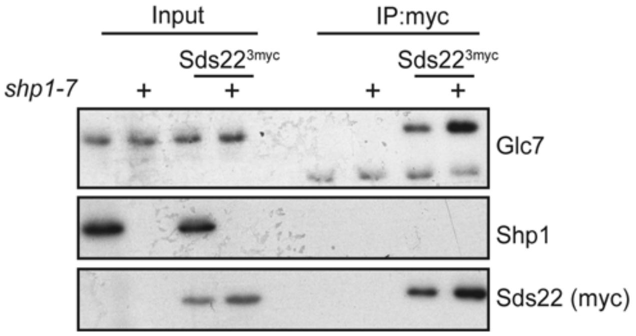

***Fig. 36.* Intact interaction of Glc7 with the nuclear targeting subunit Sds22 in *shp1-7*.** Co-immunoprecipitation of Glc7 with Sds22 from lysates of wild-type (WT) and *shp1-7 SDS22*^{3myc} cultures. Western blot against Glc7, Shp1 and Sds22 (myc).

Co-immunoprecipitation of Glc7 with Sds22 from lysates of wild-type and *shp1-7* strains demonstrated that the interaction was not reduced in *shp1-7* (*Fig. 36*). Assuming that the majority of Sds22 interacts with Glc7 in the nucleus (Peggie et al., 2002), this leads to the conclusion that a major reduction of nuclear Glc7 in *shp1-7* is highly unlikely.

In summary, the presented results rule out the possibility that the nuclear localization of Glc7 is grossly affected in *shp1* null mutants. They are in agreement with the fact that no altered localization of Glc7 was detected in biochemical fractionation assays performed during the initial study that identified *shp1* alleles as suppressors of *GLC7* overexpression (Zhang et al., 1995). However, Shp1 appears to affect Glc7^{GFP} nuclear transport under certain conditions. If untagged Glc7 is present in addition to Glc7^{GFP}, it is preferentially transported into the nucleus of *shp1* cells (*Fig. 35a*). This may either be due to impaired nuclear import of the larger Glc7^{GFP}, or result from preferential binding of Sds22 to the untagged Glc7.

3.6.4 Ubiquitination of Glc7 differs in *shp1*

As neither protein levels nor cellular localization of Glc7 are significantly affected in *shp1*, Glc7 activity in *shp1* mutants could be reduced due to altered posttranslational modification. Mammalian, fission yeast and several other PP1 variants are regulated by inhibitory phosphorylation through Cdc2 early in mitosis. However, this Cdc2 consensus site is not conserved in *S. cerevisiae*, and phosphorylation of Glc7 has not been reported (Dohadwala et al., 1994; Yamano et al., 1994; Cannon, 2010). However, Glc7 peptides were identified in a large-scale purification of ubiquitinated proteins (Tagwerker et al., 2006).

To directly analyze Glc7 ubiquitination *in vivo*, denaturing Ni-NTA pull-downs from yeast strains expressing Glc7^{3myc} and overexpressing ^{His}ubiquitin were performed. In wild-type strains Glc7 was clearly modified by monoubiquitination and perhaps some polyubiquitination (*Fig. 37*). In *Δshp1,* however, the ubiquitination of Glc7 was noticeably shifted to multi or polyubiquitination (*Fig. 37*). Glc7 was modified with multiple ubiquitins (three to four), and a slight reduction of the monoubiquitinated form could be observed. This increase of Glc7 ubiquitination in null alleles of *shp1* was also observed in strains expressing Glc7^{GFP} instead of Glc7^{3myc} (*data not shown*).

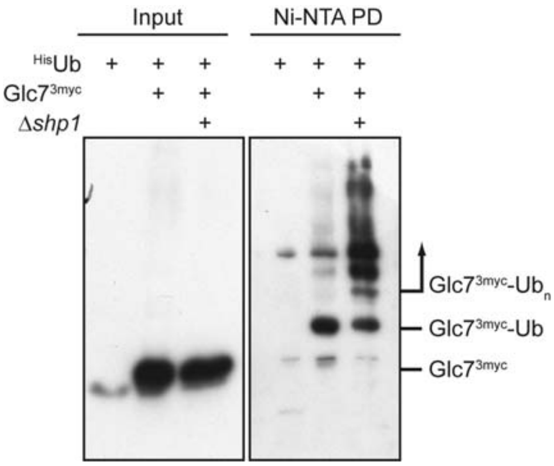

Fig. 37. **Enhanced ubiquitination of Glc7 in *shp1*.** Cultures of wild-type (WT), *GLC7^{3myc}* and *Δshp1 GLC7^{3myc}* strains, all overexpressing ^{His}ubiquitin, were lysed and denaturing Ni-NTA pull-downs of ^{His}ubiquitin performed. Glc7 was detected by Western blot against myc.

However, both myc and GFP epitope tags contain lysine residues that could be unspecifically ubiquitinated. Due to the fact that Glc7^{3HA} is not fully functional (*Fig. 34c*) no Glc7 variant without an additional lysine within the epitope tag could be tested for ubiquitination. Furthermore, analysis of untagged endogenous Glc7 was not possible, as the Glc7 antiserum caused very high background signals in Western blots of ^{His}ubiquitin pull-down samples.

Glc7 protein levels were reported to be constant throughout the cell cycle (Nigavekar et al., 2002). Consequently, Glc7 was stable in wild-type and *Δshp1* during a cycloheximide shut-off experiment (*data not shown*). It is therefore unlikely that this modification of Glc7 by ubiquitin would serve as a degradation signal for the majority of Glc7. Ubiquitination of Glc7 could only affect a very small fraction of the total cellular Glc7 protein, or rather have a non-proteolytic signaling function.

Alternatively, or in result of the increased ubiquitination of Glc7, null mutation of *shp1* could also affect Glc7 interaction with one or more of its regulatory subunits, resulting in altered Glc7 activity.

3.7 Shp1 influences the interaction of Glc7 with Glc8

3.7.1 Genetic interaction of *shp1* with Glc7 targeting subunits

Glc7 itself possesses little or no substrate specificity, therefore the interaction with numerous subunits is required to mediate activity, localization, and substrate recruitment (Stark, 1996; Cannon, 2010). Because altered interaction of Glc7 with its subunits could cause the reduced phosphatase activity in *shp1*, the genetic interaction of *FIN1*, *SDS22,* and *GLC8* with *SHP1* was analyzed.

Fin1 has been proposed to recruit Glc7 to the kinetochore, where Glc7 opposes Ipl1 and mediates exit from the spindle assembly checkpoint (Akiyoshi et al., 2009b). As *FIN1* is not an essential gene and a *Δfin1* mutant does not exhibit any cell cycle defect or a delay in spindle checkpoint silencing, an additional factor responsible for Glc7 kinetochore recruitment must exit (Akiyoshi et al., 2009b). Considering that the cell cycle delay of *shp1* cells depends on the SAC (*Fig. 26*) and that Shp1 possibly interacts with the kinetochore protein Ndc80 (*Fig. 20*), the genetic interaction between *shp1* and *Δfin1* was tested. If Shp1 were required to recruit Glc7 to the kinetochore in *Δfin1*, then the double mutant *Δfin1 shp1-7* should presumably exhibit stronger defects in cell cycle progression or even be synthetically lethal. However, no negative genetic interaction between *Δfin1 and shp1-7* was observed (*data not shown*).

Increased levels of the nuclear targeting subunit Sds22 have been demonstrated to suppress the mitotic phenotype of *glc7-12,* as well as the temperature sensitivity of *ipl1-321* (MacKelvie et al., 1995; Pinsky et al., 2006a). The suppression of *ipl1-321* by *SDS22* is speculated to be due to competition of Sds22 with the critical, still unknown, Glc7 subunit opposing Ipl1, thereby reducing Glc7 function antagonizing Ipl1. As described above, null mutation *shp1* does not alter Glc7 interaction with the nuclear subunit Sds22 (*Fig. 36*).

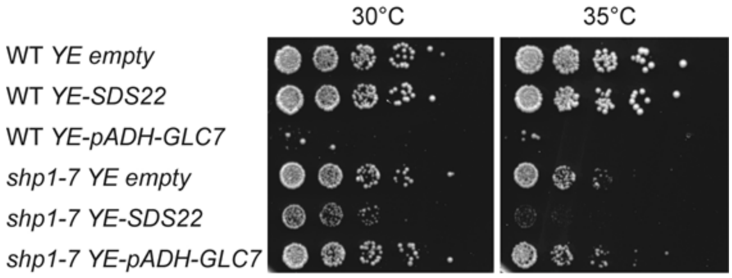

Fig. 38. **Overexpression of *SDS22* is toxic for *shp1-7***. Wild-type (WT) and *shp1-7* strains were transformed with *YEplac195, YEplac195-SDS22*, or *YEplac195-pADH-GLC7,* respectively. Cultures of these strains were spotted in serial dilutions on SC-Ura plates and incubated at the indicated temperatures. Overexpression of *GLC7* serves as a positive control.

Consistent with the hypothesis that null mutation of *shp1* results in decreased mitotic activity of Glc7, *shp1-7* was sensitive towards increased amounts of *SDS22* (*Fig. 38*). Lack of Shp1 could itself affect the interaction of Glc7 with the unknown critical mitotic targeting subunit or substrate and overexpression of *SDS22* would further reduce the interaction below a threshold required for cell cycle progression. Alternatively, null mutation of *shp1* may result in reduced overall Glc7 activity and additionally titrating Glc7 from its critical mitotic subunit could result in even further reduced mitotic Glc7 activity.

Glc8 is a positive regulator of Glc7 activity, whose Glc7 activating function depends on Pho85 mediated phosphorylation at residue T118 (Tung et al., 1995; Cannon, 2010). Deletion of *GLC8* does not result in any major detectable growth or cell cycle defects (*Fig. 39a,c*), but has been shown to cause a reduction of cellular glycogen levels and of Glc7 phosphatase activity (Cannon et al., 1994). Interestingly, the double mutant *shp1-7 Δglc8* was found to be inviable (*Fig. 39a*), indicating that either Glc8 or Shp1 is required for viability, presumably to ensure sufficient Glc7 activity.

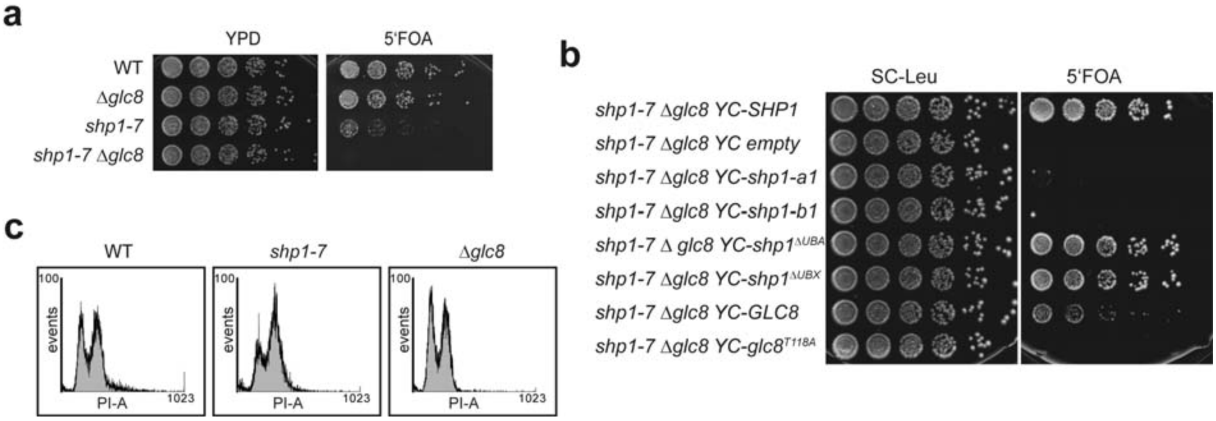

Fig. 39. **Synthetic lethality of *Δglc8* and *shp1-7*.** a) Spotting of fivefold serial dilutions of cultures of the indicated haploid spores of one *shp1-7* x *Δglc8* tetrad, all carrying an additional *YC33-SHP1* (URA) plasmid, on control YPD and 5'FOA plates to counter-select against the wild-type *SHP1* plasmid. Plates were incubated at 25°C. b) *Δglc8 shp1-7* lethality depends on Cdc48 binding of Shp1. *Δglc8 shp1-7* cells carrying the *YC33-SHP1* plasmid were additionally transformed with *YC111* plasmids encoding different *shp1* mutants as well as *GLC8* and *glc8*^{T118A}. Cultures of these strains were spotted in fivefold serial dilutions on control SC-Leu and 5'FOA plates to counter-select against *YC33-SHP1*. Plates were incubated at 25°C. c) FACS analysis of DNA content of wild-type (WT)*, shp1-7, and Δglc8.* Cultures of the indicated strains were grown at RT and the DNA content was measured by flow cytometry.

Some *glc7* alleles are synthetically lethal in combination with *Δglc8* or non-phosphorylatable T118 mutants of Glc8 (Tan et al., 2003). This is consistent with the finding that *glc8*^{T118A} cannot rescue the synthetic lethality of *shp1-7 Δglc8*, while *GLC8* restores growth (*Fig. 39b*). Thus demonstrating that the negative genetic interaction of *shp1-7* and *Δglc8* depends on the Glc7 activating function of Glc8. In addition to the phosphorylation state of Glc8, the binding of Shp1 to Cdc48 is also required for suppression of *shp1-7 Δglc8* lethality (*Fig. 39b*). This again demonstrates that Cdc48 binding of Shp1 is required for normal Glc7 regulation and activity.

As phosphorylated Glc8 binds and activates Glc7, and is required for viability upon null mutation of *shp1*, the interaction of Glc7 and Glc8 *in vivo* was analyzed in wild-type and *shp1* mutants.

3.7.2 The Glc7-Glc8 interaction is reduced in *shp1* null mutants

Glc8 has been demonstrated to physically interact with Glc7 *in vivo* and *in vitro* (Tung et al., 1995). The effect of *shp1* null mutation on the Glc7-Glc8 interaction was analyzed by co-immunoprecipitation. A *shp1-7 GLC8*^{3HA} strain was viable and did not exhibit any synthetic growth defect, indicating that Glc8^{3HA} was functional (*data not shown*). Glc7 co-immunoprecipitation with Glc8^{3HA} from lysates of asynchronous cultures, as well as cultures arrested in G1 by α-factor, was analyzed. The interaction of Glc7 with Glc8 in *shp1-7* was reduced under all tested conditions. Quantification of Glc7 co-immunoprecipitation versus Glc8 immunoprecipitation in wild-type and *shp1-7* asynchronous cultures revealed that the Glc7-Glc8 interaction was reduced by approximately 50% in *shp1-7* (*Fig. 40a,c*).

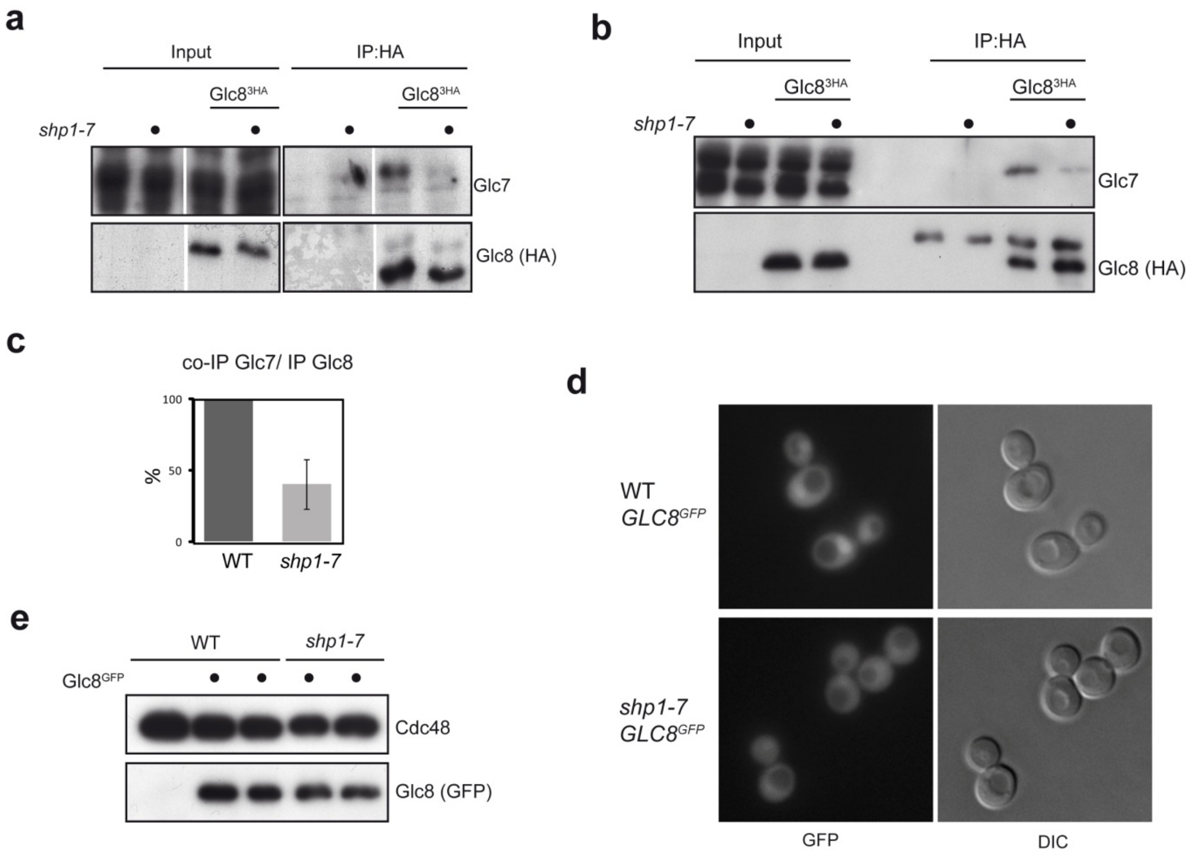

Fig. 40. **Reduced binding of Glc8 to Glc7 in *shp1*.** a) The co-immunoprecipitation (IP) of Glc7 with Glc8^{3HA} is reduced in *shp1-7*. Glc8^{3HA} was immunoprecipitated from lysates of asynchronous wild-type (WT) *GLC8^{3HA}* and *shp1-7 GLC8^{3HA}* cultures. Co-immunoprecipitation of Glc7 was analyzed by Western blot against endogenous Glc7. Note that unrelated, irrelevant lanes were removed from the figure. All samples were on the same Western blot membrane and film and therefore exposed identically. b) The reduced Glc7-Glc8 interaction in *shp1-7* is not caused by the cell cycle delay of *shp1* mutants. Glc8^{3HA} was immunoprecipitated from lysates of WT *Δbar1 GLC8^{3HA}* and *shp1-7 Δbar1 GLC8^{3HA}* strains arrested in G1 with α-factor. Co-immunoprecipitation of Glc7 was detected by Western blot against endogenous Glc7. c) Quantification of three independent co-immunoprecipitation experiments of Glc7 with Glc8 from lysates of asynchronous WT and *shp1-7 GLC8^{3HA}* strains as in a). The Western blot signal of the immunoprecipitated Glc8^{3HA} and the co-immunoprecipitated Glc7 was quantified using ImageJ. The ratio of Glc7 co-IP to Glc8 IP was calculated and normalized to WT. d) Live-cell microscopy of Glc8^{GFP}. FITC (GFP) and DIC images of asynchronous logarithmic cultures of WT and *shp1-7 GLC8^{GFP}* were acquired by live-cell fluorescence microscopy. e) Expression levels of Glc8^{GFP} during microscopy. Cell lysates of strains as in d) were analyzed by Western blot against GFP and Cdc48 (loading control). Two independent clones of each strain were analyzed by Western blot.

The reduced Glc7-Glc8 interaction is not an effect of the altered cell cycle distribution of wild-type and *shp1-7*, as the co-immunoprecipitation from G1 arrested cells shows (*Fig. 40b*). Even though the α-factor arrest efficiency of *shp1-7* is reproducibly lower than that of wild-type, this cannot be the cause of the reduced Glc7-Glc8 interaction. Co-immunoprecipitation of Glc7 with Glc8^{3HA} from asynchronous and arrested wild-type cultures showed that the Glc7-Glc8 interaction slightly fluctuates during the cell cycle, with a peak in metaphase (or during an activated SAC) (*data not shown*). Thus, the inefficient G1 arrest of *shp1-7* would have caused an increased Glc7-Glc8 interaction and the significantly reduced co-immunoprecipitation of Glc7 with Glc8^{3HA} in *shp1-7* after α-factor treatment may be an underestimate of the actual reduction (*Fig. 40b*). This indicates that Shp1 enhances the interaction of Glc7 with its positive regulator Glc8.

How this is achieved remains unclear. Shp1 could not be detected in complex with Glc7 and Glc8 (*data not shown*). Nevertheless, detection of Glc7 interaction with regulatory subunits by co-immunoprecipitation is difficult *in vivo* and this negative evidence therefore does not completely exclude the existence of such a ternary complex.

Alternatively, altered localization of Glc8 could cause a reduced interaction with Glc7. This indeed appears to be the case. In wild-type cells Glc8$^{\mathrm{GFP}}$ exhibits nuclear and cytosolic localization (*Fig. 40d*), consistent with published results (Huh et al., 2003). In contrast, *shp1* null mutants impair the nuclear localization of Glc8$^{\mathrm{GFP}}$ (*Fig. 40d*). This could possibly account for the reduced Glc7-Glc8 interaction in *shp1*, as the nuclear fraction of Glc7 would not be able to interact with Glc8. Glc8$^{\mathrm{GFP}}$ is the only source of Glc8 in *shp1-7* and this strain is viable, indicating that Glc8$^{\mathrm{GFP}}$ must be able to fulfill its role as an activator of Glc7. Furthermore, Glc8$^{\mathrm{GFP}}$ levels were similar in wild-type and *shp1-7* (*Fig. 40e*), indicating that the C-terminal epitope tagging of Glc8 was equally efficient in both strains.

3.7.3 Overexpression of *GLC8* suppresses *shp1-7* temperature sensitivity

Overexpression of *GLC8* has been demonstrated to suppress the *ipl1* temperature sensitivity. This effect was proposed to be due to an inhibitory function of Glc8 towards Glc7 when it is overexpressed. Furthermore, it has been shown that overexpression of non-phosphorylatable T118 mutants of Glc8 is more effective in suppressing *ipl1* temperature sensitivity (Tung et al., 1995).

In order to determine the effect of *GLC8* in *shp1* mutants, *GLC8* was overexpressed under control of the *MET25* promoter in wild-type and *shp1-7*. This construct was able to rescue the *ipl1-321* temperature sensitivity when fully induced, demonstrating that it was functional (*data not shown*). If *GLC8* overexpression is indeed inhibitory to Glc7 activity, it should be toxic to cells already compromised for Glc7 activity. In contrast to this model, the overexpression of *GLC8* and *GLC8*^{3HA} partially suppressed *shp1-7* phenotypes, rather than being toxic. The temperature sensitivity of *shp1-7* at 37°C was slightly suppressed by overexpression of *GLC8*^{3HA} and improved growth could be observed at 35°C (*Fig. 41a*). In contrast, overexpression of *glc8*^{T1183HA} was toxic in *shp1-7* cells (*Fig. 41a*), indicating that the ability of Glc8 to activate Glc7 is critical for the suppression of *shp1-7* phenotypes.

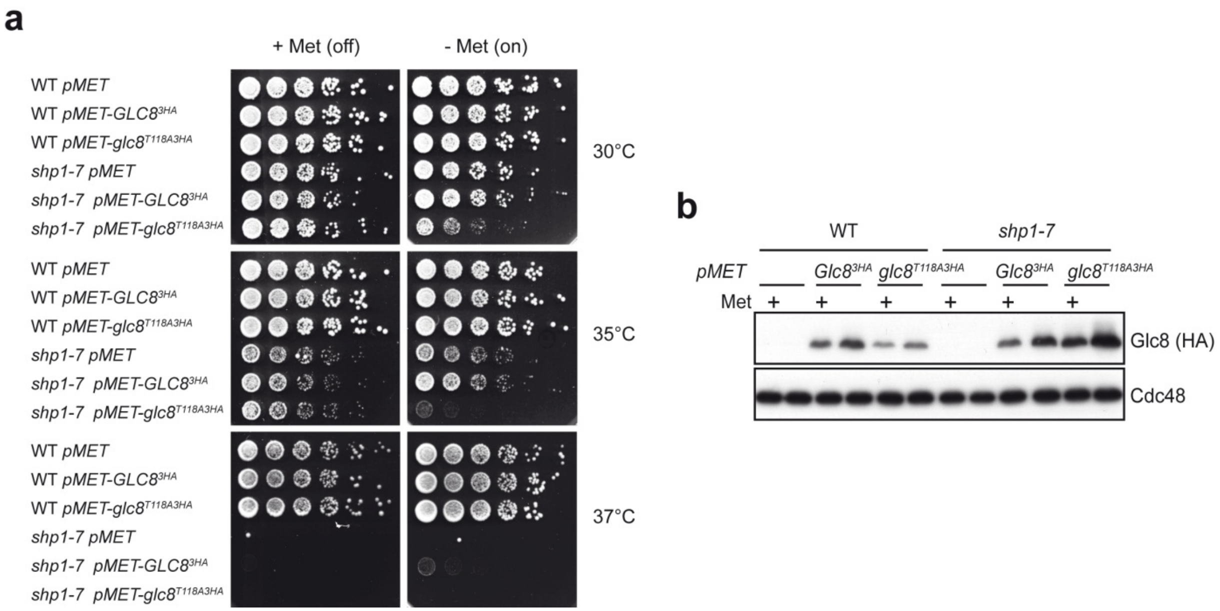

Fig. 41. **Overexpression of *GLC8* suppresses the temperature sensitivity of *shp1-7*.** a) Overexpression of *GLC8* partially suppresses the *shp1-7* temperature sensitivity. Cultures of the indicated strains were spotted in fivefold dilutions on plates containing (promoter off) or lacking methionine (promoter on). Plates were incubated at the indicated temperatures. b) Expression levels of Glc8^{3HA} and Glc8^{T118A3HA} in a). Whole cell lysates of strains spotted on plates at 30°C were analyzed by Western blot against Glc8 (HA) and Cdc48 (loading control).

Even though *GLC8* overexpression partially suppressed the *shp1-7* growth defects at higher temperatures, it did not reproducibly rescue the cell cycle defect of *shp1-7 (data not shown*). Integration of the *pMET-GLC8* construct in *shp1-7*, but not *pMET-glc8*^{T118A}, resulted in a strongly varying degree of suppression of the G2/M accumulation. However, when there was any detectable rescue of the cell cycle defect it was far weaker than that observed after *GLC7* overexpression (*Fig. 33*). Furthermore, overexpression of *GLC8*^{3HA} under control of the stronger constitutive GPD promoter did not rescue the G2/M accumulation to any extent, even though *GLC8*^{3HA} was significantly overexpressed (*data not shown*). Thus, the most plausible interpretation is that *GLC8* overexpression partially suppresses temperature sensitivity, but does not affect the cell cycle defect of *shp1-7,* in agreement with previous evidence that both phenotypes are not strictly linked (*Fig. 33*).

However, some uncertainties remain, as Glc8 previously has been described to regulate Glc7 by inhibition, inactivation, and activation depending on the stoichiometry of the two proteins (Tan et al., 2003; Cannon, 2010). Strong overexpression of *GLC8* is supposedly inhibitory, while a certain amount of Glc8 is required for Glc7 activity. If the ratio of Glc7 to Glc8 is tightly restricted in order for Glc8 to be activating, and in turn for being able to rescue Glc7 activity in *shp1-7*, the wild-type Glc7 to Glc8 ratio would first have to be determined and the experiments repeated with different degrees of *GLC8* overexpression.

4. Discussion

During the course of this work the Cdc48^{Shp1} complex was identified as a regulator of cell cycle progression during the metaphase to anaphase transition by positive regulation of protein phosphatase 1/Glc7.

Deletion of *SHP1* was found to result in severe growth defects and a mitotic delay, phenotypes similar to those of *glc7* alleles. s*hp1* mutants exhibited impaired cell cycle progression at the metaphase to anaphase transition caused by activation the spindle assembly checkpoint (SAC). Furthermore, null mutations of *shp1* reduced nuclear Glc7 activity, as illustrated by the finding that two Glc7 substrates were hyperphosphorylated in *shp1*. The mitotic delay of *shp1* could be suppressed by deletion of a SAC component or by overexpression of *GLC7.* Unperturbed cell cycle progression requires Ipl1 kinase activity to be opposed by Glc7 phosphatase activity (Francisco et al., 1994; Sassoon et al., 1999; Hsu et al., 2000; Pinsky et al., 2006a). Consequently, *shp1* null mutants, like *glc7* alleles (Pinsky et al., 2006a), suppressed the *ipl1-321* temperature sensitivity. Cell cycle progression and wild-type Glc7 activity required the Cdc48^{Shp1} complex, as evident from the analysis of a Cdc48 binding mutant of *shp1*. Shp1 was furthermore demonstrated to interact with Glc7 *in vivo*, and the double mutant of *shp1* and *glc7-129* was found to be inviable.

While all evidence indicates that the severe *shp1* phenotypes are the result of reduced Glc7 activity, the mechanism of Glc7 regulation by Cdc48^{Shp1} remains elusive. Neither Glc7 protein levels nor localization were significantly altered in *shp1*. Glc7, however, was ubiquitinated to a considerably higher degree in *shp1* than in wild-type, which could possibly account for reduced phosphatase activity. Furthermore, the interaction of Glc7 with its positive regulator Glc8 was substantially reduced in *shp1*. Deletion of *GLC8,* or mutation of its phosphorylation site required for Glc7 activation, was lethal in combination with *shp1* null alleles, indicating a requirement of Glc7 activation by Glc8 in *shp1*. The reduced Glc7 activity in *shp1* mutants could be a direct result of the altered ubiquitination, which could in turn negatively affect the interaction between Glc7 and Glc8. Alternatively, the by other mechanisms reduced Glc7-Glc8 interaction in *shp1* could cause the decreased phosphatase activity.

4.1 Phenotypic characterization of *shp1* mutants

The mammalian homolog of Shp1, p47, has been implicated in the regulation of homotypic membrane fusion processes of the Golgi, ER, and nuclear envelope as part of the p97^{p47} complex (Kondo et al., 1997; Hetzer et al., 2001; Meyer, 2005). Even though several large-scale approaches which assayed the yeast knockout libraries for drug sensitivities (SGD, www.yeastgenome.org/), had identified numerous phenotypes of *Δshp1*, no molecular function or substrate of the budding yeast Cdc48^{Shp1} complex was known at the beginning of this work.

Very recently, however, a role of the Cdc48^{Shp1} complex in autophagy has been reported (Krick et al., 2010). The authors demonstrate that *Δshp1* mutants block starvation induced macroautophagy and do not degrade the model substrate GFP-Atg8. Furthermore, *Δshp1* mutants do not accumulate autophagic bodies in the vacuole, indicating a defect in autophagosome biogenesis. Shp1 was shown to directly interact with Atg8 *in vivo* an *in vitro.* The authors propose that Cdc48^{Shp1} functions by extracting Atg8 from a complex with an unknown fusion mediator (Krick et al., 2010). While the interaction of Shp1 with Atg8 was demonstrated to be direct, the authors did not rule out an effect of reduced Glc7 activity in the assays addressing autophagy. No function of Glc7 in autophagy has been demonstrated, however, Glc7 has been reported to regulate intracellular membrane fusion processes, including vacuolar vesicle fusion (Peters et al., 1999; Bryant and James, 2003).

4.1.1 Null mutants of *shp1* exhibit severe growth defects or lethality

Deletion of *SHP1* in *S. cerevisiae* resulted in a strong growth defect in the DF5 strain background and was lethal in the W303 strain background. Substrate specificity of the AAA ATPase Cdc48 is partially mediated by binding of two mutually exclusive substrate-recruiting cofactors, the Ufd1-Npl4 heterodimer and Shp1. Taking into account that Cdc48 as well as Ufd1 and Npl4 are essential for viability, it was not unexpected that deletion of *SHP1* resulted in a severe growth defect as well.

The surprising finding that *SHP1* deletion was lethal in the W303 strain background but viable in DF5, was addressed by analyzing differences between the two commonly used yeast laboratory strain backgrounds, W303 and S288C. The mutation of *RAD5* to *rad5-535* in earlier W303 strains was not responsible for lethality, as W303 *Δshp1 RAD5* was also inviable. A probable cause of this difference in viability of *Δshp1* is the polymorphic gene *SSD1*, which differs in S288C and W303 (see Results).

Ssd1 has been demonstrated to function in the maintenance of cell wall morphology (Kaeberlein and Guarente, 2002). Consequently, *Δssd1* mutants are sensitive to cell wall damaging agents such as osmotin or calcofluor white (Ibeas et al., 2001; Kaeberlein and Guarente, 2002). It has been proposed that Ssd1 functions in a pathway parallel to Pkc1 in regulating cell wall morphogenesis, and is thought to become essential once the Pkc1 pathway is impaired (Doseff and Arndt, 1995; Kaeberlein and Guarente, 2002).

Due to the finding that the temperature sensitivity of *shp1* mutants could be suppressed by 1 M Sorbitol, it appears likely that the loss of Shp1 results in a cell wall defect. Consistently, *shp1* is sensitive to calcofluor white ((Ando et al., 2007) and *data not shown*). It is therefore conceivable that the *ssd1-d2* allele found in W303 increases the cell wall defects already present in *shp1* cells. In agreement with this is the finding that 1 M Sorbitol enables growth of W303 *Δshp1* (*Fig. 14b*). Interestingly, *PKC1* overexpression or high osmolarity also suppresses the *glc7-10* temperature sensitivity, suggesting that Pkc1 signaling is impaired in this mutant (Andrews and Stark, 2000). This could possibly indicate that the s*hp1* cell wall defect is caused by reduced Glc7 activity, which results in decreased Pkc1 signaling and therefore sensitivity towards *ssd1-d2*.

However, as this assumption could experimentally not yet be confirmed, further possibilities were analyzed. The genomes of several yeast strains have been sequenced and can be publically accessed (Wellcome Trust Sanger Institute). Comparison of the sequencing results confirmed the published data that W303 contains an *ssd1* allele with a point mutation (bp 2094) leading to a premature stop codon and C-terminal truncation of the protein by 553 amino acids. In contrast, comparing the W303 and S288C sequences of Cdc48 and its adaptors did not reveal any differences, nor are there mutations resulting in amino acid changes in Glc7 or the PP1 like phosphatases Ppz1 and Ppz2. The only difference found in this limited search was a point mutation within the *GLC8* gene, resulting in an exchange of the terminal amino acid from proline (S288C) to glutamine (W303). No alteration in any other analyzed Glc7 subunit was found. This presumably indicates a complex genetic interaction between the mutation or alteration present in W303 and *shp1*, as would possibly be true for *SSD1*.

4.1.2 The cell cycle defect of *shp1*

One central finding of this work was that null mutations of *shp1* resulted in an accumulation of cells in the G2/M phases of the cell cycle. *shp1* cells arrested with separated spindle pole bodies, a short mitotic spindle, and 2 n DNA content when shifted to the non-permissive temperature 14°C (*Fig. 24*), indicating an arrest during metaphase or early anaphase. This time-point of delay was further confirmed using arrest/release experiments at the permissive temperature of *shp1* null alleles. *shp1* mutants stalled at the metaphase to anaphase transition, as illustrated by stabilized Clb2 and Pds1 (*Fig. 24*). This phenotype had also been reported in an earlier study addressing the role of Shp1 in membrane fusion (Thoms, 2002), and was recently demonstrated for a glucose repressible W303 *pGAL-3HA-SHP1* strain (Cheng and Chen, 2010). As deletion of *SHP1* in W303 is lethal, Cheng and Chen employed a galactose inducible *3HA-SHP1* strain to study the effects of Shp1 depletion upon galactose removal.

Progression though mitosis is thus evidently impaired in *shp1* null mutants. The cause of the G2/M delay could either be a spindle or bi-orientation defect that triggers the SAC or activation of the G2 DNA damage checkpoint. Activation of either checkpoint results in an arrest at the metaphase to anaphase transition with stabilization of Pds1 and Clb2, one of the major defects observed in *shp1* mutants.

Upon DNA damage, the checkpoint kinase Chk1 inhibits the transition to anaphase by phosphorylating Pds1, and Rad53-Dun1 phosphorylation of Bfa1 prevents Clb2 degradation and mitotic exit (Gardner et al., 1999; Wang et al., 2001). Pds1 is hyperphosphorylated in a Rad9 and Mec1 dependent manner only in response to DNA damage (Cohen-Fix and Koshland, 1997; Wang et al., 2001), which inhibits APC/C^{Cdc20} mediated Pds1 ubiquitination and degradation (Agarwal et al., 2003). Additionally, activation of the DNA damage checkpoint induces Rad53-Dun1 mediated hyperphosphorylation of Bfa1, which keeps the Tem1 GAP Bfa1-Bub2 active and thereby inhibits mitotic exit (Hu et al., 2001). Taken together, the phosphorylation state of Bfa1 and Pds1 shows characteristic differences during an activated SAC compared to an active DNA damage checkpoint. Furthermore, mutants of the DNA damage checkpoint such as *Δrad53* and *Δmec1* are not sensitive to benomyl, while all spindle checkpoint components are (Clemenson and Marsolier-Kergoat, 2006).

Pds1 phosphorylation is not strikingly altered in *shp1* compared to wild-type (*Fig. 24b*), suggesting that the DNA damage checkpoint does not induce Pds1 stabilization. Analysis of the Bfa1 phosphorylation state in *Δshp1* was difficult to interpret, as the G1 and mitotic arrest efficiencies of *shp1* cells differed strongly from those of wild-type cells (*data not shown*). However, as it was demonstrated that *shp1* mutants are not defective in mitotic exit (*Fig. 23*), Bfa1 is most likely not hyperphosphorylated by Rad53-Dun1 in *shp1*.

Moreover, *shp1* mutants are sensitive to benomyl, and negatively interact with deletion mutants of spindle checkpoint components such as Mad1 (Collins et al., 2007; Costanzo et al., 2010), Mad2 ((Costanzo et al., 2010) and *Fig. 26*), Bub2 (*Fig. 26)*, and Bub3 (Costanzo et al., 2010), indicating the requirement of an intact spindle checkpoint in *shp1* mutants.

While deletion of the spindle assembly checkpoint component *MAD2* led to an enhanced growth defect in combination with *shp1*, it suppressed the G2/M accumulation of cells observed by flow cytometry (*Fig. 26*). These findings were nearly identical to those published for the depletion of Shp1 in W303 *pGAL-3HA-SHP1 ∆mad2* (Cheng and Chen, 2010). Upon deletion of the central SAC component *MAD2*, the cell cycle delay or arrest induced by SAC activation is abrogated, while the primary defect leading to SAC activation is not resolved.

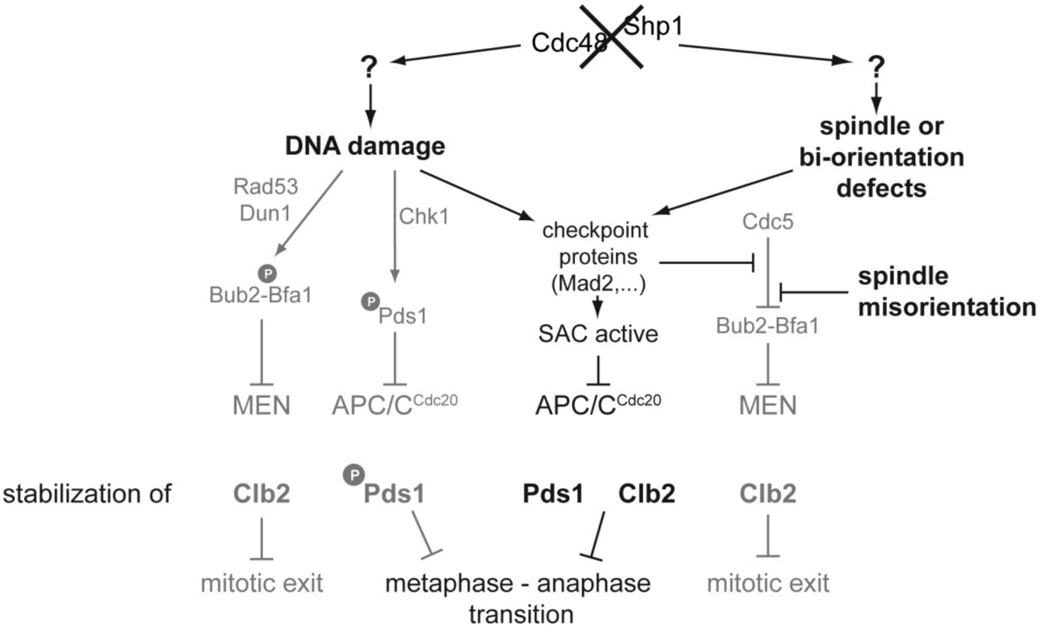
Cdc48 Shp1
?
?
DNA damage
spindle or bi-orientation defects
Rad53 Dun1
Chk1
checkpoint proteins (Mad2,...)
Cdc5
spindle misorientation
P
Bub2-Bfa1
P Pds1
SAC active
Bub2-Bfa1
MEN
APC/C^Cdc20
APC/C^Cdc20
MEN
stabilization of
Clb2
P Pds1
Pds1
Clb2
Clb2
mitotic exit
metaphase - anaphase transition
mitotic exit

***Fig. 42.* Activation of the SAC causes the metaphase to anaphase delay in *shp1* mutants.** Schematic overview of possible mechanisms resulting in a metaphase to anaphase delay with stabilization of Pds1 and Clb2, as observed for *shp1* null mutants. If the Cdc48^{Shp1} complex is lacking, either DNA damage or a spindle/ chromosome bi-orientation defect causes activation of the spindle assembly checkpoint (SAC). An active SAC inhibits the APC/C^{Cdc20} mediated degradation of Pds1 and Clb2. Stabilized Pds1 and Clb2 inhibit the metaphase to anaphase transition. Phosphorylation of Pds1 or inhibition of the mitotic exit network (MEN) independently of the SAC is unlikely, as mitotic exit was demonstrated to be unimpaired in *shp1* mutants and the cell cycle delay was shown to depend on the SAC (therefore depicted in gray).

Therefore, it is evident that the G2 DNA damage checkpoint does not cause the metaphase to anaphase delay independently of the SAC in *shp1*. Thus, stabilization of Clb2 and Pds1 in *shp1* occurs by activation of the SAC and not by phosphorylation of Pds1 by Chk1 upon DNA damage, as SAC inactivation would not enable cells to overcome the inhibitory effect of Pds1 phosphorylation (*Fig. 42*).

However, even though the G2 DNA damage checkpoint and the spindle assembly checkpoint were thought to function mostly independent of each other, emerging evidence suggests a certain degree of crosstalk. Nocodazole treatment, and thereby activation of the SAC, also results in Mad2 dependent phosphorylation of the DNA damage checkpoint regulators Rad53 and Rad9, in the absence and presence of additional DNA damage (Clemenson and Marsolier-Kergoat, 2006). In turn, replication defective *cdc6* mutants activate the SAC (Stern and Murray, 2001). Additionally, it has been demonstrated that DNA damage can activate the SAC independently of a functional kinetochore, but dependent on the kinases Mec1 (ATR) and Tel1 (ATM) (Kim and Burke, 2008).

This interdependence of the G2 DNA damage checkpoint and the SAC make it even more difficult to speculate on the nature of the primary defect in *shp1* mutants based on the presented data. The SAC causes the delay in *shp1* null mutants, as the G2/M accumulation observed in FACS could be suppressed by deletion of the central SAC component *MAD2*. However, so far it cannot be ruled out that some DNA damage results in activation of the SAC in *shp1* (*Fig. 42*).

4.1.3 The cell cycle function of Shp1 depends on the Cdc48^{Shp1} complex

This work demonstrates that the cell cycle function of Shp1 depends on the Cdc48^{Shp1} complex for the first time. Mutation of the Cdc48 binding sites within Shp1 caused a metaphase to anaphase delay and a synthetic growth defect in combination with *Δmad2* (*Fig. 27,28*), which was nearly identical to the phenotypes observed for *shp1* null mutants.

The mitotic phenotype described for the original cold sensitive *cdc48-1* allele was an arrest with unseparated spindle pole bodies, aberrant microtubules, and a large bud (Moir et al., 1982; Frohlich et al., 1991). This suggests a defect in spindle pole body duplication and/or separation, which then leads to a defect in mitosis as no mitotic spindle can be formed. In contrast to this early study, Cheng and Chen report a SAC dependent metaphase arrest for the temperature sensitive *cdc48-3* allele. The authors suggest that a defect in kinetochore-microtubule attachment is responsible for spindle assembly checkpoint activation (Cheng and Chen, 2010), which would be consistent with the defects identified for the Cdc48 binding mutant of *shp1*.

However, as Cdc48 fulfills more than one critical role during cell cycle progression (Moir et al., 1982; Latterich et al., 1995; Cao et al., 2003; Fu et al., 2003; Archambault et al., 2004; Cheng and Chen, 2010), conditional alleles such as *cdc48-1* and *cdc48-3* presumably do not affect one isolated function mediated by one specific Cdc48 sub-complex. Therefore, the phenotypes of these alleles are difficult to interpret as they may arise from the combination of multiple Cdc48 functions and defects. In contrast, the Cdc48 binding mutant of *shp1* is predicted to only affect Cdc48^{Shp1} functions and should not impair further critical processes that depend on other Cdc48 sub-complexes. Using this mutant, it could clearly be demonstrated that at least one cell cycle function of Cdc48, namely the regulation of the metaphase to anaphase transition, is mediated by the Cdc48^{Shp1} complex.

4.2 Regulation of Glc7 cell cycle function by Cdc48^{Shp1}

4.2.1 Reduction of Glc7 activity in *shp1* mutants

Shp1 has been proposed to be a positive regulator of Glc7 phosphatase activity (Zhang et al., 1995; Cannon, 2010). *shp1* cells tolerate *GLC7* overexpression, have reduced PP1 activity, and phenocopy certain *glc7* alleles (Zhang et al., 1995; Wilson et al., 2005). Therefore, investigating the relationship between Shp1 and Glc7 was the main focus of this work.

4.2.1.1 Genetic interaction of shp1 with glc7

The *shp1-7* null allele was found to be synthetically lethal with the cell cycle allele *glc7-129*. This negative genetic interaction depended on Cdc48 binding of Shp1, as demonstrated by the fact that the *shp1* binding mutants *shp1-a1* and *shp1-b1* were unable to rescue the synthetic lethality of *shp1-7 glc7-129* (*Fig. 30*). These findings are consistent with the negative genetic interaction reported for *cdc48-3* and *glc7-12* in the W303 background (Cheng and Chen, 2010). Therefore it is conceivable that Cdc48^{Shp1} regulates a process which is essential in *glc7* mutants.

Furthermore, it was demonstrated that the cell cycle delay of the *shp1* null and the *shp1-a1* binding mutant could be suppressed by *GLC7* overexpression (*Fig. 33*). *GLC7* overexpression has been reported to be involved in silencing an activated SAC (Pinsky et al., 2009). Indeed, *shp1* mutants were demonstrated to delay the cell cycle at the metaphase to anaphase transition in dependence of an activated SAC (*Fig. 26*). Therefore, *GLC7* overexpression could silence the activated checkpoint in *shp1* mutants and result in cell cycle progression and a wild-type FACS profile. This effect would be similar to that observed upon checkpoint inactivation by deletion of *MAD2*.

In contrast, the effect of *GLC7* overexpression in *shp1* mutants significantly differed from the phenotypes observed for the double mutant *shp1 Δmad2*. Deletion of the SAC component *MAD2* in *shp1* resulted in an even stronger growth defect than that observed for the single mutant *shp1* (*Fig. 26,28*), while *GLC7* overexpression in *shp1* had no negative effect on growth (*Fig. 33*). This difference was also reflected by the FACS profiles, as only *GLC7* overexpression resulted in a FACS profile very similar to wild-type, indicating that these cells did not accumulate massive defects. Therefore it is likely that *GLC7* overexpression in *shp1* mutants does not rescue the cell cycle distribution by mere SAC silencing, but rather by increasing nuclear Glc7 activity against still elusive targets above a critical threshold required for cell cycle progression.

4.2.1.2 The Ipl1/Glc7 balance at the kinetochore is impaired in shp1 mutants

Consistent with the assumption that loss of Shp1 reduces Glc7 phosphatase activity, *shp1-7* was shown to exhibit decreased nuclear Glc7 activity towards Ipl1 substrates. Null mutation of *shp1* partially rescued viability of *ipl1-321* at the non-permissive temperature (*Fig. 31*), presumably by decreasing Glc7 phosphatase activity and thereby restoring the kinase to phosphatase balance. Furthermore, the Ipl1/Glc7 substrates histone H3 and Dam1 were demonstrated to be hyperphosphorylated in *shp1* null mutants (*Fig. 32*). Both the suppression of the *ipl1-321* temperature sensitivity as well as hyperphosphorylation of histone H3 was dependent on the loss of Cdc48 binding of Shp1. Therefore, the Shp1 function in regulating Glc7 activity towards Ipl1 substrates is apparently mediated by the Cdc48^{Shp1} complex.

W303 depleted of Shp1 was also demonstrated to suppress *ipl1-321* temperature sensitivity, while *cdc48-3* was not able to suppress this phenotype (Cheng and Chen, 2010). This may indicate that Cdc48 is not involved in regulating the Glc7 function in opposing Ipl1. However, the authors speculate that additional defects of *cdc48-3* prevent the rescue of the *ipl1-321* ts phenotype (Cheng and Chen, 2010). This explanation is likely, as the data for the different *shp1* mutants clearly show that suppression of *ipl1-321* temperature sensitivity inversely correlates with the degree of Cdc48 binding to Shp1 (*Fig. 31*).

shp1 mutants are delayed at the metaphase to anaphase transition due to an activated spindle assembly checkpoint. As discussed in 4.1.2 the delay depends on an intact SAC and is not caused solely by Pds1 and Clb2 stabilization through the G2 DNA damage checkpoint. However, which defect or event triggers the SAC activation is still elusive.
Given the fact that Glc7 has been demonstrated to counteract Ipl1 in regulating attachment of kinetochores to microtubules (Biggins et al., 1999; Sassoon et al., 1999; Kang et al., 2001; Cheeseman et al., 2002; Pinsky et al., 2006a), hyperactivity of Ipl1 at kinetochores in *shp1* is conceivable to be the cause of the attachment defect leading to SAC activation (*Fig. 43*). Unbalanced activity of Ipl1 would result in hyperphosphorylation of one or more critical kinetochore substrates and thereby in an increased number of unattached kinetochores, which in turn activate the SAC (*Fig. 43b*). Consistently, Cheng and Chen demonstrated that lack of Shp1 negatively affects kinetochore-microtubule attachments. Upon Shp1 depletion, one fourth of the analyzed large budded cells exhibited an attachment defect, as indicated by localization of GFP-chromosome III close to one SPB (Cheng and Chen, 2010).
If this assumption were correct, it would be expected that decreasing Ipl1 activity in *shp1* should suppress the attachment defect (*Fig. 43e*). Indeed, reducing Ipl1 activity mutually suppressed the temperature sensitivity of both single mutants, as demonstrated for *ipl1-321 shp1-7* and *ipl1-321* upon Shp1 depletion (*Fig. 31* and (Cheng and Chen, 2010)). Secondly, if Ipl1 phosphorylates certain kinetochore proteins and, due to decreased Glc7 activity in *shp1* mutants, causes an accumulation of kinetochores lacking attachment, the SAC should be activated. Inactivation of the SAC would enable cells to progress through anaphase with chromosomes lacking attachment, leading to chromosome missegregation and presumably decreased viability (*Fig. 43c*), which is consistent with the observed defects in *shp1-7 Δmad2* (*Fig. 26,28*). Furthermore, overexpression of *GLC7* rescued the mitotic delay of *shp1* (*Fig. 33*), possibly by balancing Ipl1 activity at the kinetochore and reducing the number of unattached kinetochores by dephosphorylation of a critical Ipl1 target (*Fig. 43d*).

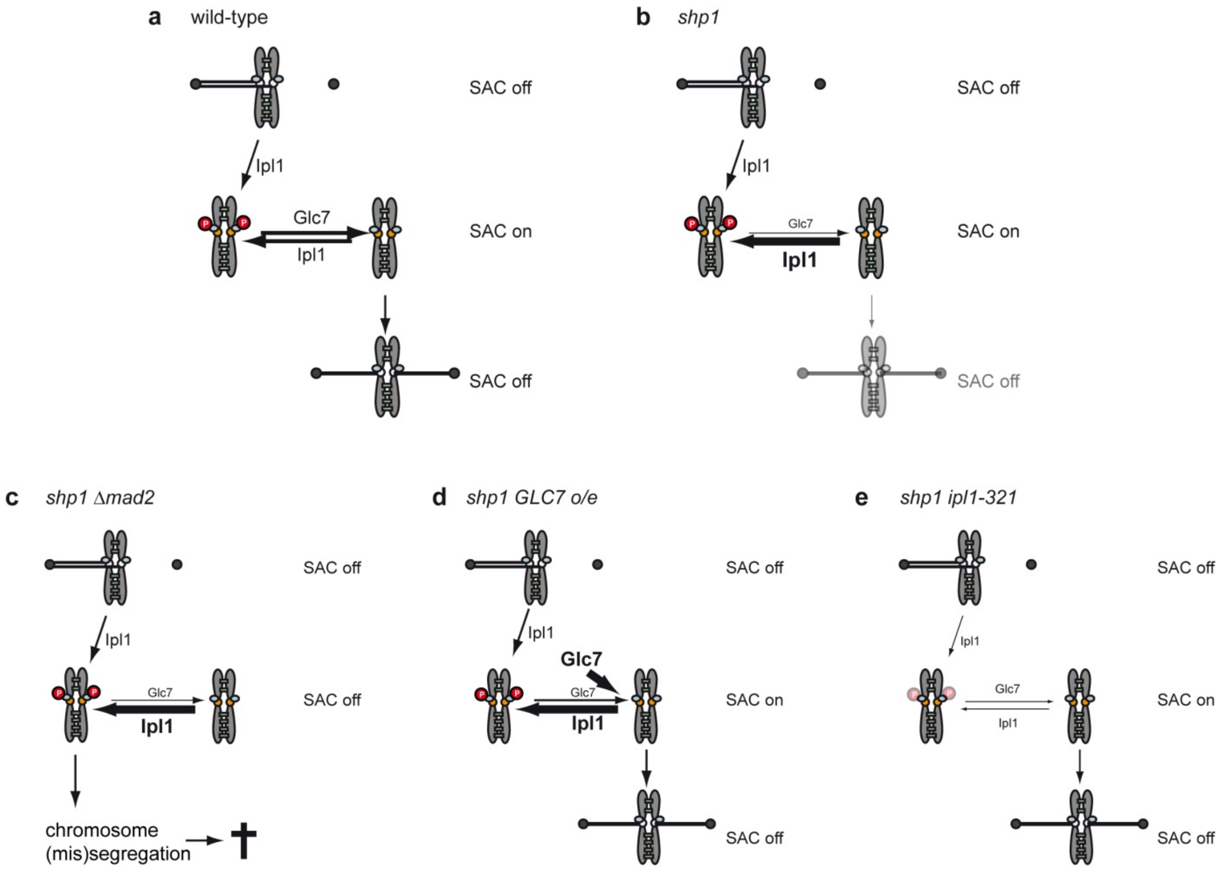

***Fig. 43.* Reduced Glc7 activity in *shp1* results in Ipl1 hyperactivity at the kinetochore and causes SAC activation due to lack of attachment.** Hypothetical model of the Glc7/Ipl1 balance at the kinetochore in different strains. a) In a wild-type situation Ipl1 senses syntelic attachments to SPBs (black) and phosphorylates critical kinetochore proteins (red). This phosphorylation results in impairment of the kinetochore-microtubule interaction and generates kinetochores lacking attachment (orange). Lack of attachment activates the SAC and causes a cell cycle arrest. Glc7 counter-acts the Ipl1 kinase activity towards these substrates and thereby enables microtubule binding and bi-orientation, resulting in cell cycle progression. b) In *shp1* mutants Glc7 activity is reduced and not sufficient to fully balance Ipl1 kinase activity. Ipl1 activity at the kinetochore is therefore high and microtubule binding is reduced. This causes a sustained activation of the SAC and a cell cycle delay. c) Deletion of the SAC component *MAD2* in *shp1* prevents the SAC activation and the cell cycle delay. However, as Ipl1 activity is not balanced at the kinetochore, chromosomes lacking attachment are missegregated and viability is decreased. d) *GLC7* overexpression (o/e) presumably increases Glc7 activity at the kinetochore and the kinase to phosphatase balance is restored. The critical kinetochore protein is more efficiently dephosphorylated by Glc7 and microtubule binding and bi-orientation achieved. e) Reduced Ipl1 activity in *shp1 ipl1-321* double mutants restores the kinase to phosphatase balance at the kinetochore. Additionally, the reduced activity of Ipl1 results in an impaired detection of syntelic attachments lacking tension, presumably causing increased chromosome missegregation. This may also partially be counteracted by the reduction of Glc7 activity in *shp1-7*, further increasing the number of properly bi-oriented chromosomes.

The critical Ipl1 substrate, which must be dephosphorylated by Glc7 to allow proper cell cycle progression, remains to be identified. However, Ipl1 mediated Dam1 phosphorylation is essential for viability, as simultaneous mutation of all phosphorylation sites is lethal (Cheeseman et al., 2002). Furthermore, phospho-mimicking mutants of Dam1 are severely impaired in growth, but can partially suppress the temperature sensitivity of *ipl1-2* mutants. Conversely, such Dam1 serine to aspartate mutants are synthetically lethal with *glc7-10*, while the corresponding alanine mutants of the phosphorylation sites are not (Cheeseman et al., 2002). This suggests that Dam1 could be a critical

Glc7/Ipl1 target. Thus, it will be interesting to test the Dam1 phosphorylation mutants in *shp1* during future studies. If Ipl1 mediated phosphorylation of Dam1 were responsible for the increased lack of attachment and subsequent cell cycle delay in *shp1*, then the Dam1 serine to alanine mutants should at least partially rescue this effect.
Alternatively or additionally, other kinetochore proteins such as Ndc10 or Ndc80 could also be critical Ipl1 substrates that must be dephosphorylated by Glc7 to enable microtubule binding to kinetochores (Biggins et al., 1999; Sassoon et al., 1999; Akiyoshi et al., 2009a). However, a phospho-mimicking mutant of Ndc80 has been demonstrated to exhibit intact kinetochore-microtubule interactions and to arrest with bipolar attached chromosomes (Kemmler et al., 2009), indicating that Ndc80, or these Ndc80 phosphorylation sites, are not involved in regulating the kinetochore-microtubule interaction.

4.2.2 Phosphorylation of Shp1 at five major sites is not required for regulation of Glc7 activity

Recently it was reported that Glc7 activity towards Dam1 and histone H3 is positively regulated by the TOR complex 1 (TORC1) (Tatchell et al., 2011). Mutations of the Tco89 subunit of TORC1 suppress the temperature sensitivity of *ipl1-321* and exhibit hyperphosphorylation of histone H3 and Dam1. Glc7 nuclear localization is reduced by approximately 25% upon Tco89 mutation (Tatchell et al., 2011). As no Glc7 phosphorylation has been reported so far, the authors speculate that regulatory subunits of Glc7 are modified by TORC1 (Tatchell et al., 2011). Shp1 residues S106 and S108 were identified as potential TORC1 sites (Huber et al., 2009), leading the authors to propose that Cdc48^{Shp1} may act downstream of TORC1 to regulate Glc7 (Tatchell et al., 2011).

If Cdc48^{Shp1} indeed acts downstream of TORC1 to regulate Glc7, mutation of the predicted phosphorylation sites within Shp1 should suppress the *ipl1-321* temperature sensitivity. No effect on *ipl1-321* temperature sensitivity was observed in combination with the three phosphorylation mutants of Shp1 (*shp1*^{S106,108A}, *shp1*^{S315,321,322A}, *shp1*^{5A}) (*data not shown*). Furthermore, all three serine to alanine mutants rescued the lethality of *shp1-7 glc7-129* and *shp1-7 Δglc8* and did not display a growth or mitotic defect in FACS (*Fig. 19* and *data not shown*). Unless a dephosphorylation event on Shp1 promotes Glc7 activity, these results indicate that phosphorylation of Shp1 by any kinase at the analyzed sites is not required for regulation of Glc7 activity. As the null mutant of *shp1* exhibits decreased Glc7 activity, it is rather unlikely that the dephosphorylation of Shp1 is required for Glc7 activation. However, to exclude this possibility, phospho-mimicking mutants of Shp1 would have to be tested for genetic interaction with *ipl1*, *glc7,* and *glc8*. Nonetheless, in contrast to the Cdc48 binding mutants, the analyzed phosphorylation mutants of Shp1 clearly do not affect the cell cycle function of the Cdc48^{Shp1} complex.

4.2.3 Mechanism of Glc7 regulation by Cdc48^{Shp1}

Many of the phenotypes identified for *shp1* mutants can be attributed to a process that requires Glc7 activity. For example, *shp1* mutants have been demonstrated to be deficient in glycogen storage, meiosis, and vacuolar fusion, all processes known to be regulated by Glc7 (Cannon, 2010). However, the only process during which an effect on Glc7 substrates has been shown in *shp1* is, as discussed, cell cycle regulation. Dam1 and histone H3 are so far the only Glc7 substrates demonstrated to be hyperphosphorylated in *shp1*.

Even though Shp1 is considered a positive regulator of Glc7, no mechanism or model of regulation has been identified, nor has an interaction between Glc7 and Shp1 been reported (Cannon, 2010). However, the co-immunoprecipitation experiments presented in this work demonstrate that Glc7 does interact with Shp1 *in vivo* (*Fig. 29*).

Shp1 could regulate Glc7 protein levels, localization, posttranslational modification, or the interaction with certain subunits and thereby mediate phosphatase activity. Removal of an unidentified inhibitor from Glc7 may also be plausible. However, strong overexpression of *GLC7* should generate a large excess over the inhibitor and completely restore Glc7 activity. As *GLC7* overexpression neither fully rescues *shp1* nor is toxic in *shp1*, this mechanism of regulation appears unlikely.

4.2.3.1 Protein levels and localization of Glc7 in shp1

Protein levels and localization of Glc7 have been demonstrated to be unaffected by *shp1* null mutation (Zhang et al., 1995), a finding that was verified in this work.

Cheng and Chen, however, postulate that the Cdc48^{Shp1} complex mediates nuclear transport or localization of Glc7 and thereby regulates the Glc7/Ipl1 balance required for proper chromosome bi-orientation (Cheng and Chen, 2010). The authors demonstrate that ^{GFP}Glc7 is excluded from the nucleus upon Shp1 depletion in a W303 *pGAL-3HA-SHP1 GLC7* strain. This is contradictory to what was observed in the DF5 *shp1-7 GLC7*^{GFP} strain (*Fig. 34,35*). Nuclear levels of Glc7^{GFP} are, if at all, slightly reduced in *shp1-7*, but Glc7^{GFP} is by no means excluded from the nucleus. Furthermore, the interaction of Glc7 with its nuclear targeting subunit Sds22 was also demonstrated to be intact in *shp1-7* (*Fig. 36*). The study by Cheng and Chen employed a strain expressing ^{GFP}Glc7 in addition to the endogenous untagged Glc7. The authors did not analyze protein levels of ^{GFP}Glc7 compared to endogenous Glc7, nor did they comment on the functionality of the N-terminally epitope tagged Glc7 variant (Cheng and Chen, 2010). Additional expression of untagged Glc7 in *shp1* strains resulted in a reduced nuclear Glc7^{GFP} signal (*Fig. 35*). This most likely reflects the difference between the results presented in this work and by Cheng and Chen. Therefore, it is improbable that nuclear localization of Glc7 in *shp1* is significantly reduced and it is highly unlikely to be the cause of reduced Glc7 activity towards Ipl1 substrates.

Moreover, Shp1 is thought to be a positive regulator of global Glc7 activity (Cannon, 2010). Lysates of *shp1* strains have reduced total phosphatase activity and deletion mutants are defective in glycogen accumulation (Zhang et al., 1995; Wilson et al., 2005). If the only effect of *SHP1* deletion were decreased nuclear localization of Glc7, one would expect that cytosolic functions of Glc7 should not be affected. Therefore, other or additional mechanisms of Glc7 activity regulation by Cdc48^{Shp1} must exist. The observed slightly decreased nuclear localization could be a consequence rather than the cause of the actual regulatory mechanism, such as posttranslational modification or altered interaction with targeting subunits.

4.2.3.2 Glc7 ubiquitination is altered in shp1

As Glc7 protein stability, expression, and localization are not altered in *shp1* mutants, one further possible regulatory mechanism of phosphatase activity is alteration of posttranslational modification. This work demonstrates for the first time that Glc7 is ubiquitinated *in vivo* and this modification was furthermore shown to be significantly altered in *Δshp1* cells.

Activity of Glc7 must be regulated during the cell cycle by some mechanism, as Glc7 has been demonstrated to be required for chromosome bi-orientation and silencing of the spindle checkpoint. While Glc7 activity is required at the kinetochore to counteract Ipl1 during chromosome bi-orientation, Glc7 must at the same time be restrained from prematurely silencing the spindle checkpoint. This could either be achieved by altering Glc7 localization or by modulating its activity either by binding of regulatory subunits or by modification.

Ubiquitination of Glc7 *in vivo* could directly inhibit phosphatase activity and thereby mediate Glc7 function. Alternatively, ubiquitination could result in degradation of Glc7. However, Glc7 protein levels have been demonstrated to be constant throughout the cell cycle (Nigavekar et al., 2002) therefore, degradation could only affect small amounts of the overall protein. Furthermore, ubiquitination could serve as a non-proteolytic signal and mediate extraction of Glc7 from certain cellular structures, possibly by Cdc48. If Glc7 ubiquitination would function to enable Glc7 extraction, then the sub-complexes from which it must be removed are most likely inhibitory, as it is otherwise not reasonable why Glc7 activity should be reduced in *shp1*. Inhibition of Glc7 within these complexes could be caused by the inability of activating or other regulatory subunits to bind Glc7.

Either degradation or deubiquitination of Glc7 would depend on Cdc48$^{\text{Shp1}}$, as ubiquitinated forms of Glc7 are enriched in *shp1* cells. Interestingly, the DUB Otu1 has been found to exhibit a synthetic growth defect in combination with a *glc7* allele (Logan et al., 2008). Furthermore, Cdc48 and Shp1 have been demonstrated to interact with Otu1 (Rumpf and Jentsch, 2006). In a highly speculative model Cdc48$^{\text{Shp1}}$ in complex with Otu1 could regulate Glc7 ubiquitination. The DUB Otu1 would trim ubiquitin chains on Glc7 required for activation of the phosphatase. Null mutation of *shp1* would result in increased ubiquitination as Cdc48 and Otu1 could not be recruited to the substrate Glc7 by Shp1. This altered ubiquitination of Glc7 could in turn result in reduction of phosphatase activity and cause a cell cycle defect due to decreased Glc7 activity.

This would be similar to the mechanism described for the p97$^{\text{p47}}$ dependent regulation of homotypic membrane fusion during Golgi reassembly (Wang et al., 2004; Meyer, 2005). During Golgi fragmentation so far unidentified critical components are ubiquitinated. Upon activation of p47 in telophase, the p97$^{\text{p47}}$ complex binds these ubiquitinated substrates and the associated deubiquitinating enzyme VCIP135 removes ubiquitin, enabling Golgi reassembly (Wang et al., 2004).

4.2.3.3 Interaction of Glc7 with regulatory subunits in shp1

The described altered posttranslational modification or other mechanisms could also influence the interaction of Glc7 with its regulatory subunits. As Glc7 has little or no substrate specificity this could result in phenotypes resembling *glc7* alleles.

As discussed, binding of the nuclear targeting subunit Sds22 to Glc7 was not affected by *shp1* null mutation. However, overexpression of *SDS22* was toxic in *shp1* cells. Increased expression of *SDS22* suppresses both the mitotic phenotype of *glc7-12* as well as the *ipl1* temperature sensitivity (MacKelvie et al., 1995; Pinsky et al., 2006a). It has been proposed that *SDS22* suppresses *ipl1* by titrating the critical targeting subunit opposing Ipl1 away from Glc7 and thereby reducing phosphatase activity at the kinetochore (Pinsky et al., 2006a). This suggests that the interaction of Glc7 with the critical Ipl1 opposing subunit is essential in *shp1*, presumably because Glc7 activity is reduced.

Furthermore, Shp1 was found to genetically interact with the positive Glc7 regulator Glc8. The double mutant of *shp1* and *Δglc8* was demonstrated to be inviable, supporting the hypothesis that both Glc8 and Shp1 are activators of Glc7. However, the mechanism of Glc7 activation by Glc8 is poorly understood. Several *glc7* alleles have been demonstrated to depend on phosphorylatable Glc8 for viability (Tan et al., 2003). The mammalian Glc8 homolog I-2 presumably fulfills a chaperone analogous function towards PP1 (Alessi et al., 1993). Hence, it has been speculated that Glc8 modulates Glc7 conformation and function, which becomes essential for viability in strains that have particular, not yet defined, Glc7 defects (Cannon, 2010). The synthetic lethality of *shp1-7 Δglc8* could not be rescued by Cdc48 binding mutants of *shp1*, nor by the phosphorylation mutant of *glc8* (*Fig. 39b*), indicating a requirement of Glc7 activation by Cdc48$^{\mathrm{Shp1}}$ or phospho-Glc8. The decreased Glc7 activation in *Δglc8* combined with a reduced Glc7 activity in *shp1* mutants may therefore cause lethality due to insufficient phosphatase activity.

Interestingly, the interaction of Glc7 with Glc8 was significantly impaired in *shp1* null mutants. However, no ternary complex of Shp1, Glc7 and Glc8 could be demonstrated *in vivo*. Thus, if Shp1 does not directly mediate the interaction of Glc7 with Glc8, an altered localization of Glc8, the ubiquitination state of Glc7, or other mechanisms may be responsible for the reduced interaction.

Glc8$^{\mathrm{GFP}}$ nuclear localization appears to be reduced in *shp1* cells (*Fig. 40d*). Therefore, the nuclear pool of Glc7 presumably cannot interact with Glc8, which may account for the observed reduction of the Glc7-Glc8 interaction in *shp1-7*. Additionally, impaired nuclear localization of Glc8 could also affect its phosphorylation state, as Pho85 kinase has been reported to localize mainly to the nucleus (Huh et al., 2003). A reduction of Glc8 phosphorylation would in turn result in a reduced ability of Glc8 to activate Glc7. However, it remains unclear if the altered localization of Glc8 is caused by defects or modification of Glc7 or indicates a mislocalization of Glc8 due to the lack of Shp1.

Nonetheless, consistent with the assumption that a reduced Glc7-Glc8 interaction in *shp1* results in decreased Glc7 activity was the finding that overexpression of *GLC8* partially suppressed the temperature sensitivity of *shp1*. Consequently, overexpression of the *glc8*^{T118A} mutant, which cannot be phosphorylated by Pho85 and is therefore impaired in Glc7 activation, was toxic in *shp1* mutants (*Fig. 41*).

This is in contrast to what has been observed for the suppression of *ipl1* temperature sensitivity. Deletion of *GLC8* and overexpression both suppress the *ipl1* temperature sensitivity. According to the currently accepted model *GLC8* overexpression inhibits Glc7 activity. Furthermore, the suppression of the *ipl1* temperature sensitivity is increased by overexpression of non-phosphorylatable mutants of *GLC8* (Tung et al., 1995). As the suppression of the *shp1-7* temperature sensitivity by overexpression of *GLC8* depended on the phosphorylation sites required for Glc7 activation, it is conceivable that Glc7 activity was not inhibited but rather increased upon overexpression of *GLC8* in *shp1*. The finding that overexpression of the *glc8*^{T118A} mutant was toxic in *shp1* suggests that this Glc8 mutant further reduces Glc7 activity in *shp1*. The non-phosphorylatable Glc8 mutant presumably interacts with Glc7 without being able to activate phosphatase activity, and, as it is overexpressed, titrates the “active” Glc8 away from Glc7, further reducing phosphatase activity.

The presented results are so far consistent with a model in which Cdc48$^{\mathrm{Shp1}}$ regulates the interaction of Glc7 with its activating subunit Glc8. Impairing the interaction of Glc8 with Glc7 in *shp1* reduces Glc7 activity and therefore leads to the observed phenotypes. However, inconsistent with this hypothesis is the fact that *GLC8* is neither essential, nor does the deletion mutant display any strong phenotype. Deletion of *GLC8* results in slightly reduced glycogen levels and reduced Glc7 phosphatase activity, but does not lead to a growth or cell cycle defect ((Cannon et al., 1994), *Fig. 39*). Therefore, the impaired interaction of Glc7 with Glc8 in *shp1* mutants cannot be the only cause of the severe phenotypes of *shp1* mutants.

Furthermore, *GLC8* overexpression does not clearly rescue the cell cycle defect of *shp1*, as overexpression of *GLC7* does. Conversely, *GLC7* overexpression restores a wild-type FACS profile, but does not rescue the temperature sensitivity of *shp1*. This would suggest that *GLC7* and *GLC8* overexpression affect two distinct aspects of *shp1* phenotypes.

The temperature sensitivity of *shp1* was partially suppressed by 1 M Sorbitol, suggesting that this phenotype may be caused by cell wall defects that result in cell lysis at higher temperatures. The cell lysis defect of *glc7-10* at 37°C and the growth defect are suppressed by 1 M Sorbitol or *PKC1* overexpression, while the mitotic defect is unaffected (Andrews and Stark, 2000). This indicates that at least two distinct substrates cause the cell morphology and the mitotic defect of *glc7* mutants. Similarly, overexpression of *GLC8* in *shp1* could possibly affect a Glc7 function required for cell wall morphogenesis and be independent of the mitotic function of Glc7. If the Glc8 interaction with Glc7 were required for the function in cell wall morphogenesis, *GLC7* overexpression may not be sufficient to suppress this defect, as “active” or correctly localized Glc8 could be limiting. The reduced interaction of Glc7 with Glc8 found in *shp1* could in turn cause the cell wall integrity defect and temperature sensitivity. As *Δglc8* mutants are not temperature sensitive (*data not shown*) and do not have any reported cell wall defect, the interaction of Glc7 with Glc8 is not required for cell wall morphogenesis in wild-type yeast cells. However, negative genetic interactions of *Δglc8* with *Δssd1* (*see 4.1.1*) and deletion mutants of the kinases Bck1 and Slt2, which act downstream of Pkc1, have been reported (Fiedler et al., 2009), suggesting a requirement of Glc8 in mutants with cell wall defects.

However, further complicating an interpretation is the reported requirement of a certain Glc7-Glc8 stoichiometry for activation of Glc7 phosphatase activity by a so far poorly understood mechanism (Tan et al., 2003; Cannon, 2010). Therefore, the results of *GLC7* and *GLC8* overexpression may also differ due to the degree of induction and cellular abundance of the respective binding partner. Further experiments have to be performed to address the stoichiometry of Glc7 to Glc8 required for partial suppression of *shp1* phenotypes.

Furthermore, *shp1* mutants could have multiple defects resulting in temperature sensitivity and growth impairment. This appears plausible, as the double mutant of *ipl1-321* and *shp1-7* also partially suppresses the temperature sensitivity of *shp1,* even though Ipl1 is linked to a mitotic function of Glc7. It may therefore be useful to test combinations of partially suppressing conditions, such as the simultaneous overexpression of *GLC7* and *GLC8* in *shp1*, or the phenotypic analysis of *ipl1-321 shp1* in 1 M Sorbitol or upon *PKC1* overexpression.

In summary, at least two Shp1-dependent mechanisms appear to regulate Glc7 activity. First, Shp1 affects the activating Glc8-Glc7 interaction, possibly by mediating nuclear localization of Glc8. Second, the Cdc48$^{\mathrm{Shp1}}$ complex positively regulates the activity of nuclear Glc7 opposing Ipl1 kinase and thereby ensures unperturbed cell cycle progression.

5. Material and Methods

5.1. Material

5.1.1 Chemicals and reagents

Unless otherwise indicated commonly used chemicals were obtained from Roth, Sigma Aldrich, Merck, and Serva.

5.1.2 Databases

The following electronic databases were used: PubMed (http://www.ncbi.nlm.nih.gov/pubmed/), the “Saccharomyces Genome Database” (SGD, http://www.yeastgenome.org/), the Biological General Repository for Interaction Datasets (BioGRID, http://thebiogrid.org/index.php), UniProt (http://www.uniprot.org/), the Saccharomyces Genome Resequencing Project BLAST server (http://www.moseslab.csb.utoronto.ca/sgrp/), and the vector database (VectorDB, http://genome-www.stanford.edu/vectordb/).

5.1.3 Media and plates

5.1.3.1 S. cerevisiae media and plates

YPD (Yeast Peptone Dextrose)

2% (w/v)	glucose (Sigma Aldrich)
1% (w/v)	bacto yeast extract (Difco, BD)
2% (w/v)	bacto peptone (Difco, BD)

Master-mix for drop-out mixtures

20 g	alanine	(Merck)
20 g	arginine	(Merck)
20 g	asparagine	(Merck)
20 g	aspartic acid	(Sigma Aldrich)
20 g	cysteine	(Merck)
20 g	glutamine	(Merck)
20 g	glutamic acid	(Fluka)
20 g	glycine	(Merck)
20 g	inositol	(Sigma Aldrich)
20 g	isoleucine	(Merck)
20 g	lysine	(Merck)
2 g	para-aminobenzoic acid	(Merck)
20 g	phenylalanine	(Merck)
20 g	proline	(Merck)
20 g	serine	(Merck)
20 g	threonine	(Merck)
20 g	tyrosine	(Merck)
20 g	valine	(Merck)

Drop-out mixtures for SC-media and plates

36.7 g	master-mix

addition of the following supplements with the exception of the drop-out(s) of interest

2 g	histidine	(Merck)
4 g	leucine	(Merck)
2 g	uracil	(Sigma Aldrich)
2 g	tryptophan	(Merck)
2 g	methionine	(Merck)
0.5 g	adenine	(Sigma Aldrich)

SC (Synthetic Complete)

2% (w/v)	glucose (Sigma Aldrich) *added after autoclaving*
0.67% (w/v)	yeast Nitrogen Base (Difco, BD)
0.2% (w/v)	drop-out mixture

For most applications 2xSC was used and the pH adjusted to 5.8 prior to autoclaving (if necessary)

YPD and SC- plates

2% (w/v) agar (Difco, BD) was added directly to YPD medium or after autoclaving to 2xSC-medium

Antibiotic selection plates (YPD)

G418 (Roth)	200 mg/l
Nourseothricin (HKI Jena)	100 mg/l
Hygromycin B (Calbiochem)	300 mg/l

added to YPD with 2% (w/v) agar after autoclaving at 55°C

5'FOA plates

2% (w/v)	glucose (Sigma Aldrich) *added after autoclaving*
0.67% (w/v)	yeast Nitrogen Base (Difco, BD)
0.2% (w/v)	SC-complete drop-out powder
0.003% (w/v)	adenine (Sigma Aldrich)
0.003% (w/v)	uracil (Sigma Aldrich)
2% (w/v)	agar (Difco, BD)
0.1% (w/v)	5'fluoroorotic acid (Zymo Research) *added after autoclaving*

Benomyl plates

The appropriate amount of a 1.5 mg/ml Benomyl (Sigma Aldrich) stock solution in DMSO was added to YPD/ 2% (w/v) agar directly after autoclaving.

Further plates for phenotypic analysis

All drugs, with the exception of benomyl, were added to YPD/ 2% (w/v) agar after autoclaving at 55°C.

5.1.3.2 E. coli media and plates

Luria-Bertani-Medium (LB)

1% (w/v)	tryptone (Difco, BD)
0.5% (w/v)	yeast extract (Difco, BD)
1% (w/v)	NaCl

LB-ampicillin/ -kanamycin plates

ampicillin	50 mg/l
kanamycin	30 mg/l

added to LB/ 1.5% (w/v) agar after autoclaving at 55°C

5.1.4 Plasmids

Plasmid	**Source**
pGBD-C1,2,3 *pGAD-C1,2,3*	(James et al., 1996)
YIplac 211, 204, 128 *YCplac 33, 22, 111* *YEplac 195, 112, 181*	(Gietz and Sugino, 1988)
pUG36	(Niedenthal et al., 1996)
pGBT9-SHP1	(Schuberth et al., 2004)
pGBD-shp1$^{\Delta UBX}$	(Schuberth, 2006)
pGBD-shp1$^{S4\Delta UBX}$	(Neves, 2005)
pGBD-shp1^{S1S3S4}	(Neves, 2005)
pGBT9-CDC48	(Braun et al., 2002)
pGAD-CUE3	this work
pGAD-YGL108c	this work
pGAD-YNL155w	this work
pGAD-HDA2	this work
pGAD-TEM1	this work
pGAD-NDC80	this work
pGAD-GLC7	this work
pGBD-GLC7	this work
YEpCUP-^{6xHis}*ubiquitin*	(Hoege et al., 2002)
YCplac33-SHP1	(Schuberth, 2006)
YCplac111-SHP1	(Schuberth, 2006)
YCplac111-shp1-a1	this work
YCplac111-shp1$^{\Delta UBA}$	(Schuberth, 2006)
YCplac111-shp1$^{\Delta UBX}$	(Schuberth, 2006)
pUG36-GFP-tubulin	this work
YCplac111-GLC7	this work
YCplac111-GLC8	this work
YCplac111-glc8^{T118A}	this work
YEplac195-pADH-GLC7	this work
YCplac111-shp1^{SS106108AA}	this work
YCplac111-shp1^{S315,321,322A}	this work
YCplac111-shp1^{S106,108,315,321,322A}	this work
YEplac195-SDS22	(MacKelvie et al., 1995)

Table 2. Plasmids used in this study.

5.1.5 *E. coli* strains

XL1 Blue. *supE44, hsd R17, rec A1, gyr A46, thi, rel A1, lac-, F' [proAB +, lac Iq, lacZ M15, Tn10(tet r)]*

XL10 Gold: *Tetr Δ(mcrA)183 Δ(mcrCB-hsdSMR-mrr)173 endA1 supE44 thi-1 recA1 gyrA96 relA1 lac I [F´ proAB lacIqZΔM15 Tn10 (Tetr) Amy Camr].*

5.1.6 *S. cerevisiae* strains

Strain	**Genotype**	**Source**
DF5a	MATa *ura3-52, leu2-3,-112 lys2-801, trp1-1, his3Δ200*	(Finley et al., 1987)
W303	MATa/α *leu2-3,112 trp1-1 can1-100 ura3-1 ade2-1 his3-11,15 RAD5*	(Thomas and Rothstein, 1989)
PJ69-4a	MATa, *trp1-901, leu2-3,-112, ura3-52, his3D200,gal4Δ, gal80Δ, GAL2-ADE2, LYS2::GAL1-HIS3, met2::GAL7-lacZ*	(James et al., 1996)
RCY3-1C	MATa *leu2-3,112 ura3-52 HIS3*::*GAL10-FLP1* [cir0]	(Zhang et al., 1995)
YPH499	MATa, *ura3-52, lys2-801amber, ade2-101ochre, trp1Δ63, his3Δ200, leu2Δ*	(Sikorski and Hieter, 1989)
SUB280	MATa *lys2-801 leu2-3,112 ura3-52 his3- Δ 200 trp1-1[am] ubi1·Δ1*::*TRP1 ubi2-Δ2*::*ura3 ubi3·Δub-2 ubi4-Δ2*::*LEU2* [pUB39] [pUB100]	(Spence et al., 1995)
SUB413	MATa *lys2-801 leu2-3,112 ura3-52 his3- Δ 200 trp1-1[am] ubi1·Δ1*::*TRP1 ubi2-Δ2*::*ura3 ubi3·Δub-2 ubi4-Δ2*::*LEU2* [pUB-K63R] [pUB100]	(Spence et al., 1995)
shp1-1	RCY MATa *leu2-3,112 ura3-52 HIS3*::*GAL10-FLP1 shp1-1* [cir0]	(Zhang et al., 1995)
shp1-2	RCY MATa *leu2-3,112 ura3-52 HIS3*::*GAL10-FLP1 shp1*-2 [cir0]	(Zhang et al., 1995)
Δshp1	DF5a *Δshp1::kanMX6*	(Braun et al., 2002)
ySB838/ shp1-7	DF5a *shp1 ATG->ACC* pop-in pop-out	this work
ySB958/ shp1-b1	DF5a *shp1*$^{\Delta Cdc48}$ pop-in pop-out	this work
ySB944/ shp1-a1	DF5a *shp1a-1* pop-in pop-out	this work
ySB185/ shp1-a1	DF5a *Δshp1::kanMX6 YIplac211-shp1a-1::URA3*	this work
ySB218/ shp1-a3	DF5a *Δshp1::kanMX6 YIplac211-shp1a-3::URA3*	this work
ySB219/ shp1-a4	DF5a *Δshp1::kanMX6 YIplac211-shp1a-4::URA3*	this work
ySB220/ shp1-a5	DF5a *Δshp1::kanMX6 YIplac211-shp1a-5::URA3*	this work
ySB155/ shp1$^{\Delta UBA}$	DF5a *Δshp1::kanMX6 YIplac211-shp1*$^{\Delta UBA}$*::URA3*	this work
ySB154/ shp1$^{\Delta UBX}$	DF5a *Δshp1::kanMX6 YIplac211-shp1*$^{\Delta UBX}$*::URA3*	this work
ySB320	W303a/α *Δshp1::kanMX6/SHP1*	this work
ySB272	W303a *Δshp1::kanMX6 YC33-SHP1*	this work
ySB756/757	W303a *Δshp1::kanMX6* (1 M Sorbitol)	this work
ySB217	DF5 *shp1*^{myc7His}*::kanMX4*	this work
ySB293	DF5 *shp1*^{7His}*::kanMX4*	this work
ySB196	DF5a *Δshp1::kanMX6 YIplac211-shp1*^{SSAA}*::URA3*	this work
ySB565	DF5a *SHP1*^{3HA}*::HIS3MX6*	this work
yCS160	YPH499 *SHP1*^{9myc}*::klTRP1*	(Schuberth, 2006)
ySB30	YPH499 *CUE3*^{3HA}*::HIS3MX6 SHP1*^{9myc}*::klTRP1*	this work
ySB29	YPH499 *YGL108c*^{3HA}*::HIS3MX6 SHP1*^{9myc}*::klTRP1*	this work
ySB31	YPH499 *YNL155w*^{3HA}*::HIS3MX6 SHP1*^{9myc}*::klTRP1*	this work
ySB36	DF5 *HDA2*^{9myc}*::HIS3MX6*	this work
ySB37	DF5a *TEM1*^{9myc}*::HIS3MX6*	this work
ySB38	DF5 *NUT2*^{9myc}*::HIS3MX6*	this work
ySB223	DF5 *YI211-pADH-*^{His}*Ub::URA3*	this work
ySB234	DF5a *YI211-pADH-*^{His}*UbK63R::URA3*	this work
ySB448	DF5a *CLN2*^{3HA}*::klTRP1*	this work
ySB449	DF5a *Δshp1::kanMX6 CLN2*^{3HA}*::klTRP1*	this work
ySB423/424	DF5a *Δshp1::kanMX6 YIplac128-pMET25-CDC14*^{3HA}*::LEU2* (clone 4 and 5)	this work

cdc15-2	W303 a *cdc15-2*	W. Seufert
ySB425/426	W303 a *cdc15-2 YIplac128-pMET25-CDC14*^{3HA}*::LEU2* (clone 2 and 3)	this work
ySB967	DF5 a *SIC1*^{3HA}*::klTRP1*	this work
ySB427	DF5 a *Δshp1::kanMX6 SIC1*^{3HA}*::klTRP1*	this work
ySB332	DF5a *SPC42*^{Mars}*:: nat-NT2*	this work
ySB341	DF5a *Δshp1::kanMX6 SPC42*^{Mars}*::nat-NT2*	this work
ySB1164	DF5a *PDS1*^{18myc}*::klTRP1*	this work
ySB1165	DF5a *shp1-7 PDS1*^{18myc}*::klTRP1*	this work
ySB1039	DF5a *Δmad2::HIS3MX6*	this work
ySB1036	DF5a *shp1-7Δmad2::HIS3MX6*	this work
ySB370	DF5α *Δbub2::HIS3MX6*	this work
ySB369	DF5 *Δbub2::HIS3MX6 Δshp1::kanMX6*	this work
ySB566	DF5a *GLC7*^{3myc}*::HIS3MX6 SHP1*^{3HA}*::klTRP1*	this work
ySB542	DF5a *GLC7*^{3myc}*::HIS3MX6*	this work
ySB554	DF5a *Δshp1::kanMX6 GLC7*^{3myc}*::HIS3MX6*	this work
ySB569	DF5a *SHP1*^{3HA}*:: klTRP1*	this work
ySB501	DF5a *GLC7*^{3HA}*::klTRP1*	this work
ySB1040	DF5α *glc7-127* pop-in pop-out	this work
ySB1042	DF5α *glc7-129* pop-in pop-out	this work
ySB1088	DF5 *shp1-7 glc7-129 YC33-SHP1*	this work
ySB1098	DF5α *ipl1-321* pop-in pop-out	this work
ySB1168	DF5 *shp1-7 ipl1-321*	this work
ySB506	DF5a *DAM1*^{9myc}*::HIS3MX6*	this work
ySB1204	DF5α *ipl1-321 DAM1*^{9myc}*::klTRP1*	this work
ySB1203	DF5α *glc7-129 DAM1*^{9myc}*::klTRP1*	this work
ySB1205	DF5 *shp1-7 ipl1-321 DAM1*^{9myc}*::klTRP1*	this work
ySB676	DF5a *YIplac128-pMET25::LEU2*	this work
ySB1220	DF5a *shp1-7 YIplac128-pMET25::LEU2*	this work
ySB581	DF5a *YIplac128-pMET25-GLC7::LEU2*	this work
ySB933	DF5a *shp1-7 YIplac128-pMET25-GLC7::LEU2*	this work
ySB1209	DF5a *shp1-a1 YIplac128-pMET25::LEU2*	this work
ySB1210	DF5a *shp1-a1 YIplac128-pMET25-GLC7::LEU2*	this work
ySB497	DF5a *GLC7*^{GFP}*::klTRP1*	this work
ySB886/1061	DF5a *shp1-7 GLC7*^{GFP}*::klTRP1*	this work
ySB1078	DF5a *shp1-b1 GLC7*^{GFP}*::klTRP1*	this work
ySB665	DF5α *Δglc8::hph-NT1*	this work
ySB1178	DF5 *shp1-7Δglc8::hph-NT1 YC33-SHP1*	this work
ySB688	DF5a *SDS22*^{3myc}*::klTRP1*	this work
ySB927	DF5a *shp1-7 SDS22*^{3myc}*::klTRP1*	this work
ySB924	DF5a *GLC8*^{3HA}*::klTRP1*	this work
ySB925	DF5a *shp1-7 GLC8*^{3HA}*::klTRP1*	this work
ySB460	DF5a *Δbar1::hph-NT1*	this work
ySB1064	DF5a *shp1-7 Δbar1::hph-NT1*	this work
ySB1066	DF5a *GLC8*^{3HA}*::klTRP1 Δbar1::hph-NT1*	this work
ySB1067	DF5a *shp1-7 GLC8*^{3HA}*::klTRP1Δbar1::hph-NT1*	this work
ySB1216	DF5a *YIplac128-pMET25-GLC8*^{3HA}*::LEU2*	this work
ySB1218	DF5a *YIplac128-pMET25-glc8*^{T118A3HA}*::LEU2*	this work
ySB1224	DF5a *shp1-7 YIplac128-pMET25-GLC8*^{3HA}*::LEU2*	this work
ySB1227	DF5a *shp1-7 YIplac128-pMET25-glc8*^{T118A3HA}*::LEU2*	this work
ySB1256/1257	DF5a *GLC8*^{GFP}*::klTRP1* (clone 1 and 2)	this work
ySB1258/1259	DF5a *shp1-7 GLC8*^{GFP}*::klTRP1* (clone 1 and 3)	this work

Table 3. S. cerevisiae strains used in this study.

5.1.7 Antibodies

5.1.7.1 Primary antibodies

Antigen	Type	Dilution for Western blot	Amount for IP	Source
Shp1	rabbit polyclonal	1:1000- 1:10000	2 µl	Jentsch Department (MPI of Biochemistry, Martinsried)
Cdc48	rabbit polyclonal	1:1000- 1:5000		AB95, Jentsch Department (MPI of Biochemistry, Martinsried)
Myc (9E10)	mouse monoclonal		4.5 µl	Sigma Aldrich
Myc (9E10)	mouse monoclonal	1:1000		Santa Cruz Biotechnology Inc.
HA (F7)	mouse monoclonal	1:1000		Santa Cruz Biotechnology Inc.
Glc7	goat antiserum	1:5000		C. Chan, University of Texas at Austin- ICMB (Tung et al., 1995)
Clb2	rabbit polyclonal	1:2000		Santa Cruz Biotechnology Inc.
GFP	mouse monoclonal	1:1000		Clontech
Phospho-Histone H3	rabbit polyclonal	1:1000		Millipore (Upstate)
Histone H3 ChiP grade	rabbit polyclonal	1:1000		Abcam

Table 4. Primary antibodies used in this study.

5.1.7.2 Secondary antibodies, horseradish peroxidase (HRP) coupled

Goat anti-rabbit	Jackson Immunoreseach (Dianova)	dilution 1:7500
Goat anti-mouse	Jackson Immunoreseach (Dianova)	dilution 1:7500
Donkey anti-goat	Jackson Immunoreseach (Dianova)	dilution 1:7500

5.2. Methods

The following methods are based on standard biochemical, microbiological and molecular biological protocols previously described (Ausubel et al., 1987; Sambrook and Russell, 2001) and were modified and applied as denoted. Certain *S. cerevisiae* protocols were adapted from methods described in (Abelson et al., 1991; Abelson et al., 1997).

5.2.1 Protein biochemical methods

5.2.1.1 SDS-polyacrylamide gel electrophoresis (SDS-PAGE)

Denatured protein samples were applied to 8%, 10%, 12%, or 15% polyacrylamide gels and separated by electrophoresis as described (Laemmli, 1970). Separating gels were of the above mentioned acrylamide (Acrylamide/Bis Solution, 37.5:1, Serva) concentrations, stacking gels were always 4%. To denature protein samples they were incubated at 65°C for 10 min in HU buffer/ DTT (8 M urea, 5% SDS, 0.2 M Tris pH 6.8, bromophenol blue and 0.1M DTT prior to use). Electrophoresis of mini gels (Hoefer Mini Gel System) was carried out using Laemmli running buffer (25 mM Tris, 192 mM glycine, 0.1 % SDS) at 20 mA per gel and depending on application a maximum of 150 V. Approximate protein size was estimated by comparison to a pre-stained protein standard (AllBlue, BioRad).

5.2.1.2 Western blot

After SDS-PAGE proteins were blotted to PVDF membrane (Millipore) using a semi-dry blotting system. The membrane and Whatman filter papers were cut to gel size and soaked in blotting buffer (25 mM Tris, 192 mM glycine, 0.01 % SDS, 20 % methanol). Gels were blotted at constant current

(150 mA per mini gel) and limited to 15 V for 2-3 hours. After blotting the membranes were blocked using 5 % non-fat milk (Merck) in TBS-T (TBS/ 0.02% Tween20) for at least 30 min. For immunological detection of blotted proteins incubation with primary antibody in blocking solution (with 0.065% sodium azide) was carried out overnight at 4°C. After washing with TBS-T (1x5min, 3x10min) the membrane was incubated with horseradish peroxidase coupled secondary antibody for 1-2 h at room temperature. This was again followed by washing with TBS-T (6x10 min) and once with ddH$_2$O. For chemiluminescent detection the ECL reagent mixture (GE Healthcare) was added to each membrane, spread evenly, and the signal detected using ECL-Hyperfilm (GE Healthcare). Developed films were scanned and processed using Adobe Photoshop (Adobe Systems Inc.) and/ or ImageJ (http://imagej.nih.gov/ij/) software.

5.2.1.3 Yeast whole cell lysates- TCA precipitation

The necessary amount of cells (release/ FACS cell amount in 1 ml of OD$_{600}$=0.6, otherwise in 1 ml of OD$_{600}$=1; OD$_{600}$=1 is approximately equal to 10^7 cells/ ml) was harvested by centrifugation and then resuspended in 1 ml ddH$_2$O. Alternatively the appropriate amount of cells was resuspended in 1 ml ddH$_2$O directly from plates. To lyse cells, 150 μl 1.85% NaOH/ 7.5 % β-mercaptoethanol were added and the samples were vortexed. After incubation for 10 min on ice 150 μl 55 % TCA were added to the samples, they were vortexed and again incubated on ice for 10 min. Protein precipitates were then collected by centrifugation (20000 g, 10 min, 4°C), the supernatant was aspirated, and the pellet was centrifuged again to remove the remaining liquid. Pellets were then resuspended in 50 μl HU/ DTT and incubated at 65°C for 10 min. If necessary the pH of the samples was adjusted by addition of 2-4 μl 2 M Tris-base.

5.2.1.4 Immunoprecipitation (IP)

Yeast cultures were grown in YPD to an OD$_{600}$ of 1, harvested and washed once with cold ddH$_2$O/ 1 mM PMSF (1000 g, 4°C, 5 min). Cells were then lysed in IP buffer (50 mM Tris/ HCl pH 7.5, 100 mM KCl, 5 mM MgCl$_2$, 0.1% NP-40, 10% glycerol, 10 mM NaF, 2 mM PMSF, complete protease inhibitor cocktail (Roche)) by addition of zirconia beads (Biospec) and vortexing (6x 30sec). After lysis the NP-40 concentration was increased to 1%, and the extracts were centrifuged at 2,600 g for 5 min, followed by centrifugation at 20,000 g for 25 min. An input sample (10 μl) was taken prior to antibody addition and denatured by adding an equal amount of HU/ DTT and incubation at 65°C for 10 min. The supernatants were incubated with 20 μl pre-coupled HA-antibody (Santa Cruz Biotechnology Inc.), or 4.5 μl myc, or 2 μl Shp1 antibodies and rotation at 4°C over night. Immunocomplexes were then either bound to 20 μl protein A sepharose beads (GE Healthcare) for three hours (4°C) or directly washed if pre-coupled beads were used. Beads were washed four times (600 μl IP buffer/ 1% NP-40 for 10 min, 800 μl IP buffer/ 1%NP-40 8 min, 800 ml IP-buffer 5 min, 1 ml IP buffer) and eluted in 25 μl HU/ DTT, 10 min, 65°C.

5.2.1.5 Denaturing Ni-NTA Pull-down

Denaturing Ni-NTA pull-downs of yeast overexpressing 6xHis epitope tagged ubiquitin were used to detect *in vivo* ubiquitination of proteins. Yeast strains were either transformed with *YE-pCUP-*^{His}*Ub*, or strains in which *Yl211-pADH-^{His}Ub* had been integrated were used. Overnight cultures were grown in selective medium without induction of the copper promoter. 200 ml selective medium were inoculated to OD_{600} of 0.1 and incubated at 30°C or 25°C. In the case of strains carrying *pCUP-^{His}Ub*, overexpression of ^{His}ubiquitin was induced approximately 3 h before harvesting the cultures by addition of 100 µM $CuSO_4$ to the culture. Upon reaching OD_{600} 0.8-1.0, the cultures were harvested by centrifugation (5500 g, 10 min, 4°C), were resuspended in 10 ml ice-cold sterile ddH_2O and were transferred to 50 ml round-bottom tubes. After centrifugation (3500 g, 10 min, 4°C), the supernatant was discarded and the pellets were frozen in liquid nitrogen. Cells were lysed by resuspending the frozen pellet in 5 ml 1.85 N NaOH/ 7.5 % β-mercaptoethanol and incubation on ice for 15 min. 5 ml 55 % (w/v) TCA were added, the samples were vortexed and incubated on ice for 15 min. Precipitated proteins were collected by centrifugation (3500 g, 10 min, 4°C) and the pellet was washed twice with 5 ml ice cold (-20°C) acetone. The protein pellets were then thoroughly resuspended in 2 ml denaturing buffer A (6 M guanidinium chloride, 0.1 M NaH_2PO_4, 10 mM Tris, 0.05 % Tween20 pH 8) and were incubated at RT and 80 rpm for one hour to further increase solubilization of the TCA-precipitate. Remaining insoluble material was removed by centrifugation (23000 g, 20 min, 4°C). The imidazole concentration of the supernatant was increased to 20 mM and a 10 % input sample was taken. The lysate was then incubated with 50 µl magnetic Ni-NTA agarose (Qiagen) at 4°C overnight. Using a magnetic rack (Dynal), the beads were washed three times with 800 µl buffer A/ 20 mM imidazole and then five times with 800 µl buffer C (8 M urea, 0.1 M NaH_2PO_4, 10 mM Tris pH 6.3 and 0.05% Tween20). To elute bound proteins the beads were incubated with 30 µl 1 % SDS for 10 min at 65°C. The eluate was then concentrated using a speed-vac (25 min, 45°C) and was resuspended in 15 µl HU/ DTT and 10 µl ddH_2O. Input samples were subjected to TCA-precipitation (*see 5.2.1.3*) and were finally resuspended in 25 µl HU/ DTT. Both samples were incubated at 65°C for 10 min prior to SDS-PAGE. Typically 3 µl input and 7 µl pull-down were loaded on SDS-PAGE gels.

5.2.1.6 Two step purification of phosphorylated Shp1 for mass-spectrometry

Strains expressing Shp1^{myc7His} were grown to OD_{600} of 1-1.5 and harvested. Lysis and Ni-NTA pull-down were performed as described above for ^{His}ubiquitin pull-downs. Most (25 µl) of the SDS eluate was directly diluted 1:24 with RIPA*** (50 mM Tris, 5 mM EDTA, 150 mM NaCl, 1.25 % Triton X-100) buffer and incubated with 20 µl of pre-coupled anti-myc beads (Santa Cruz Biotechnology Inc.) overnight. The remaining 5 µl were used as a PD eluate/ IP-input control. The beads were then transferred to empty protein columns (BioRad), the flow-through was collected and the beads were then washed six times with 600 µl RIPA* (50 mM Tris, 5 mM EDTA, 150 mM NaCl, 1.25 % Triton X-100, 0.1 % SDS) buffer and bound protein was eluted in 50 µl 1 % SDS. The eluate was concentrated using a speed-vac and then resuspended in 7.5 µl HU/ DTT and 12.5 µl ddH_2O.

For mass-spectrometry the sample was analyzed on a pre-cast 10% Gel and run with MOPS buffer (Invitrogen). The strong band at approximately 50 kD was excised and analyzed using an OrbiTrap mass spectrometer and peptides were identified using Mascot Daemon software (all performed by Frank Siedler MPI of Biochemistry, Martinsried).

5.2.2 *E. coli* Methods

5.2.2.1 Preparation of competent E. coli

Electrocompetent E. coli

An overnight culture of XL1 blue cells in LB-tetracycline was diluted in LB medium and grown at 37°C to a final OD_{600} of 0.7. The culture was then rapidly cooled by incubation on ice for 30-60min. Cells were harvested by centrifugation (10 min, 4°C), quickly washed with 500 ml sterile ice-cold ddH_2O and were resuspended in 250 ml sterile ice-cold 10% glycerol. After 30 min incubation on ice the cells were harvested and resuspended in 10 ml ice cold 10 % glycerol and again incubated on ice for 30 min. After harvesting the cells (6000 rpm, 10min) the pellet was resuspended in an approximately equal volume of 10% glycerol and aliquots were frozen in liquid nitrogen and stored at -80°C.

$CaCl_2$ competent E. coli

The overnight culture of XL1 blue cells was diluted in LB medium and grown at 37°C to final OD of 0.6-0.8. Cultures were then cooled on ice and cells were harvested by centrifugation. The pellet was resuspended in 100 mM ice-cold sterile $CaCl_2$ solution and incubated on ice for 10 min. Cells were harvested (5000 rpm, 4°C, 10 min) and the pellet was resuspended in 1/10 volume $CaCl_2$, incubated at least 10 min on ice and DMSO was added to a final concentration of 10%. Aliquots of cells were frozen in liquid nitrogen and stored at -80°C.

5.2.2.2 Transformation of E. coli with DNA

To transform $CaCl_2$ competent *E. coli* 50 µl of cells were incubated with approximately 250 ng plasmid DNA on ice for 20 min. They were then subjected to heat-shock for 1 min at 42°C and cooled on ice. Depending on the application phenotypic expression was carried out for at least 30 min at 37°C.

Electrocompetent cells were transformed by transferring the mixture of 50 µl cells and 1.5 µl ligation product or plasmid DNA to a 0.1 cm electroporation cuvette (BioRad, VWR). The pre-installed settings for *E .coli* and 0.1 cm cuvettes were used (1.8 kV, 1 pulse; Micropulser, BioRad). Directly after electroporation LB medium was added and phenotypic expression was carried out for 45 min at 37°C.

5.2.2.3 Plasmid isolation from E. coli cultures

Small amounts of plasmid DNA were extracted from *E. coli* by mini preparation. Single clones were inoculated in 5 ml LB medium with the applicable antibiotic. After harvesting the cells different mini preparation kits (Machery Nagel, Bioneer, Qiagen, Zymoprep) were used for isolation of plasmid DNA. All kits were based on the alkaline lysis method (Birnboim and Doly, 1979).

5.2.3 Molecular biology methods

5.2.3.1 Polymerase chain reaction (PCR)

For amplification of DNA fragments from plasmids or genomic DNA Phusion DNA polymerase (NEB) was used. Annealing temperature and elongation time were chosen depending on primer composition and fragment length. For the amplification of fragments from genomic DNA, polymerase activity of about 1 kb/ min was used for calculation of the elongation time.

To amplify the knockout and tagging cassettes used for yeast strain construction, a mixture of Taq and Vent polymerases (NEB) was used. PCR reaction conditions and buffers were used as described (Knop et al., 1999; Janke et al., 2004).

5.2.3.2 Site-directed mutagenesis

Site-directed mutagenesis was carried out using the QuikChange Multi, XL and Lightning Kits (Stratagene/ Agilent) according to the manufacturer's protocol. In most cases more DpnI digested mutagenesis reaction was transformed into XL10 Gold cells (Stratagene/ Agilent) than denoted in the protocol.

5.2.3.3 Restriction digest

Manufacturer (NEB or Fermentas) instructions for buffer and digest conditions were followed. For cloning generally 2 μg plasmid DNA were digested and 600 ng of mini-prep DNA for control digests.

5.2.3.4 Electrophoresis and DNA extraction from agarose gels

Depending on the application 0.8- 1.6% agarose gels in TBE buffer were used. DNA was visualized by addition of 0.2 μg/ml ethidium bromide (Roth). Prior to applying the DNA samples to the gel, loading buffer (0.1 M EDTA, 1 % SDS, 20 % glycerol, 0.2 % bromophenol blue and xylencyanol) was added. The DNA samples, as well as a DNA size standard (1 kb ladder, Invitrogen; GeneRuler 1 kb ladder, Fermentas) were separated by electrophoresis at 80- 120 V. After 20- 60 min DNA was visualized using a UV-transilluminator and size and amount of the DNA samples was estimated by comparison with the DNA standard.

In case of preparative digests for cloning, the appropriate DNA fragment was excised using a scalpel. The DNA was isolated from the agarose as described in the manufacturer's protocol for gel extraction kits (Machery Nagel, Bioneer). The extracted DNA was typically eluted in 30 μl of the supplied elution buffer.

5.2.3.5 Vector dephosphorylation and ligation

To reduce the number of false-positive transformants due to vector re-ligation during cloning, digested vector fragments were dephosphorylated according to the manufacturer's protocol using Antarctic Phosphatase (NEB). Approximate amounts of dephosphorylated vector and insert were determined by agarose gel electrophoresis and a ratio of about 5:1 for insert to vector was used for the ligation reaction. DNA fragments were ligated using T4 DNA ligase (NEB, Fermentas) and in most cases the reaction was carried out at 16°C overnight.

5.2.3.6 Sequencing

Sequencing reactions were either performed by the MPI core facility (MPI of Biochemistry, Martinsried) or by GATC Biotec (Konstanz). Sequencing results were analyzed using the Lasergene software package (DNASTAR, Inc.).

5.2.4 *S. cerevisiae* methods

5.2.4.1 Preparation of competent yeast cells (Knop et al., 1999)

Overnight cultures of yeast strains grown in the appropriate medium were diluted to OD_{600} of 0.1 and grown at 25°C or 30°C until reaching a final OD_{600} of 0.5-0.7. The cells were then harvested by centrifugation (1000 g, 5 min, 24°C) and washed once with an equal volume of sterile ddH_2O. The cells were pelleted again and were resuspended in 0.2 volumes of SORB buffer (100 mM LiOAc, 10 mM Tris-HCl pH 8, 1 mM EDTA/ NaOH pH 8, 1 M Sorbitol; pH 8 with acetic acid). After centrifugation excess SORB buffer was removed and the pellet was resuspended in 360 µl SORB buffer per 50 ml culture volume. 40 µl of denatured salmon sperm DNA (10 mg/ml, Invitrogen) were added and the competent cells were aliquoted and stored at -80°C.

5.2.4.2 Transformation of competent yeast cells (Knop et al., 1999)

To transform yeast either with plasmid DNA or PCR products and integrative plasmids, 10 or 50 µl competent cells were thawed, respectively. After addition of the DNA to the cells, six volumes PEG buffer (10 mM Tris-HCl pH 8.0; 1 mM EDTA; 100 mM lithium acetate (Sigma Aldrich); 40% PEG3350 (Sigma Aldrich)) were added, the mixture was vortexed, and incubated for 30 min at RT. Prior to the heat shock 1/9 Vol DMSO was added and the transformation mixture was then incubated at 42°C for 15 min in a water bath (less for ts alleles). After cooling on ice, the cells were pelleted (500 g, 2 min, 24°C) and resuspended in ddH_2O or SC-medium and plated on the respective selection plates. For PCR cassettes with antibiotic resistance markers the transformed cells were incubated in 5 ml YPD for 3 h (G418) or 6 h (*hph-NT1*, *nat-NT2*) and then pelleted and plated on the antibiotic containing plates.

5.2.4.3 Integration of YIplac plasmids using homologous recombination

YIplac plasmids (Gietz and Sugino, 1988) do not contain an origin of replication and therefore must be integrated into the yeast genome in order to be stably propagated. By linearization either within the selection marker or within the cloned yeast genomic insert, these constructs can be integrated into the chromosomal *leu*, *trp* or *ura* loci, or the genomic locus of interest, respectively. To this end, approximately 2 µg of *YIplac* constructs were digested using a restriction enzyme that cuts once either within the auxotrophy marker or the insert (typically: *URA3*: StuI, *LEU2:* ClaI, EcoRV, BstXI, *TRP1:* EcoRV). One fifth of the restriction digest was then directly transformed into 50 µl competent yeast cells. Once proper integration of the plasmid had been confirmed, the strains were also cultured using non-selective YPD or SC media.

5.2.4.4 Yeast colony-PCR

To verify chromosomal integration of knockout or epitope tagging cassettes, as well as for the identification of positive pop-in/ pop-out transformants, colony-PCR was used. A small amount of yeast cells was resuspended in 20 µl 0.02 N NaOH and approximately the same volume glass beads (Roth) were added. After 5 min incubation at 99°C and 1400 rpm the supernatant was collected and 2 µl were directly used as a template for PCR. The PCR reaction was carried out using Thermopol buffer and Taq polymerase (both NEB) and was set up in 25 µl. For standard products smaller than

1kb the following PCR program used: 94°C 30 sec, 52°C 30 sec, 72°C 1 min for 30 cycles. 10 µl PCR product was analyzed on an agarose gel.

5.2.4.5 Extraction of genomic DNA (gDNA)

Genomic DNA was extracted using a protocol based on glass bead lysis and phenol/ chloroform extraction. At least 5 ml stationary overnight culture were harvested and washed with 1 ml ddH_2O. The cell pellet was resuspended in 400 µl breaking buffer (100 mM NaCl, 10 mM Tris pH 8.0, 1 mM EDTA, 1 % SDS, 2 % Triton X-100) and glass beads (Roth) as well as a mixture of phenol:chloroform:isoamyl alcohol (25:24:1) was added. The mixture was then vigorously vortexed for 5 min at RT. 200 µl TE buffer (10 mM Tris pH 8.0, 1 mM EDTA) were added, the mixture was shortly vortexed, and the phases were separated by centrifugation (10 min, 5000 g, RT). 500 µl aqueous supernatant were collected and extracted twice with equal volumes of chloroform. 1 ml 100 % EtOH was added to the aqueous supernatant and the DNA was precipitated by incubation at -20 C for 1-2 hours. The genomic DNA was harvested and was washed once with 1 ml 70 % EtOH. The DNA pellet was dried and resuspended in 25 µl ddH_2O.

Alternatively, a kit for extraction of yeast genomic DNA (Yeast-Geno-DNA-Template Kit, Gbiosciences). The protocol of the manufacturer was followed, in which the major difference to the previous protocol was a zymolyase digest to enable lysis. The genomic DNA extracted with the kit yielded better results regarding quantity and template quality for a subsequent (Phusion) PCR.

5.2.4.6 Pop-in/ pop-out gene replacement

The pop-in/ pop-out two-step method allows replacement of genes without introduction of any exogenous sequence elements such as resistance marker cassettes or loxP sites (Scherer and Davis, 1979; Rothstein, 1991). The *URA3* plasmid carrying the mutant gene is first integrated into the chromosomal locus, resulting in a duplication containing the wild-type gene and the mutant version separated by the plasmid sequence. By subsequent 5'FOA counter-selection, one of the two copies is removed and clones are screened for mutant phenotypes. This method was used to construct the *shp1* mutant strains as well as for the introduction of *glc7* and *ipl1* conditional alleles into the DF5 background.

shp1 ATG→ACC mutagenesis was performed on *YIplac211-SHP1* including promoter and terminator sequences. The mutated plasmid was linearized within the *SHP1* ORF by restriction digest with BamHI and was then integrated into *ura3-52* of DF5a. Clones were selected for URA auxotrophy, and positive transformants were identified by colony-PCR and subsequent KpnI digestion of the PCR fragment (a KpnI site is introduced by the mutation). Positive clones (2/10) were streaked twice on 5'FOA and single colonies were selected. These clones were then analyzed by Western blot for Shp1 expression and by PCR for the *SHP1* ORF to exclude aberrant pop-out events that remove entire sequence stretches. 2/12 positive clones identified: *shp1-7* and *shp1-9*. All mutants were then sequenced, either by cloning the ORF +/- 1kb (*shp1-7/9*) or by sequencing of a PCR product of the mutated region (*shp1-a1, shp-b1*, *glc7-129*, *ipl1-321*).

5.2.4.7 Mating of yeast strains

Overnight cultures of two strains with the opposite mating types were inoculated to OD_{600} of 0.1 and incubated for approximately 3 h so that logarithmic growth phase was reached. 10 µl of each culture, adjusted to an equal OD_{600}, were spotted on top of each other on a pre-warmed YPD plate. After at least 6 hours of incubation at 30°C, zygotes were either selected according to their characteristic morphology using a micro-manipulator (MSM100, Singer Instruments), or streaked on appropriate selection plates and incubated for 1-2 days.

5.2.4.8 Mating type test

To test yeast strains for their mating type or to verify zygotes, plates containing either a (RH449) or α (RC757-58) reporter strains were used. The respective reporter strain was resuspended in sterile ddH_2O from freshly streaked plates, and 30 µl of this suspension were added to 8 ml liquid YPD 1 % (w/v) agar. The mixture was briefly vortexed and poured on top of a YPD plate to completely cover its surface. After drying the plates, DF5a and α, as well as the strains to be tested were streaked on both reporter plates. The plates were incubated at least one day at 30°C and analyzed for the formation of halos around cells of opposite mating types.

5.2.4.9 Sporulation and tetrad dissection

0.5 ml stationary culture of zygotes were harvested (500 g, 3 min, RT) and washed twice with an equal volume of sterile ddH_2O. The pellet was then resuspended in 5 ml sporulation medium (2 % KAc) and incubated at least 4 days at RT with shaking. For tetrad dissection, 10 µl sporulated culture were digested with 10 µl zymolyase solution (1 mg/ml 20T, Seikagaku) for 8-10 min at RT. The spheroplasts were carefully transferred to a YPD plate and spread in a line dividing the plate in two halves. Tetrads were selected and separated into the four spores using a micro-manipulator (MSM100, Singer Instruments). Spores were incubated at least two days at 25°C or 30°C, depending on the phenotypes. Genotypes of the haploid progeny were identified using marker selection, colony-PCR and Western blot.

5.2.4.10 Spotting of serial dilutions for phenotypic analysis

To analyze phenotypes mutants, serial dilutions of yeast cultures were spotted on selective plates or plates containing drugs and incubated at varying temperatures. Overnight cultures were diluted with sterile ddH_2O to OD_{600} of 0.1 (in some cases 0.3) and five fivefold serial dilutions were prepared in microtiter-plates. Approximately 5 µl of each dilution were transferred to the respective plates using a replica stamp with 96 pins. The plates were then incubated at the indicated temperatures for 3-7 days.

5.2.4.11 Interaction studies using directed yeast two hybrid (Y2H) assays

The coding sequences of bait and prey genes were cloned into pGBD-C1 and pGAD-C1 (James et al., 1996), respectively. These vectors then express an N-terminal fusion of Gal4 transcriptional activator with the prey or an N-terminal fusion of the Gal4 DNA binding domain fused in frame to the bait. Different combinations of bait and prey plasmids were transformed into PJ69-4a yeast cells (James et al., 1996) and selected on SC-Leu-Trp plates. After 2-3 days the amount of cells in 1 ml OD_{600}=0.5 was spotted on SC-Leu-Trp (control), SC-Leu-Trp-His and SC-Leu-Trp-Ade and incubated 3-7 days at

30°C. To reduce background on SC-Leu-Trp-His plates 3 mM 3'amino triazole (3AT, Sigma Aldrich) was added to the plates.

5.2.4.12 Robot-based Y2H screen

The robot-based Y2H screens were conducted using a library of yeast strains expressing each of the >6000 yeast ORFs N-terminally fused to the Gal4 AD, spatially ordered on arrays (Cagney et al., 2000; Gera et al., 2002). To introduce the bait plasmid into the strains of this array a mating strategy was used. PJ69-4α was transformed with the Gal4 BD fusion of the bait and mated to the Y2H array. Diploids carrying both plasmids were selected by growth on SC-Leu-Trp plates. Interaction of bait and prey was analyzed by growth on SC-Leu-Trp-His and SC-Leu-Trp-Ade plates. To increase stringency 3 mM 3AT (Sigma Aldrich) was added to the SC-Leu-Trp-His plates. Plates were incubated for 5- 7 days at 30°C and then scored for positive interactors. All steps were carried out using the Biomek FX automated workstation (Beckman Coulter) and a 384 pin replica tool.

5.2.4.13 Live-cell microscopy (fluorescence and spinning disk confocal)

Yeast strains were grown in the applicable sterile filtered SC or SC-complete media to avoid high background fluorescence. To immobilize cells, the cover slips were coated with 1 mg/ml concanavalin A (Type 5, Sigma Aldrich) and incubated for at least 30 min. The undiluted logarithmic culture was spotted on the cover slip, shortly incubated and sealed with Vaseline. Live-cell microscopy was carried out using different microscopes and software:

	DM RXA (Leica)	**Axiovert 200M (Zeiss)**	**Spinning Disk Confocal**
Camera	Orca-ER (Hamatsu)	AxioCam MRm TV2/3" 0.63x (Zeiss)	D-977 iXon EMCCD+ and twofold magnification (Andor Technology)
Software	OpenLab 5.2 (Improvision)	AxioVision LE (Zeiss)	(Andor Technology)
Objective	PL APO (Leica) 100x/1.4-0.7 oil	Axio Apochrom (Zeiss) 100x/1.4 oil	TIRFM (Olympus) 100x/1.45 oil
Detection of green fluorophores (GFP)	GFP excitation BP 470/40 beamsplitter FT 500 emission BP 525/50	FITC (#10) excitation BP 450-490 beamsplitter FT 510 emission BP 515-565	diode pumped solid state lasers (488 nm and 561 nm) Samrock emission filters in a Sutter filter wheel
Detection of red fluorophores (Mars)	TexasRed excitation BP 62/40 beamsplitter LP 593 emission BP 624/40	Rhodamine (#20) excitation BP 546/12 beamsplitter FT 560 emission BP 575-640	

Table 5. Details of microscope setups used in this study. BP: bandpass, FT:"farb teiler" beamsplitter, LP: longpass

Data sets were analyzed and processed using ImageJ software (http://imagej.nih.gov/ij/) and the MBF ImageJ for Microscopy collection of plug-ins (http://www.macbiophotonics.ca/imagej/).

5.2.5 Cell cycle experiments in *S. cerevisiae*

5.2.5.1 Analysis of DNA content by flow cytometry (FACS)

Flow cytometry of yeast was carried out essentially as described (Lew et al., 1992). Yeast cultures were inoculated to an OD_{600} 0.1 in YPD or SC medium and grown to a final OD_{600} of 0.7- 1.0 at RT. The amount of cells corresponding to 1 ml of OD_{600}=0.6 was harvested by centrifugation (3500 g, 3 min, 4°C) and washed once with 5 ml ddH_2O. The cell pellet was then resuspended in 70% ethanol under constant vortexing to avoid clumping of cells. Fixation in ethanol at 4°C was carried out for at least 1 h, but mostly overnight. After fixation the cells were again harvested by centrifugation and washed once with 5 ml PBS. The cell pellet was then resuspended in 0.9 ml PBS and briefly sonified (6 pulses on lowest setting). To remove RNA 0.5 mg/ml RNase (Sigma Aldrich) were added and the sample was incubated overnight at 37°C (in case of shorter incubation times the RNase concentration was increased to 1 mg/ ml). Before propidium iodide (PI, Sigma Aldrich) staining, the cells were washed once with 5 ml PBS. DNA was stained overnight by gentle shaking at 4°C in 1 ml PBS/ 0.05 mg/ml PI. For FACS measurement the cells were resuspended in PBS/ 0.005 mg/ml PI, sonified briefly and diluted approximately 1:4 in PBS. FACS analysis was carried using either a BD FACS Calibur and Cell Quest Pro software, a BD FACS Canto and FACS Diva software, or, for some measurements, a Beckman Coulter FC500 and CXP software. For post-acquisition analysis and quantification, WinMDI software (http://facs.scripps.edu/software.html) was used.

5.2.5.2 α-factor arrest/ release

Overnight cultures of wild-type and mutant strains were diluted to OD_{600} of 0.1 (for *shp1* 0.15) in 50 ml YPD for arrest/ release experiments or in 15 ml for arrests only. The cultures were then grown at 24°C for approximately four hours until reaching a maximal OD_{600} of 0.3-0.35. For a G1 arrest in *BAR1* strains, 10 μM α-factor in DMSO (Core facility, MPI of Biochemistry, Martinsried) were added and the cells were allowed to arrest for three hours, at 25°C. Directly before addition of α-factor, a control sample from the asynchronous culture was collected, and the pellet was frozen in liquid nitrogen. The efficiency of the arrest was determined by FACS analysis and/ or Western blot for Clb2 levels after three hours of arrest. In case of release experiments, the cultures were then washed two times with equal volumes of YPD (500 g, 3 min, 24°C) and resuspended to a final OD_{600} of approximately 0.5 in YPD. The released cultures were incubated at 25°C and samples for each time-point of the release were taken. Per time-point, an amount of cells corresponding to 1 ml of OD_{600}=0.6 was removed from the culture, quickly pelleted and frozen in liquid nitrogen. Time-point 0 min was taken after the two washing steps, as shaking incubation of the cultures was continued. Typically time-points every 20 min were taken for at least 180 min. The pellets were then subjected to TCA precipitation (*see 5.2.1.3*) and were resuspended in 50 μl HU/DTT. Fluctuation of Clb2 or other cell cycle marker proteins was analyzed by Western blot. For some experiments FACS samples were taken in addition to Western blot samples. As for the Western blot samples, the amount of cells corresponding to 1 ml of OD_{600}=0.6 was collected per time-point, but processed directly for FACS analysis rather than frozen in liquid nitrogen.

5.2.5.3 Nocodazole arrest/ release

For mitotic arrests the spindle depolymerizing drug nocodazole (Sigma Aldrich, Enzo Life Sciences) was added to logarithmic yeast cultures. A protocol similar to the α-factor arrest was used, but cells were arrested with 150 µg/ml nocodazole in YPD. (A 1.5 mg/ml nocodazole stock solution in water-free DMSO (Sigma Aldrich) was stored at -80°C and thawed only once prior to use.) After three hours, the arrest efficiency was monitored by Western blot of Clb2 levels or FACS profiles of DNA content. For release experiments, the cultures were washed twice with YPD/ 1% DMSO to remove all traces of the water insoluble nocodazole. The release was then monitored as described above for the α-factor arrest.

6. References

Abelson, J.N., Simon, M.I., and Dunphy, W.G., eds. (1997). Cell Cycle Control (Elsevier Academic Press).

Abelson, J.N., Simon, M.I., Guthrie, C., and Fink, G.R., eds. (1991). Guide to Yeast Genetics and Molecular Biology (Elsevier Academic Press).

Agarwal, R., Tang, Z., Yu, H., and Cohen-Fix, O. (2003). Two distinct pathways for inhibiting pds1 ubiquitination in response to DNA damage. J Biol Chem *278*, 45027-45033.

Akiyoshi, B., Nelson, C.R., Ranish, J.A., and Biggins, S. (2009a). Analysis of Ipl1-mediated phosphorylation of the Ndc80 kinetochore protein in Saccharomyces cerevisiae. Genetics *183*, 1591-1595.

Akiyoshi, B., Nelson, C.R., Ranish, J.A., and Biggins, S. (2009b). Quantitative proteomic analysis of purified yeast kinetochores identifies a PP1 regulatory subunit. Genes Dev *23*, 2887-2899.

Alberts, S.M., Sonntag, C., Schafer, A., and Wolf, D.H. (2009). Ubx4 modulates cdc48 activity and influences degradation of misfolded proteins of the endoplasmic reticulum. J Biol Chem *284*, 16082-16089.

Albuquerque, C.P., Smolka, M.B., Payne, S.H., Bafna, V., Eng, J., and Zhou, H. (2008). A multidimensional chromatography technology for in-depth phosphoproteome analysis. Mol Cell Proteomics *7*, 1389-1396.

Alessi, D.R., Street, A.J., Cohen, P., and Cohen, P.T. (1993). Inhibitor-2 functions like a chaperone to fold three expressed isoforms of mammalian protein phosphatase-1 into a conformation with the specificity and regulatory properties of the native enzyme. Eur J Biochem *213*, 1055-1066.

Amerik, A.Y., and Hochstrasser, M. (2004). Mechanism and function of deubiquitinating enzymes. Biochim Biophys Acta *1695*, 189-207.

Andersen, M.P., Nelson, Z.W., Hetrick, E.D., and Gottschling, D.E. (2008). A genetic screen for increased loss of heterozygosity in Saccharomyces cerevisiae. Genetics *179*, 1179-1195.

Ando, A., Nakamura, T., Murata, Y., Takagi, H., and Shima, J. (2007). Identification and classification of genes required for tolerance to freeze-thaw stress revealed by genome-wide screening of Saccharomyces cerevisiae deletion strains. FEMS Yeast Res *7*, 244-253.

Andrews, P.D., and Stark, M.J. (2000). Type 1 protein phosphatase is required for maintenance of cell wall integrity, morphogenesis and cell cycle progression in Saccharomyces cerevisiae. J Cell Sci *113 (Pt 3)*, 507-520.

Archambault, V., Chang, E.J., Drapkin, B.J., Cross, F.R., Chait, B.T., and Rout, M.P. (2004). Targeted proteomic study of the cyclin-Cdk module. Mol Cell *14*, 699-711.

Ausubel, F. M., B., R., K., R. E., M., D. D.,, Seidman, J.G., Smith, J.A., and Struhl, K., ed, eds. (1987). Current Protocols in Molecular Biology (NY, John Wiley & Sons).

Axton, J.M., Dombradi, V., Cohen, P.T., and Glover, D.M. (1990). One of the protein phosphatase 1 isoenzymes in Drosophila is essential for mitosis. Cell *63*, 33-46.

Baker, S.H., Frederick, D.L., Bloecher, A., and Tatchell, K. (1997). Alanine-scanning mutagenesis of protein phosphatase type 1 in the yeast Saccharomyces cerevisiae. Genetics *145*, 615-626.

Bardin, A.J., and Amon, A. (2001). MEN and SIN: what's the difference? Nat Rev Mol Cell Biol *2*, 815-826.

Bardin, A.J., Visintin, R., and Amon, A. (2000). A mechanism for coupling exit from mitosis to partitioning of the nucleus. Cell *102*, 21-31.

Bazzi, M., Mantiero, D., Trovesi, C., Lucchini, G., and Longhese, M.P. (2010). Dephosphorylation of gamma H2A by Glc7/protein phosphatase 1 promotes recovery from inhibition of DNA replication. Mol Cell Biol *30*, 131-145.

Beuron, F., Dreveny, I., Yuan, X., Pye, V.E., McKeown, C., Briggs, L.C., Cliff, M.J., Kaneko, Y., Wallis, R., Isaacson, R.L.*, et al.* (2006). Conformational changes in the AAA ATPase p97-p47 adaptor complex. Embo J *25*, 1967-1976.

Bharucha, J.P., Larson, J.R., Gao, L., Daves, L.K., and Tatchell, K. (2008). Ypi1, a positive regulator of nuclear protein phosphatase type 1 activity in Saccharomyces cerevisiae. Mol Biol Cell *19*, 1032-1045.

Biggins, S., and Murray, A.W. (2001). The budding yeast protein kinase Ipl1/Aurora allows the absence of tension to activate the spindle checkpoint. Genes Dev *15*, 3118-3129.

Biggins, S., Severin, F.F., Bhalla, N., Sassoon, I., Hyman, A.A., and Murray, A.W. (1999). The conserved protein kinase Ipl1 regulates microtubule binding to kinetochores in budding yeast. Genes Dev *13*, 532-544.

Birnboim, H.C., and Doly, J. (1979). A rapid alkaline extraction procedure for screening recombinant plasmid DNA. Nucleic Acids Res *7*, 1513-1523.

Black, S., Andrews, P.D., Sneddon, A.A., and Stark, M.J. (1995). A regulated MET3-GLC7 gene fusion provides evidence of a mitotic role for Saccharomyces cerevisiae protein phosphatase 1. Yeast *11*, 747-759.

Bloecher, A., and Tatchell, K. (1999). Defects in Saccharomyces cerevisiae protein phosphatase type I activate the spindle/kinetochore checkpoint. Genes Dev *13*, 517-522.

Bloecher, A., and Tatchell, K. (2000). Dynamic localization of protein phosphatase type 1 in the mitotic cell cycle of Saccharomyces cerevisiae. J Cell Biol *149*, 125-140.

Bloom, J., and Cross, F.R. (2007). Multiple levels of cyclin specificity in cell-cycle control. Nat Rev Mol Cell Biol *8*, 149-160.

Böhm, S., Lamberti, G., Fernandez-Saiz, V., Stapf, C., and Buchberger, A. (2011). Cellular functions of Ufd2 and Ufd3 in proteasomal protein degradation depend on Cdc48 binding. Mol Cell Biol.

Brachmann, C.B., Davies, A., Cost, G.J., Caputo, E., Li, J., Hieter, P., and Boeke, J.D. (1998). Designer deletion strains derived from Saccharomyces cerevisiae S288C: a useful set of strains and plasmids for PCR-mediated gene disruption and other applications. Yeast *14*, 115-132.

Braun, S., Matuschewski, K., Rape, M., Thoms, S., and Jentsch, S. (2002). Role of the ubiquitin-selective CDC48(UFD1/NPL4)chaperone (segregase) in ERAD of OLE1 and other substrates. Embo J *21*, 615-621.

Bruderer, R.M., Brasseur, C., and Meyer, H.H. (2004). The AAA ATPase p97/VCP interacts with its alternative co-factors, Ufd1-Npl4 and p47, through a common bipartite binding mechanism. J Biol Chem *279*, 49609-49616.

Bryant, N.J., and James, D.E. (2003). The Sec1p/Munc18 (SM) protein, Vps45p, cycles on and off membranes during vesicle transport. J Cell Biol *161*, 691-696.

Buchberger, A. (2006). Cdc48 (p97) and Its Cofactors. In Protein Degradation Cell Biology of the Ubiquitin-Proteasome System, A.C. R. John Mayer, Martin Rechsteiner, ed. (Weinheim, Wiley-VCH).

Buchberger, A. (2010). Control of ubiquitin conjugation by cdc48 and its cofactors. Subcell Biochem *54*, 17-30.

Buchberger, A., Howard, M.J., Proctor, M., and Bycroft, M. (2001). The UBX domain: a widespread ubiquitin-like module. J Mol Biol *307*, 17-24.

Cagney, G., Uetz, P., and Fields, S. (2000). High-throughput screening for protein-protein interactions using two-hybrid assay. Methods Enzymol *328*, 3-14.

Cannon, J.F. (2010). Function of protein phosphatase-1, Glc7, in Saccharomyces cerevisiae. Adv Appl Microbiol *73*, 27-59.

Cannon, J.F., Pringle, J.R., Fiechter, A., and Khalil, M. (1994). Characterization of glycogen-deficient glc mutants of Saccharomyces cerevisiae. Genetics *136*, 485-503.

Cao, K., Nakajima, R., Meyer, H.H., and Zheng, Y. (2003). The AAA-ATPase Cdc48/p97 regulates spindle disassembly at the end of mitosis. Cell *115*, 355-367.

Ceulemans, H., and Bollen, M. (2004). Functional diversity of protein phosphatase-1, a cellular economizer and reset button. Physiol Rev *84*, 1-39.

Cheeseman, I.M., Anderson, S., Jwa, M., Green, E.M., Kang, J., Yates, J.R., 3rd, Chan, C.S., Drubin, D.G., and Barnes, G. (2002). Phospho-regulation of kinetochore-microtubule attachments by the Aurora kinase Ipl1p. Cell *111*, 163-172.

Cheng, Y.L., and Chen, R.H. (2010). The AAA-ATPase Cdc48 and cofactor Shp1 promote chromosome bi-orientation by balancing Aurora B activity. J Cell Sci *123*, 2025-2034.

Ciechanover, A., and Ben-Saadon, R. (2004). N-terminal ubiquitination: more protein substrates join in. Trends Cell Biol *14*, 103-106.

Clemenson, C., and Marsolier-Kergoat, M.C. (2006). The spindle assembly checkpoint regulates the phosphorylation state of a subset of DNA checkpoint proteins in Saccharomyces cerevisiae. Mol Cell Biol *26*, 9149-9161.

Cohen-Fix, O., and Koshland, D. (1997). The anaphase inhibitor of Saccharomyces cerevisiae Pds1p is a target of the DNA damage checkpoint pathway. Proc Natl Acad Sci U S A *94*, 14361-14366.

Collins, S.R., Miller, K.M., Maas, N.L., Roguev, A., Fillingham, J., Chu, C.S., Schuldiner, M., Gebbia, M., Recht, J., Shales, M.*, et al.* (2007). Functional dissection of protein complexes involved in yeast chromosome biology using a genetic interaction map. Nature *446*, 806-810.

Costanzo, M., Baryshnikova, A., Bellay, J., Kim, Y., Spear, E.D., Sevier, C.S., Ding, H., Koh, J.L., Toufighi, K., Mostafavi, S.*, et al.* (2010). The genetic landscape of a cell. Science *327*, 425-431.

Costigan, C., Gehrung, S., and Snyder, M. (1992). A synthetic lethal screen identifies SLK1, a novel protein kinase homolog implicated in yeast cell morphogenesis and cell growth. Mol Cell Biol *12*, 1162-1178.

Dalal, S., Rosser, M.F., Cyr, D.M., and Hanson, P.I. (2004). Distinct roles for the AAA ATPases NSF and p97 in the secretory pathway. Mol Biol Cell *15*, 637-648.

Decottignies, A., Evain, A., and Ghislain, M. (2004). Binding of Cdc48p to a ubiquitin-related UBX domain from novel yeast proteins involved in intracellular proteolysis and sporulation. Yeast *21*, 127-139.

Deluca, K.F., Lens, S.M., and Deluca, J.G. (2011). Temporal changes in Hec1 phosphorylation control kinetochore-microtubule attachment stability during mitosis. J Cell Sci *124*, 622-634.

Deshaies, R.J., and Joazeiro, C.A. (2009). RING domain E3 ubiquitin ligases. Annu Rev Biochem *78*, 399-434.

Dohadwala, M., da Cruz e Silva, E.F., Hall, F.L., Williams, R.T., Carbonaro-Hall, D.A., Nairn, A.C., Greengard, P., and Berndt, N. (1994). Phosphorylation and inactivation of protein phosphatase 1 by cyclin-dependent kinases. Proc Natl Acad Sci U S A *91*, 6408-6412.

Dombradi, V., Axton, J.M., Barker, H.M., and Cohen, P.T. (1990). Protein phosphatase 1 activity in Drosophila mutants with abnormalities in mitosis and chromosome condensation. FEBS Lett *275*, 39-43.

Doseff, A.I., and Arndt, K.T. (1995). LAS1 is an essential nuclear protein involved in cell morphogenesis and cell surface growth. Genetics *141*, 857-871.

Dreveny, I., Kondo, H., Uchiyama, K., Shaw, A., Zhang, X., and Freemont, P.S. (2004). Structural basis of the interaction between the AAA ATPase p97/VCP and its adaptor protein p47. Embo J *23*, 1030-1039.

Dumitrescu, T.P., and Saunders, W.S. (2002). The FEAR Before MEN: networks of mitotic exit. Cell Cycle *1*, 304-307.

Egloff, M.P., Johnson, D.F., Moorhead, G., Cohen, P.T., Cohen, P., and Barford, D. (1997). Structural basis for the recognition of regulatory subunits by the catalytic subunit of protein phosphatase 1. Embo J *16*, 1876-1887.

Fan, H.Y., Cheng, K.K., and Klein, H.L. (1996). Mutations in the RNA polymerase II transcription machinery suppress the hyperrecombination mutant hpr1 delta of Saccharomyces cerevisiae. Genetics *142*, 749-759.

Feldman, R.M., Correll, C.C., Kaplan, K.B., and Deshaies, R.J. (1997). A complex of Cdc4p, Skp1p, and Cdc53p/cullin catalyzes ubiquitination of the phosphorylated CDK inhibitor Sic1p. Cell *91*, 221-230.

Feng, Z.H., Wilson, S.E., Peng, Z.Y., Schlender, K.K., Reimann, E.M., and Trumbly, R.J. (1991). The yeast GLC7 gene required for glycogen accumulation encodes a type 1 protein phosphatase. J Biol Chem *266*, 23796-23801.

Fernandez, A., Brautigan, D.L., and Lamb, N.J. (1992). Protein phosphatase type 1 in mammalian cell mitosis: chromosomal localization and involvement in mitotic exit. J Cell Biol *116*, 1421-1430.

Ficarro, S.B., McCleland, M.L., Stukenberg, P.T., Burke, D.J., Ross, M.M., Shabanowitz, J., Hunt, D.F., and White, F.M. (2002). Phosphoproteome analysis by mass spectrometry and its application to Saccharomyces cerevisiae. Nat Biotechnol *20*, 301-305.

Fiedler, D., Braberg, H., Mehta, M., Chechik, G., Cagney, G., Mukherjee, P., Silva, A.C., Shales, M., Collins, S.R., van Wageningen, S*., et al.* (2009). Functional organization of the S. cerevisiae phosphorylation network. Cell *136*, 952-963.

Finley, D. (2009). Recognition and processing of ubiquitin-protein conjugates by the proteasome. Annu Rev Biochem *78*, 477-513.

Finley, D., Ozkaynak, E., and Varshavsky, A. (1987). The yeast polyubiquitin gene is essential for resistance to high temperatures, starvation, and other stresses. Cell *48*, 1035-1046.

Finley, D., Sadis, S., Monia, B.P., Boucher, P., Ecker, D.J., Crooke, S.T., and Chau, V. (1994). Inhibition of proteolysis and cell cycle progression in a multiubiquitination-deficient yeast mutant. Mol Cell Biol *14*, 5501-5509.

Flick, K., Ouni, I., Wohlschlegel, J.A., Capati, C., McDonald, W.H., Yates, J.R., and Kaiser, P. (2004). Proteolysis-independent regulation of the transcription factor Met4 by a single Lys 48-linked ubiquitin chain. Nat Cell Biol *6*, 634-641.

Francisco, L., Wang, W., and Chan, C.S. (1994). Type 1 protein phosphatase acts in opposition to IpL1 protein kinase in regulating yeast chromosome segregation. Mol Cell Biol *14*, 4731-4740.

Frohlich, K.U., Fries, H.W., Rudiger, M., Erdmann, R., Botstein, D., and Mecke, D. (1991). Yeast cell cycle protein CDC48p shows full-length homology to the mammalian protein VCP and is a member of a protein family involved in secretion, peroxisome formation, and gene expression. J Cell Biol *114*, 443-453.

Fu, X., Ng, C., Feng, D., and Liang, C. (2003). Cdc48p is required for the cell cycle commitment point at Start via degradation of the G1-CDK inhibitor Far1p. J Cell Biol *163*, 21-26.

Gardner, R., Putnam, C.W., and Weinert, T. (1999). RAD53, DUN1 and PDS1 define two parallel G2/M checkpoint pathways in budding yeast. Embo J *18*, 3173-3185.

Gera, J.F., Hazbun, T.R., and Fields, S. (2002). Array-based methods for identifying protein-protein and protein-nucleic acid interactions. Methods Enzymol *350*, 499-512.

Geymonat, M., Spanos, A., de Bettignies, G., and Sedgwick, S.G. (2009). Lte1 contributes to Bfa1 localization rather than stimulating nucleotide exchange by Tem1. J Cell Biol *187*, 497-511.

Gietz, R.D., and Sugino, A. (1988). New yeast-Escherichia coli shuttle vectors constructed with in vitro mutagenized yeast genes lacking six-base pair restriction sites. Gene *74*, 527-534.

Gruhler, A., Olsen, J.V., Mohammed, S., Mortensen, P., Faergeman, N.J., Mann, M., and Jensen, O.N. (2005). Quantitative phosphoproteomics applied to the yeast pheromone signaling pathway. Mol Cell Proteomics *4*, 310-327.

Gustafsson, C.M., Myers, L.C., Beve, J., Spahr, H., Lui, M., Erdjument-Bromage, H., Tempst, P., and Kornberg, R.D. (1998). Identification of new mediator subunits in the RNA polymerase II holoenzyme from Saccharomyces cerevisiae. J Biol Chem *273*, 30851-30854.

Hanson, P.I., and Whiteheart, S.W. (2005). AAA+ proteins: have engine, will work. Nat Rev Mol Cell Biol *6*, 519-529.

Hardwick, K.G., and Murray, A.W. (1995). Mad1p, a phosphoprotein component of the spindle assembly checkpoint in budding yeast. J Cell Biol *131*, 709-720.

Hardwick, K.G., Weiss, E., Luca, F.C., Winey, M., and Murray, A.W. (1996). Activation of the budding yeast spindle assembly checkpoint without mitotic spindle disruption. Science *273*, 953-956.

Hartmann-Petersen, R., Wallace, M., Hofmann, K., Koch, G., Johnsen, A.H., Hendil, K.B., and Gordon, C. (2004). The Ubx2 and Ubx3 cofactors direct Cdc48 activity to proteolytic and nonproteolytic ubiquitin-dependent processes. Curr Biol *14*, 824-828.

Hartwell, L.H., Culotti, J., Pringle, J.R., and Reid, B.J. (1974). Genetic control of the cell division cycle in yeast. Science *183*, 46-51.

Hemmings, B.A., Resink, T.J., and Cohen, P. (1982). Reconstitution of a Mg-ATP-dependent protein phosphatase and its activation through a phosphorylation mechanism. FEBS Lett *150*, 319-324.

Heo, J.M., Livnat-Levanon, N., Taylor, E.B., Jones, K.T., Dephoure, N., Ring, J., Xie, J., Brodsky, J.L., Madeo, F., Gygi, S.P.*, et al.* (2010). A stress-responsive system for mitochondrial protein degradation. Mol Cell *40*, 465-480.

Hetzer, M., Meyer, H.H., Walther, T.C., Bilbao-Cortes, D., Warren, G., and Mattaj, I.W. (2001). Distinct AAA-ATPase p97 complexes function in discrete steps of nuclear assembly. Nat Cell Biol *3*, 1086-1091.

Heubes, S., and Stemmann, O. (2007). The AAA-ATPase p97-Ufd1-Npl4 is required for ERAD but not for spindle disassembly in Xenopus egg extracts. J Cell Sci *120*, 1325-1329.

Hicke, L. (2001). Protein regulation by monoubiquitin. Nat Rev Mol Cell Biol *2*, 195-201.

Hisamoto, N., Frederick, D.L., Sugimoto, K., Tatchell, K., and Matsumoto, K. (1995). The EGP1 gene may be a positive regulator of protein phosphatase type 1 in the growth control of Saccharomyces cerevisiae. Mol Cell Biol *15*, 3767-3776.

Hisamoto, N., Sugimoto, K., and Matsumoto, K. (1994). The Glc7 type 1 protein phosphatase of Saccharomyces cerevisiae is required for cell cycle progression in G2/M. Mol Cell Biol *14*, 3158-3165.

Hitt, R., and Wolf, D.H. (2004). Der1p, a protein required for degradation of malfolded soluble proteins of the endoplasmic reticulum: topology and Der1-like proteins. FEMS Yeast Res *4*, 721-729.

Hoege, C., Pfander, B., Moldovan, G.L., Pyrowolakis, G., and Jentsch, S. (2002). RAD6-dependent DNA repair is linked to modification of PCNA by ubiquitin and SUMO. Nature *419*, 135-141.

Hofmann, K., and Bucher, P. (1996). The UBA domain: a sequence motif present in multiple enzyme classes of the ubiquitination pathway. Trends Biochem Sci *21*, 172-173.

Hoyt, M.A. (2000). Exit from mitosis: spindle pole power. Cell *102*, 267-270.

Hoyt, M.A., Totis, L., and Roberts, B.T. (1991). S. cerevisiae genes required for cell cycle arrest in response to loss of microtubule function. Cell *66*, 507-517.

Hsu, J.Y., Sun, Z.W., Li, X., Reuben, M., Tatchell, K., Bishop, D.K., Grushcow, J.M., Brame, C.J., Caldwell, J.A., Hunt, D.F.*, et al.* (2000). Mitotic phosphorylation of histone H3 is governed by Ipl1/aurora kinase and Glc7/PP1 phosphatase in budding yeast and nematodes. Cell *102*, 279-291.

Hu, F., Wang, Y., Liu, D., Li, Y., Qin, J., and Elledge, S.J. (2001). Regulation of the Bub2/Bfa1 GAP complex by Cdc5 and cell cycle checkpoints. Cell *107*, 655-665.

Huber, A., Bodenmiller, B., Uotila, A., Stahl, M., Wanka, S., Gerrits, B., Aebersold, R., and Loewith, R. (2009). Characterization of the rapamycin-sensitive phosphoproteome reveals that Sch9 is a central coordinator of protein synthesis. Genes Dev *23*, 1929-1943.

Huh, W.K., Falvo, J.V., Gerke, L.C., Carroll, A.S., Howson, R.W., Weissman, J.S., and O'Shea, E.K. (2003). Global analysis of protein localization in budding yeast. Nature *425*, 686-691.

Hwang, L.H., Lau, L.F., Smith, D.L., Mistrot, C.A., Hardwick, K.G., Hwang, E.S., Amon, A., and Murray, A.W. (1998). Budding yeast Cdc20: a target of the spindle checkpoint. Science *279*, 1041-1044.

Ibeas, J.I., Yun, D.J., Damsz, B., Narasimhan, M.L., Uesono, Y., Ribas, J.C., Lee, H., Hasegawa, P.M., Bressan, R.A., and Pardo, J.M. (2001). Resistance to the plant PR-5 protein osmotin in the model fungus Saccharomyces cerevisiae is mediated by the regulatory effects of SSD1 on cell wall composition. Plant J *25*, 271-280.

Ikai, N., and Yanagida, M. (2006). Cdc48 is required for the stability of Cut1/separase in mitotic anaphase. J Struct Biol *156*, 50-61.

Ishii, K., Kumada, K., Toda, T., and Yanagida, M. (1996). Requirement for PP1 phosphatase and 20S cyclosome/APC for the onset of anaphase is lessened by the dosage increase of a novel gene sds23+. Embo J *15*, 6629-6640.

Ishii, T., Funakoshi, M., and Kobayashi, H. (2006). Yeast Pth2 is a UBL domain-binding protein that participates in the ubiquitin-proteasome pathway. Embo J *25*, 5492-5503.

Iwai, K., and Tokunaga, F. (2009). Linear polyubiquitination: a new regulator of NF-kappaB activation. EMBO Rep *10*, 706-713.

James, P., Halladay, J., and Craig, E.A. (1996). Genomic libraries and a host strain designed for highly efficient two-hybrid selection in yeast. Genetics *144*, 1425-1436.

Janke, C., Magiera, M.M., Rathfelder, N., Taxis, C., Reber, S., Maekawa, H., Moreno-Borchart, A., Doenges, G., Schwob, E., Schiebel, E.*, et al.* (2004). A versatile toolbox for PCR-based tagging of yeast genes: new fluorescent proteins, more markers and promoter substitution cassettes. Yeast *21*, 947-962.

Jarosch, E., Taxis, C., Volkwein, C., Bordallo, J., Finley, D., Wolf, D.H., and Sommer, T. (2002). Protein dislocation from the ER requires polyubiquitination and the AAA-ATPase Cdc48. Nat Cell Biol *4*, 134-139.

Jaspersen, S.L., and Winey, M. (2004). The budding yeast spindle pole body: structure, duplication, and function. Annu Rev Cell Dev Biol *20*, 1-28.

Jentsch, S., and Rumpf, S. (2007). Cdc48 (p97): a "molecular gearbox" in the ubiquitin pathway? Trends Biochem Sci *32*, 6-11.

Johnson, E.S., Ma, P.C., Ota, I.M., and Varshavsky, A. (1995). A proteolytic pathway that recognizes ubiquitin as a degradation signal. J Biol Chem *270*, 17442-17456.

Kaeberlein, M., and Guarente, L. (2002). Saccharomyces cerevisiae MPT5 and SSD1 function in parallel pathways to promote cell wall integrity. Genetics *160*, 83-95.

Kamada, Y., Jung, U.S., Piotrowski, J., and Levin, D.E. (1995). The protein kinase C-activated MAP kinase pathway of Saccharomyces cerevisiae mediates a novel aspect of the heat shock response. Genes Dev *9*, 1559-1571.

Kang, J., Cheeseman, I.M., Kallstrom, G., Velmurugan, S., Barnes, G., and Chan, C.S. (2001). Functional cooperation of Dam1, Ipl1, and the inner centromere protein (INCENP)-related protein Sli15 during chromosome segregation. J Cell Biol *155*, 763-774.

Kano, F., Kondo, H., Yamamoto, A., Kaneko, Y., Uchiyama, K., Hosokawa, N., Nagata, K., and Murata, M. (2005). NSF/SNAPs and p97/p47/VCIP135 are sequentially required for cell cycle-dependent reformation of the ER network. Genes Cells *10*, 989-999.

Keating, P., Rachidi, N., Tanaka, T.U., and Stark, M.J. (2009). Ipl1-dependent phosphorylation of Dam1 is reduced by tension applied on kinetochores. J Cell Sci *122*, 4375-4382.

Kemmler, S., Stach, M., Knapp, M., Ortiz, J., Pfannstiel, J., Ruppert, T., and Lechner, J. (2009). Mimicking Ndc80 phosphorylation triggers spindle assembly checkpoint signalling. Embo J *28*, 1099-1110.

Kim, E.M., and Burke, D.J. (2008). DNA damage activates the SAC in an ATM/ATR-dependent manner, independently of the kinetochore. PLoS Genet *4*, e1000015.

Kim, J.H., Kang, J.S., and Chan, C.S. (1999). Sli15 associates with the ipl1 protein kinase to promote proper chromosome segregation in Saccharomyces cerevisiae. J Cell Biol *145*, 1381-1394.

Kim, S.H., Lin, D.P., Matsumoto, S., Kitazono, A., and Matsumoto, T. (1998). Fission yeast Slp1: an effector of the Mad2-dependent spindle checkpoint. Science *279*, 1045-1047.

King, E.M., Rachidi, N., Morrice, N., Hardwick, K.G., and Stark, M.J. (2007). Ipl1p-dependent phosphorylation of Mad3p is required for the spindle checkpoint response to lack of tension at kinetochores. Genes Dev *21*, 1163-1168.

Knop, M., Siegers, K., Pereira, G., Zachariae, W., Winsor, B., Nasmyth, K., and Schiebel, E. (1999). Epitope tagging of yeast genes using a PCR-based strategy: more tags and improved practical routines. Yeast *15*, 963-972.

Koegl, M., Hoppe, T., Schlenker, S., Ulrich, H.D., Mayer, T.U., and Jentsch, S. (1999). A novel ubiquitination factor, E4, is involved in multiubiquitin chain assembly. Cell *96*, 635-644.

Kondo, H., Rabouille, C., Newman, R., Levine, T.P., Pappin, D., Freemont, P., and Warren, G. (1997). p47 is a cofactor for p97-mediated membrane fusion. Nature *388*, 75-78.

Kozubowski, L., Panek, H., Rosenthal, A., Bloecher, A., DeMarini, D.J., and Tatchell, K. (2003). A Bni4-Glc7 phosphatase complex that recruits chitin synthase to the site of bud emergence. Mol Biol Cell *14*, 26-39.

Krick, R., Bremer, S., Welter, E., Schlotterhose, P., Muehe, Y., Eskelinen, E.L., and Thumm, M. (2010). Cdc48/p97 and Shp1/p47 regulate autophagosome biogenesis in concert with ubiquitin-like Atg8. J Cell Biol *190*, 965-973.

Krogan, N.J., Cagney, G., Yu, H., Zhong, G., Guo, X., Ignatchenko, A., Li, J., Pu, S., Datta, N., Tikuisis, A.P.*, et al.* (2006). Global landscape of protein complexes in the yeast Saccharomyces cerevisiae. Nature *440*, 637-643.

Laemmli, U.K. (1970). Cleavage of structural proteins during the assembly of the head of bacteriophage T4. Nature *227*, 680-685.

Latterich, M., Frohlich, K.U., and Schekman, R. (1995). Membrane fusion and the cell cycle: Cdc48p participates in the fusion of ER membranes. Cell *82*, 885-893.

Lew, D.J., and Burke, D.J. (2003). The spindle assembly and spindle position checkpoints. Annu Rev Genet *37*, 251-282.

Lew, D.J., Marini, N.J., and Reed, S.I. (1992). Different G1 cyclins control the timing of cell cycle commitment in mother and daughter cells of the budding yeast S. cerevisiae. Cell *69*, 317-327.

Li, R., and Murray, A.W. (1991). Feedback control of mitosis in budding yeast. Cell *66*, 519-531.

Li, W., and Ye, Y. (2008). Polyubiquitin chains: functions, structures, and mechanisms. Cell Mol Life Sci *65*, 2397-2406.

Li, X., Gerber, S.A., Rudner, A.D., Beausoleil, S.A., Haas, W., Villen, J., Elias, J.E., and Gygi, S.P. (2007). Large-scale phosphorylation analysis of alpha-factor-arrested Saccharomyces cerevisiae. J Proteome Res *6*, 1190-1197.

Logan, M.R., Nguyen, T., Szapiel, N., Knockleby, J., Por, H., Zadworny, M., Neszt, M., Harrison, P., Bussey, H., Mandato, C.A.*, et al.* (2008). Genetic interaction network of the Saccharomyces cerevisiae type 1 phosphatase Glc7. BMC Genomics *9*, 336.

Lupas, A.N., and Martin, J. (2002). AAA proteins. Curr Opin Struct Biol *12*, 746-753.

MacKelvie, S.H., Andrews, P.D., and Stark, M.J. (1995). The Saccharomyces cerevisiae gene SDS22 encodes a potential regulator of the mitotic function of yeast type 1 protein phosphatase. Mol Cell Biol *15*, 3777-3785.

Makrantoni, V., and Stark, M.J. (2009). Efficient chromosome biorientation and the tension checkpoint in Saccharomyces cerevisiae both require Bir1. Mol Cell Biol *29*, 4552-4562.

Mendenhall, M.D., and Hodge, A.E. (1998). Regulation of Cdc28 cyclin-dependent protein kinase activity during the cell cycle of the yeast Saccharomyces cerevisiae. Microbiol Mol Biol Rev *62*, 1191-1243.

Meyer, H.H. (2005). Golgi reassembly after mitosis: the AAA family meets the ubiquitin family. Biochim Biophys Acta *1744*, 481-492.

Meyer, H.H., Wang, Y., and Warren, G. (2002). Direct binding of ubiquitin conjugates by the mammalian p97 adaptor complexes, p47 and Ufd1-Npl4. Embo J *21*, 5645-5652.

Moir, D., Stewart, S.E., Osmond, B.C., and Botstein, D. (1982). Cold-sensitive cell-division-cycle mutants of yeast: isolation, properties, and pseudoreversion studies. Genetics *100*, 547-563.

Mouysset, J., Deichsel, A., Moser, S., Hoege, C., Hyman, A.A., Gartner, A., and Hoppe, T. (2008). Cell cycle progression requires the CDC-48UFD-1/NPL-4 complex for efficient DNA replication. Proc Natl Acad Sci U S A *105*, 12879-12884.

Mukhopadhyay, D., and Riezman, H. (2007). Proteasome-independent functions of ubiquitin in endocytosis and signaling. Science *315*, 201-205.

Musacchio, A., and Salmon, E.D. (2007). The spindle-assembly checkpoint in space and time. Nat Rev Mol Cell Biol *8*, 379-393.

Nakajima, Y., Tyers, R.G., Wong, C.C., Yates, J.R., 3rd, Drubin, D.G., and Barnes, G. (2009). Nbl1p: a Borealin/Dasra/CSC-1-like protein essential for Aurora/Ipl1 complex function and integrity in Saccharomyces cerevisiae. Mol Biol Cell *20*, 1772-1784.

Nasmyth, K., Peters, J.M., and Uhlmann, F. (2000). Splitting the chromosome: cutting the ties that bind sister chromatids. Science *288*, 1379-1385.

Neuber, O., Jarosch, E., Volkwein, C., Walter, J., and Sommer, T. (2005). Ubx2 links the Cdc48 complex to ER-associated protein degradation. Nat Cell Biol *7*, 993-998.

Neves, A.T. (2005). Identification of substrates and cellular functions of the ubiquitin specific Cdc48Shp1 chaperone complex from Saccharomyces cerevisiae (München, Technische Universität).

Niedenthal, R.K., Riles, L., Johnston, M., and Hegemann, J.H. (1996). Green fluorescent protein as a marker for gene expression and subcellular localization in budding yeast. Yeast *12*, 773-786.

Nigavekar, S.S., Tan, Y.S., and Cannon, J.F. (2002). Glc8 is a glucose-repressible activator of Glc7 protein phosphatase-1. Arch Biochem Biophys *404*, 71-79.

Ohkura, H., Kinoshita, N., Miyatani, S., Toda, T., and Yanagida, M. (1989). The fission yeast dis2+ gene required for chromosome disjoining encodes one of two putative type 1 protein phosphatases. Cell *57*, 997-1007.

Park, I.K., Roach, P., Bondor, J., Fox, S.P., and DePaoli-Roach, A.A. (1994). Molecular mechanism of the synergistic phosphorylation of phosphatase inhibitor-2. Cloning, expression, and site-directed mutagenesis of inhibitor-2. J Biol Chem *269*, 944-954.

Pedelini, L., Marquina, M., Arino, J., Casamayor, A., Sanz, L., Bollen, M., Sanz, P., and Garcia-Gimeno, M.A. (2007). YPI1 and SDS22 proteins regulate the nuclear localization and function of yeast type 1 phosphatase Glc7. J Biol Chem *282*, 3282-3292.

Peggie, M.W., MacKelvie, S.H., Bloecher, A., Knatko, E.V., Tatchell, K., and Stark, M.J. (2002). Essential functions of Sds22p in chromosome stability and nuclear localization of PP1. J Cell Sci *115*, 195-206.

Peng, J., Schwartz, D., Elias, J.E., Thoreen, C.C., Cheng, D., Marsischky, G., Roelofs, J., Finley, D., and Gygi, S.P. (2003). A proteomics approach to understanding protein ubiquitination. Nat Biotechnol *21*, 921-926.

Peng, Z.Y., Trumbly, R.J., and Reimann, E.M. (1990). Purification and characterization of glycogen synthase from a glycogen-deficient strain of Saccharomyces cerevisiae. J Biol Chem *265*, 13871-13877.

Peters, C., Andrews, P.D., Stark, M.J., Cesaro-Tadic, S., Glatz, A., Podtelejnikov, A., Mann, M., and Mayer, A. (1999). Control of the terminal step of intracellular membrane fusion by protein phosphatase 1. Science *285*, 1084-1087.

Pickart, C.M. (2001). Mechanisms underlying ubiquitination. Annu Rev Biochem *70*, 503-533.

Pickart, C.M., and Cohen, R.E. (2004). Proteasomes and their kin: proteases in the machine age. Nat Rev Mol Cell Biol *5*, 177-187.

Pickart, C.M., and Eddins, M.J. (2004). Ubiquitin: structures, functions, mechanisms. Biochim Biophys Acta *1695*, 55-72.

Pickart, C.M., and Fushman, D. (2004). Polyubiquitin chains: polymeric protein signals. Curr Opin Chem Biol *8*, 610-616.

Pinsky, B.A., Kotwaliwale, C.V., Tatsutani, S.Y., Breed, C.A., and Biggins, S. (2006a). Glc7/protein phosphatase 1 regulatory subunits can oppose the Ipl1/aurora protein kinase by redistributing Glc7. Mol Cell Biol *26*, 2648-2660.

Pinsky, B.A., Kung, C., Shokat, K.M., and Biggins, S. (2006b). The Ipl1-Aurora protein kinase activates the spindle checkpoint by creating unattached kinetochores. Nat Cell Biol *8*, 78-83.

Pinsky, B.A., Nelson, C.R., and Biggins, S. (2009). Protein phosphatase 1 regulates exit from the spindle checkpoint in budding yeast. Curr Biol *19*, 1182-1187.

Rabouille, C., Kondo, H., Newman, R., Hui, N., Freemont, P., and Warren, G. (1998). Syntaxin 5 is a common component of the NSF- and p97-mediated reassembly pathways of Golgi cisternae from mitotic Golgi fragments in vitro. Cell *92*, 603-610.

Ramadan, K., Bruderer, R., Spiga, F.M., Popp, O., Baur, T., Gotta, M., and Meyer, H.H. (2007). Cdc48/p97 promotes reformation of the nucleus by extracting the kinase Aurora B from chromatin. Nature *450*, 1258-1262.

Rape, M., Hoppe, T., Gorr, I., Kalocay, M., Richly, H., and Jentsch, S. (2001). Mobilization of processed, membrane-tethered SPT23 transcription factor by CDC48(UFD1/NPL4), a ubiquitin-selective chaperone. Cell *107*, 667-677.

Ravid, T., and Hochstrasser, M. (2008). Diversity of degradation signals in the ubiquitin-proteasome system. Nat Rev Mol Cell Biol *9*, 679-690.

Ren, J., Wen, L., Gao, X., Jin, C., Xue, Y., and Yao, X. (2008). CSS-Palm 2.0: an updated software for palmitoylation sites prediction. Protein Eng Des Sel *21*, 639-644.

Ross, K.E., Kaldis, P., and Solomon, M.J. (2000). Activating phosphorylation of the Saccharomyces cerevisiae cyclin-dependent kinase, cdc28p, precedes cyclin binding. Mol Biol Cell *11*, 1597-1609.

Rothstein, R. (1991). Targeting, disruption, replacement, and allele rescue: integrative DNA transformation in yeast. Methods Enzymol *194*, 281-301.

Rumpf, S., and Jentsch, S. (2006). Functional division of substrate processing cofactors of the ubiquitin-selective Cdc48 chaperone. Mol Cell *21*, 261-269.

Sambrook, J., and Russell, D.W. (2001). Molecular Cloning - A Laboratory Manual, 3rd edition edn (Cold Spring Harbor, New York, Cold Spring Harbor Laboratory Press).

Sassoon, I., Severin, F.F., Andrews, P.D., Taba, M.R., Kaplan, K.B., Ashford, A.J., Stark, M.J., Sorger, P.K., and Hyman, A.A. (1999). Regulation of Saccharomyces cerevisiae kinetochores by the type 1 phosphatase Glc7p. Genes Dev *13*, 545-555.

Sato, B.K., and Hampton, R.Y. (2006). Yeast Derlin Dfm1 interacts with Cdc48 and functions in ER homeostasis. Yeast *23*, 1053-1064.

Scherer, S., and Davis, R.W. (1979). Replacement of chromosome segments with altered DNA sequences constructed in vitro. Proc Natl Acad Sci U S A *76*, 4951-4955.

Schuberth, C. (2006). UBX-Domänen-Proteine als neue Familie von Kofaktoren der AAA-ATPase Cdc48. In Fakultät für Biologie (München, Ludwig-Maximilians-Universität).

Schuberth, C., and Buchberger, A. (2005). Membrane-bound Ubx2 recruits Cdc48 to ubiquitin ligases and their substrates to ensure efficient ER-associated protein degradation. Nat Cell Biol *7*, 999-1006.

Schuberth, C., and Buchberger, A. (2008). UBX domain proteins: major regulators of the AAA ATPase Cdc48/p97. Cell Mol Life Sci *65*, 2360-2371.

Schuberth, C., Richly, H., Rumpf, S., and Buchberger, A. (2004). Shp1 and Ubx2 are adaptors of Cdc48 involved in ubiquitin-dependent protein degradation. EMBO Rep *5*, 818-824.

Schwob, E., Bohm, T., Mendenhall, M.D., and Nasmyth, K. (1994). The B-type cyclin kinase inhibitor p40SIC1 controls the G1 to S transition in S. cerevisiae. Cell *79*, 233-244.

Seeley, E.S., Kato, M., Margolis, N., Wickner, W., and Eitzen, G. (2002). Genomic analysis of homotypic vacuole fusion. Mol Biol Cell *13*, 782-794.

Shimogawa, M.M., Graczyk, B., Gardner, M.K., Francis, S.E., White, E.A., Ess, M., Molk, J.N., Ruse, C., Niessen, S., Yates, J.R., 3rd*, et al.* (2006). Mps1 phosphorylation of Dam1 couples kinetochores to microtubule plus ends at metaphase. Curr Biol *16*, 1489-1501.

Sikorski, R.S., and Hieter, P. (1989). A system of shuttle vectors and yeast host strains designed for efficient manipulation of DNA in Saccharomyces cerevisiae. Genetics *122*, 19-27.

Skibbens, R.V., and Hieter, P. (1998). Kinetochores and the checkpoint mechanism that monitors for defects in the chromosome segregation machinery. Annu Rev Genet *32*, 307-337.

Skowyra, D., Craig, K.L., Tyers, M., Elledge, S.J., and Harper, J.W. (1997). F-box proteins are receptors that recruit phosphorylated substrates to the SCF ubiquitin-ligase complex. Cell *91*, 209-219.

Smolka, M.B., Albuquerque, C.P., Chen, S.H., and Zhou, H. (2007). Proteome-wide identification of in vivo targets of DNA damage checkpoint kinases. Proc Natl Acad Sci U S A *104*, 10364-10369.

Spence, J., Sadis, S., Haas, A.L., and Finley, D. (1995). A ubiquitin mutant with specific defects in DNA repair and multiubiquitination. Mol Cell Biol *15*, 1265-1273.

Spingola, M., Grate, L., Haussler, D., and Ares, M., Jr. (1999). Genome-wide bioinformatic and molecular analysis of introns in Saccharomyces cerevisiae. RNA *5*, 221-234.

Stark, M.J. (1996). Yeast protein serine/threonine phosphatases: multiple roles and diverse regulation. Yeast *12*, 1647-1675.

Stern, B.M., and Murray, A.W. (2001). Lack of tension at kinetochores activates the spindle checkpoint in budding yeast. Curr Biol *11*, 1462-1467.

Stuart, J.S., Frederick, D.L., Varner, C.M., and Tatchell, K. (1994). The mutant type 1 protein phosphatase encoded by glc7-1 from Saccharomyces cerevisiae fails to interact productively with the GAC1-encoded regulatory subunit. Mol Cell Biol *14*, 896-905.

Sullivan, M., and Morgan, D.O. (2007). Finishing mitosis, one step at a time. Nat Rev Mol Cell Biol *8*, 894-903.

Sutton, A., Immanuel, D., and Arndt, K.T. (1991). The SIT4 protein phosphatase functions in late G1 for progression into S phase. Mol Cell Biol *11*, 2133-2148.

Tagwerker, C., Flick, K., Cui, M., Guerrero, C., Dou, Y., Auer, B., Baldi, P., Huang, L., and Kaiser, P. (2006). A tandem affinity tag for two-step purification under fully denaturing conditions: application in ubiquitin profiling and protein complex identification combined with in vivocross-linking. Mol Cell Proteomics *5*, 737-748.

Tan, Y.S., Morcos, P.A., and Cannon, J.F. (2003). Pho85 phosphorylates the Glc7 protein phosphatase regulator Glc8 in vivo. J Biol Chem *278*, 147-153.

Tanaka, T.U., Rachidi, N., Janke, C., Pereira, G., Galova, M., Schiebel, E., Stark, M.J., and Nasmyth, K. (2002). Evidence that the Ipl1-Sli15 (Aurora kinase-INCENP) complex promotes chromosome bi-orientation by altering kinetochore-spindle pole connections. Cell *108*, 317-329.

Tatchell, K., Makrantoni, V., Stark, M.J., and Robinson, L.C. (2011). Temperature-sensitive ipl1-2/Aurora B mutation is suppressed by mutations in TOR complex 1 via the Glc7/PP1 phosphatase. Proc Natl Acad Sci U S A *108*, 3994-3999.

Thomas, B.J., and Rothstein, R. (1989). Elevated recombination rates in transcriptionally active DNA. Cell *56*, 619-630.

Thoms, S. (2002). Shp1, ein neuer Faktor der Vakuolenmembranfusion von Saccharomyces cerevisiae (Universität Witten/Herdecke).

Tu, J., and Carlson, M. (1994). The GLC7 type 1 protein phosphatase is required for glucose repression in Saccharomyces cerevisiae. Mol Cell Biol *14*, 6789-6796.

Tu, J., and Carlson, M. (1995). REG1 binds to protein phosphatase type 1 and regulates glucose repression in Saccharomyces cerevisiae. Embo J *14*, 5939-5946.

Tung, H.Y., Wang, W., and Chan, C.S. (1995). Regulation of chromosome segregation by Glc8p, a structural homolog of mammalian inhibitor 2 that functions as both an activator and an inhibitor of yeast protein phosphatase 1. Mol Cell Biol *15*, 6064-6074.

Uchiyama, K., Jokitalo, E., Kano, F., Murata, M., Zhang, X., Canas, B., Newman, R., Rabouille, C., Pappin, D., Freemont, P.*, et al.* (2002). VCIP135, a novel essential factor for p97/p47-mediated membrane fusion, is required for Golgi and ER assembly in vivo. J Cell Biol *159*, 855-866.

Uchiyama, K., Jokitalo, E., Lindman, M., Jackman, M., Kano, F., Murata, M., Zhang, X., and Kondo, H. (2003). The localization and phosphorylation of p47 are important for Golgi disassembly-assembly during the cell cycle. J Cell Biol *161*, 1067-1079.

Uhlmann, F., Lottspeich, F., and Nasmyth, K. (1999). Sister-chromatid separation at anaphase onset is promoted by cleavage of the cohesin subunit Scc1. Nature *400*, 37-42.

van Leuken, R., Clijsters, L., and Wolthuis, R. (2008). To cell cycle, swing the APC/C. Biochim Biophys Acta *1786*, 49-59.

Vanoosthuyse, V., and Hardwick, K.G. (2009). A novel protein phosphatase 1-dependent spindle checkpoint silencing mechanism. Curr Biol *19*, 1176-1181.

Venturi, G.M., Bloecher, A., Williams-Hart, T., and Tatchell, K. (2000). Genetic interactions between GLC7, PPZ1 and PPZ2 in saccharomyces cerevisiae. Genetics *155*, 69-83.

Verma, R., Oania, R., Fang, R., Smith, G.T., and Deshaies, R.J. (2011). Cdc48/p97 Mediates UV-Dependent Turnover of RNA Pol II. Mol Cell *41*, 82-92.

Walsh, E.P., Lamont, D.J., Beattie, K.A., and Stark, M.J. (2002). Novel interactions of Saccharomyces cerevisiae type 1 protein phosphatase identified by single-step affinity purification and mass spectrometry. Biochemistry *41*, 2409-2420.

Wang, H., Liu, D., Wang, Y., Qin, J., and Elledge, S.J. (2001). Pds1 phosphorylation in response to DNA damage is essential for its DNA damage checkpoint function. Genes Dev *15*, 1361-1372.

Wang, Y., and Burke, D.J. (1995). Checkpoint genes required to delay cell division in response to nocodazole respond to impaired kinetochore function in the yeast Saccharomyces cerevisiae. Mol Cell Biol *15*, 6838-6844.

Wang, Y., Hu, F., and Elledge, S.J. (2000). The Bfa1/Bub2 GAP complex comprises a universal checkpoint required to prevent mitotic exit. Curr Biol *10*, 1379-1382.

Wang, Y., Satoh, A., Warren, G., and Meyer, H.H. (2004). VCIP135 acts as a deubiquitinating enzyme during p97-p47-mediated reassembly of mitotic Golgi fragments. J Cell Biol *164*, 973-978.

Waterhouse, A.M., Procter, J.B., Martin, D.M., Clamp, M., and Barton, G.J. (2009). Jalview Version 2--a multiple sequence alignment editor and analysis workbench. Bioinformatics *25*, 1189-1191.

Weiss, E., and Winey, M. (1996). The Saccharomyces cerevisiae spindle pole body duplication gene MPS1 is part of a mitotic checkpoint. J Cell Biol *132*, 111-123.

Wilcox, A.J., and Laney, J.D. (2009). A ubiquitin-selective AAA-ATPase mediates transcriptional switching by remodelling a repressor-promoter DNA complex. Nat Cell Biol *11*, 1481-1486.

Wilson, W.A., Wang, Z., and Roach, P.J. (2005). Regulation of yeast glycogen phosphorylase by the cyclin-dependent protein kinase Pho85p. Biochemical and Biophysical Research Communications *329*, 161-167.

Winey, M., Mamay, C.L., O'Toole, E.T., Mastronarde, D.N., Giddings, T.H., Jr., McDonald, K.L., and McIntosh, J.R. (1995). Three-dimensional ultrastructural analysis of the Saccharomyces cerevisiae mitotic spindle. J Cell Biol *129*, 1601-1615.

Wolf, D.H., and Hilt, W. (2004). The proteasome: a proteolytic nanomachine of cell regulation and waste disposal. Biochim Biophys Acta *1695*, 19-31.

Woodbury, E.L., and Morgan, D.O. (2007). Cdk and APC activities limit the spindle-stabilizing function of Fin1 to anaphase. Nat Cell Biol *9*, 106-112.

Wu, J., Carmen, A.A., Kobayashi, R., Suka, N., and Grunstein, M. (2001). HDA2 and HDA3 are related proteins that interact with and are essential for the activity of the yeast histone deacetylase HDA1. Proc Natl Acad Sci U S A *98*, 4391-4396.

Wu, X., and Tatchell, K. (2001). Mutations in yeast protein phosphatase type 1 that affect targeting subunit binding. Biochemistry *40*, 7410-7420.

Xu, P., Duong, D.M., Seyfried, N.T., Cheng, D., Xie, Y., Robert, J., Rush, J., Hochstrasser, M., Finley, D., and Peng, J. (2009). Quantitative proteomics reveals the function of unconventional ubiquitin chains in proteasomal degradation. Cell *137*, 133-145.

Yamano, H., Ishii, K., and Yanagida, M. (1994). Phosphorylation of dis2 protein phosphatase at the C-terminal cdc2 consensus and its potential role in cell cycle regulation. Embo J *13*, 5310-5318.

Ye, Y., Meyer, H.H., and Rapoport, T.A. (2001). The AAA ATPase Cdc48/p97 and its partners transport proteins from the ER into the cytosol. Nature *414*, 652-656.

Yeh, E., Skibbens, R.V., Cheng, J.W., Salmon, E.D., and Bloom, K. (1995). Spindle dynamics and cell cycle regulation of dynein in the budding yeast, Saccharomyces cerevisiae. J Cell Biol *130*, 687-700.

Yuan, X., Shaw, A., Zhang, X., Kondo, H., Lally, J., Freemont, P.S., and Matthews, S. (2001). Solution structure and interaction surface of the C-terminal domain from p47: a major p97-cofactor involved in SNARE disassembly. J Mol Biol *311*, 255-263.

Yuan, X., Simpson, P., Kondo, H., McKeown, C., Dreveny, I., Zhang, X., Freemont, P.S., and Matthews, S. (2004a). Complete backbone resonance assignments of p47: the 41kDa adaptor protein of the AAA ATPase p97. J Biomol NMR *28*, 309-310.

Yuan, X., Simpson, P., McKeown, C., Kondo, H., Uchiyama, K., Wallis, R., Dreveny, I., Keetch, C., Zhang, X., Robinson, C., *et al.* (2004b). Structure, dynamics and interactions of p47, a major adaptor of the AAA ATPase, p97. Embo J *23*, 1463-1473.

Yuen, K.W., Warren, C.D., Chen, O., Kwok, T., Hieter, P., and Spencer, F.A. (2007). Systematic genome instability screens in yeast and their potential relevance to cancer. Proc Natl Acad Sci U S A *104*, 3925-3930.

Zhang, S., Guha, S., and Volkert, F.C. (1995). The Saccharomyces SHP1 gene, which encodes a regulator of phosphoprotein phosphatase 1 with differential effects on glycogen metabolism, meiotic differentiation, and mitotic cell cycle progression. Mol Cell Biol *15*, 2037-2050.

Zich, J., and Hardwick, K.G. (2010). Getting down to the phosphorylated 'nuts and bolts' of spindle checkpoint signalling. Trends Biochem Sci *35*, 18-27.

7. Abbreviations

3AT	3’amino-1,2,4-triazole
5’FOA	5-fluoroorotic acid
AAA	ATPases associated with diverse cellular activities
AD	Gal4 activation domain
Amp	ampicillin
APC/C	anaphase promoting complex/ cyclosome
APS	ammonium-peroxo-disulfate
ATM	ataxia-telangiectasia-mutated
ATP	adenosine 5’-triphosphate
ATR	ATM and Rad3-related protein
BD	Gal4 binding domain
BUB	budding uninhibited by benomyl
cdc	cell division cycle
Cdk	cyclin dependent kinase
CEN	centromeric
CHX	cycloheximide
CIN	chromosomal instability
CP	core particle
CPC	chromosomal passenger complex
cs	cold sensitive
C-terminal	carboxy-terminal
ddH$_2$O	double distilled water
DIC	differential interference contrast
DMSO	dimethyl sulfoxide
DNA	deoxyribonucleic acid
dNTP	deoxy nucleoside triphosphate
DTT	1,4-dithiothreitol
DUB	deubiquitinating enzyme
E. coli	*Escherichia coli*
ECL	enhanced chemiluminescence
EDTA	ethylene diamine tetra-acetic acid
ER	endoplasmatic reticulum
ERAD	endoplasmatic reticulum associated degradation
FACS	fluorescence activated cell sorting
FEAR	fourteen early anaphase release
FITC	fluorescein isothiocyanate
g	gravitational constant 9.81m/s^2
G1/G2	gap phases G1 and G2
G418	geneticine disulfate
GAP	GTPase activating complex
gDNA	genomic DNA
GEF	guanine nucleotide exchange factor
GFP	green fluorescent protein
GTP	guanosine-5‘-triphosphate
h	hours
HA	hemagglutinin
HECT	Homologous to E6AP Carboxy Terminus
His	histidine
HRP	horseradish peroxidase
HU	hydroxyurea

Hyg	hygromycin
I-2	inhibitor 2
IP	immunoprecipitation
Kan	kanamycin
kb	kilo basepairs
kD	kilo Dalton
LB	Luria-Bertani
Leu	leucine
LP	longpass
BP	bandpass
FT	“farb teiler”
LUBAC	linear ubiquitin chain assembly complex
mA	milli-ampere
MAD	mitotic arrest deficient
MCC	mitotic checkpoint complex
MEN	mitotic exit network
min	minutes
n.d.	not determined
NAT	nourseothricin
Noc	nocodazole
NP-40	Nonidet P-40
NSF	N-ethylmaleimide-sensitive fusion protein
N-terminal	amino-terminus
OD	optical density
ORF	open reading frame
PAGE	polyacrylamide gel electrophoresis
PBS	phosphate-buffered saline
PCR	polymerase chain reaction
PD	pull-down
PEG	polyethylene glycol
PI	propidium iodide
Pkc1	protein kinase C
PMSF	phenylmethanesulfonyl fluoride
PNGase	peptidyl-N-glycanase
PP1	protein phosphatase 1
PVDF	polyvinylidene fluoride
RING	Really Interesting New Gene
RNA	ribonucleic acid
RNA Pol II	RNA polymerase II
RNase	ribonuclease
rpm	rounds per minute
RT	room temperature, 24°C
S. cerevisiae	*Saccharomyces cerevisiae*
SAC	spindle assembly checkpoint
SC	synthetic complete
SCF	Skp1-Cullin-F-box complex
SDS	sodium dodecyl sulfate
sec	seconds
SEP	Shp1 Eyc p47
SL	synthetically lethal
SNARE	soluble NSF attachment protein
SPB	spindle pole body
SRH	second region of homology

SUMO	small ubiquitin-like modifier
TBE	tris-borate-EDTA
TBS	tris-buffered saline
TCA	trichloroacetic acid
TOR	target of rapamycin
Tris	tris (hydroxymethyl)aminomethane
Trp	tryptophan
ts	temperature sensitive
Ub	ubiquitin
UBA	ubiquitin associated domain
UBC	ubiquitin conjugating enzyme
U-box	UFD2 homology
UBX	ubiquitin regulatory ‘X’
UFD	ubiquitin fusion degradation
UIM	ubiquitin interaction motif
UPS	ubiquitin proteasome system
Ura	uracil
V	volt
VCP	Valosin containing protein
Vol	volume
w/v	weight per volume
WT	wild-type
Y2H	yeast two hybrid
YPD	yeast peptone dextrose

Acknowledgements

Zuallererst möchte ich mich bei dem Betreuer meiner Arbeit, Prof. Dr. Alexander Buchberger bedanken: für die große Freiheit bei der Bearbeitung auch dieses Projekts, die ständige Diskussionsbereitschaft, und vor allem für eine ganze Menge Geduld.

Ein besonderer Dank gilt Prof. Dr. Stefan Jentsch, nicht nur für die Übernahme des Erstgutachtens dieser Arbeit, sondern vor allem für die großzügige Unterstützung während der Zeit in München und auch noch nach dem Umzug nach Würzburg.

Bei Frau Prof. Dr. Böttger möchte ich mich herzlich für die freundliche Übernahme der Begutachtung dieser Arbeit bedanken. Auch allen anderen Mitgliedern der Prüfungskommission danke ich sehr für ihr Interesse und ihre Zeit.

Bei allen Kollegen des „alten Labors“ bedanke ich mich für die stets gute und lustige Stimmung. Ein riesengroßer Dank geht an Christian für die immer verlässliche Hilfe während der letzten Jahre und an Silke für ihre Geduld bei den Versuchen mir das Tetradenauslegen beizubringen. Michael, Olaf, Bernd und Sandrine danke ich für die hilfreichen Diskussionen zum Zellzyklus. Ganz besonders bedanken möchte ich mich bei den anderen „goats“ aus dem 2. Stock, für eine wirklich sehr schöne gemeinsame Zeit in München!

Außerdem möchte ich auch der ganzen Abteilung Jentsch für die große Diskussions- und Hilfsbereitschaft danken. Vor allem bei Dirk bedanke ich mich für das Beantworten unendlich vieler Fragen zur Labororganisation während des Umzugs und bei Jochen für Rat und Tat bei meinen ganzen Computer- und Mikroskop-Problemchen.

Ein weiteres Dankeschön geht an Dr. Tobias Walther für die Nutzung das Spinning Disk Mikroskops und vor allem an Doris für ihre Hilfe dabei.

Prof. Gaubatz und Prof. Eilers danke ich für die unkomplizierte Möglichkeit zur Nutzung der FACS Geräte in ihren Abteilungen.

Schließlich bedanke ich mich natürlich auch bei meinen Mitstreitern im „neuen Labor“: Christopher, Claudia, Erika und Sven, dass es von Anfang an so lustig zuging hat einiges leichter gemacht! Ich danke außerdem den Mitgliedern des Lehrstuhls für Biochemie, die die Hefe und mich ohne Protest in ihre Labore gelassen haben. Basti, Kathrin und Katrin- danke, dass Mikroskop und FACS nun auch bei Hefe funktionieren.

Zu guter Letzt bedanke ich mich vor allem bei Freunden und meiner Familie für ihre Geduld und Unterstützung. Besonders danke ich denjenigen, denen diese Arbeit wohl den einen oder anderen Nerv mehr geraubt hat, vor allem meiner Mutter.